

**Nesprin-2 Giant at the nuclear envelope with  
roles in cell differentiation, proliferation and  
chromatin association**

**Inaugural-Dissertation**

zur

Erlangung des Doktorgrades

der Mathematisch-Naturwissenschaftlichen Fakultät

der Universität zu Köln



vorgelegt von

**Rashmi Rudrappa Nanjundappa**

aus Birur, Indien

2011

Prüfungsvorsitzender:

Prof. Dr. Thomas Wiehe

Berichterstatter:

Prof. Dr. Angelika A. Noegel

Berichterstatter:

Prof. Dr. Siegfried Roth

Tag der mündlichen Prüfung:

13. 07. 2010

# Contents

<b>Acknowledgment</b>	<b>III</b>
<b>List of Figures</b>	<b>VI</b>
<b>List of Tables</b>	<b>VII</b>
<b>List of Abbreviations</b>	<b>XI</b>
<b>1 Introduction</b>	<b>1</b>
1.1 Nucleus and Nuclear envelope . . . . .	1
1.2 Nesprins - their roles in human disease . . . . .	3
1.2.1 Structural composition, binding partners and role of Nesprin-2 at the nuclear envelope . . . . .	5
1.3 Cell migration and wound healing . . . . .	8
1.3.1 Phases of wound healing . . . . .	8
1.4 Role of nuclear envelope proteins in transcription regulation and cell proliferation . . . . .	12
1.5 Aim of the research . . . . .	13
<b>2 Results</b>	<b>15</b>
2.1 Transcriptional profiling in Nesprin-2 knockout fibroblasts . . . . .	15
2.2 In vivo wound healing study in Nesprin-2 knock out mice . . . . .	20
2.2.1 Macroscopic observation showed a delay in wound healing in Nesprin-2 KO mice as compared to wild type . . . . .	20
2.2.2 The distance between the epidermal tips is altered in Nesprin-2 KO wounds . . . . .	21
2.2.3 Inflammatory phase-study of Macrophages . . . . .	25
2.2.4 New tissue formation and tissue remodelling phase - Study of keratinocytes migration, proliferation and fibroblast differentiation . . . . .	29
2.3 The transcriptional regulation of genes involved in wound healing is altered in Nesprin-2 Giant knock out mice . . . . .	41
2.4 c-Fos localization in Nesprin-2 KO and WT epidermis . . . . .	44
2.5 Nesprin-2 regulates the localization of c-Fos in human keratinocytes	46
2.6 Localization of c-Fos in cell scratch assay . . . . .	47

---

2.7	Apoptosis in Nesprin-2 KO cultured fibroblasts . . . . .	49
2.8	Caspase-3 in Nesprin-2 KO fibroblasts . . . . .	51
2.9	The Localization of SAFB1 has changed in Nesprin-2 KO fibroblasts	51
2.10	Nesprin-2 Giant binds to heterochromatic DNA . . . . .	54
<b>3</b>	<b>Discussion</b>	<b>59</b>
3.1	Transcriptional profiling in Nesprin-2 KO and WT fibroblasts . . . . .	59
3.2	The wound healing process is delayed in Nesprin-2 KO mice . . . . .	60
3.3	Nesprin-2 regulates the cell proliferation and differentiation under the wound healing situation by affecting transcription factors . . . . .	62
3.4	A disturbed F-actin network can cause the impaired myofibroblast differentiation in Nesprin-2 KO mice . . . . .	66
3.5	Fate of the cells which showed nuclear deformation in Nesprin-2 KO mice (an apoptotic approach) . . . . .	67
3.6	Nesprin-2 interacts with heterochromatin and associates with chro- matin . . . . .	68
3.7	Model for Nesprin-2 Giant function in wound healing . . . . .	69
<b>4</b>	<b>Materials and Methods</b>	<b>72</b>
4.1	Kits and Reagents . . . . .	72
4.2	Oligonucleotides . . . . .	75
4.3	Enzymes and Antibodies . . . . .	76
4.4	Media, Buffers and solutions . . . . .	77
4.5	Nesprin-2 Giant knock out mice . . . . .	79
4.6	Isolation of primary fibroblasts . . . . .	80
4.7	Wounding . . . . .	80
4.8	Wound tissue harvesting and sectioning . . . . .	80
4.9	Histological staining . . . . .	81
4.10	Immunohistochemistry and Immunofluorescence . . . . .	82
4.11	Western blotting . . . . .	82
4.12	RNA isolation and RT-PCR analysis . . . . .	83
4.13	Cell culture and transfection . . . . .	85
4.14	Chromatin immunoprecipitation assay (ChiP) . . . . .	85
4.15	Microarray analysis . . . . .	86
	<b>Bibliography</b>	<b>91</b>
	<b>Abstract</b>	<b>i</b>
	<b>Zusammenfassung</b>	<b>iii</b>
	<b>Erklärung</b>	<b>v</b>

# Acknowledgment

## **‘Gratitude is the memory of the heart’**

I would like to express my deep and sincere gratitude to my supervisor, **Prof. Dr. A. A. Noegel**. Her wide knowledge and her logical way of thinking have been of great value for me. Her understanding, encouraging and belief in my strength have provided a good basis for the successful completion of PhD thesis.

I avail this opportunity to express my deep sense of gratitude to other members of my thesis committee **Prof. Dr. S. Roth**, Institute of Developmental Biology and **Prof. Dr. T. Wiehe**, Institute of Genetics, University of Cologne.

I wish to express my warm and sincere thanks to Prof. Dr. Ludwig Eichinger, Dr. Iakowos Karakesisoglou, Dr. Beate Eckes (Dept. of Dermatology, Cologne), Dr. Gernot Glöckner (Berlin Center for Genomics in Biodiversity Research, Berlin) and Dr. Marco Groth (Leibniz Institute for Age Research - Fritz Lipmann Institute, Jena) for their detailed and constructive comments, for the valuable advice and friendly help.

I am very much thankful to Rosi, Maria, Martina, Berthold, Rolf, Sonya, Brigitte and Bärbel for their valuable help and co-operation in the lab. My special thanks to Dörte Püsche who helped me all the time to complete and solve official matters. I also thank Budi, Gudrun and Roman who helped me to solve computer related problems whenever I needed.

I am privileged for having Anja, Bhagyashri, Eva, Georgia, Janbo, Karl-Heinz, Karthik I, Karthik II, Liu, Margit, Martin, Raphael, Sandra, Sascha, Shahrzad,

Surayya, Vivek, Tanja, Xin and Yvonne as my colleagues who have provided me great help and company during all these years in Biochemistry Institute, Cologne. I also thank all the members of Ludwig's group for making me to feel comfortable while doing my experiments in their lab. I should not forget to thank Ralf Hallinger who helped me a lot during wound healing analysis, thanks a lot Ralf. I am very much thankful to Alex Friede for her great help in using the Latex programme for writing my thesis. I also take this opportunity to thank all the members of AG. Huelskamp who were always very friendly and made me feel as a part of their group.

I thank all my Kannadiga friends in Germany, I thank Nikki, Manoj and Ashish and other friends with whom I had wonderful time. I also thank my all other friends in India and other parts of the world.

My parents deserve special mention for their constant support, encouragement and selfless sacrifice. Without their love and blessings I would not have been what I am today. Thank you **Amma** and **Appa** for everything you have done for me. I dedicate all my success to you both. I remember with great respect and love my sister and her family and also my brother. My in laws deserve special place in my heart for their invaluable inspiration and love. Without their support this study would have scarcely been accomplished.

One more important person in my life is my husband **Rachu**, who is guiding and inspiring me all the time. I cannot imagine my personal and professional life without his love, care and encouragement. Thank you rachi.

Last but not the least I thank all the people who directly or indirectly helped me during my PhD work.

Vielen Dank an alle für alle

# List of Figures

1.1	Schematic representation of a eukaryotic cell . . . . .	2
1.2	Nesprin-2 localization and its interaction partners in mammalian cells	5
1.3	Structural features of Nesprin-2 Giant . . . . .	8
1.4	Phases of wound healing . . . . .	10
2.1	Significance analysis of microarray (SAM) plot . . . . .	16
2.2	Classification of differentially regulated genes based on GOAT . . . . .	19
2.3	Macroscopic analysis of wound closure. . . . .	22
2.4	Measurement of distance between the migrating tips. . . . .	24
2.5	Comparison of macrophage population in WT Nesprin-2KO mice. . . . .	26
2.6	The expression of the inflammation related gene SAA3 is increased in Nesprin-2 KO wounds. . . . .	27
2.7	The expression of chemokine MCP1 (CCL2) in the wounds of WT and Nesprin-2 KO. . . . .	28
2.8	The keratinocyte migration pattern during wound healing process. . . . .	31
2.9	Observation of keratinocyte proliferation in the wounds. . . . .	33
2.10	Differentiation of fibroblasts into myofibroblasts during the wound healing process. . . . .	35
2.11	Study of F-actin in primary dermal fibroblasts. . . . .	37
2.12	Nesprin-2 Giant maintains actin fibers around the nucleus in primary fibroblasts. . . . .	39
2.13	F-actin distribution and localization in shRNA knock down HaCaT cells. . . . .	40
2.14	Sirius red staining showing the granulation tissue area. . . . .	41
2.15	Transcription factors are differentially regulated in Nesprin-2 KO wounds. . . . .	43
2.16	c-Fos localization at various stages of wound healing in Nesprin-2 KO and WT mice. . . . .	45
2.17	The localization and expression of c-Fos in knock down HaCaT cells. . . . .	48
2.18	c-Fos localization in control and Nesprin-2 KD HaCaT cells after scratching. . . . .	50
2.19	Apoptosis study in Nesprin-2 KO and WT fibroblasts. . . . .	52
2.20	Caspase-3 in WT and Nesprin-2 KO fibroblasts. . . . .	53
2.21	Scaffold attachment factor-B1 (SAFB1) in WT and Nesprin-2 KO fibroblasts. . . . .	55

2.22 Heterochromatin HP1 $\beta$ distribution in WT and Nesprin-2 KO fibroblasts. . . . .	58
3.1 Model for Nesprin-2 Giant function in wound healing . . . . .	70
4.1 Principle of microarray . . . . .	90
4.2 Overview of the research findings . . . . .	ii

# List of Tables

2.1	List of differentially regulated genes from microarray analysis . . . .	16
2.2	List of up-regulated inflammation related genes from microarray analysis . . . . .	26
2.3	Chip-assay data showing the presence of centromere sequences in the CHIP carried out with mAb K20-478 . . . . .	57
2.4	Quantification of the number of HP1 $\beta$ stained speckles. . . . .	58

# List of Abbreviations

$\alpha$ -SMA	alpha smooth muscle actin
ABD	actin binding domain
AD-EDMD	autosomal dominant EDMD
AO	acridine orange
AP1	activating protein 1
BAF	barrier to autointegration factor
BMP	bone morphogenic protein
BSA	bovine serum albumin
BTF	BCL2 the associated transcription factor
cDNA	complementary deoxynucleiacid
CH	calponin homology
ChIP	chromatin immunoprecipitation
DAPI	4',6-diamidino-2-phenylindole
DAW / D	days after wounding
DEPC	diethylpyrocarbonate
DMSO	dimethyl sulfoxide
DNA	deoxyribonucleic acid
DR	death receptor
DTT	1, 4-dithiothreitol
EB	ethidium bromide
ECL	enhanced chemiluminescence
EDMD	emery Dreifuss muscular dystrophy

EDTA	ethylenediaminetetraacetic acid
Egr-1	early growth response factor 1
EGTA	ethylene-glycol-bis(2-aminoethylether)-N, N, N, N-tetraessigsacid
EMR	EGF module containing mucin like hormone receptor
ER	endoplasmic reticulum
ERK	extracellular signal-regulated kinases
EtOH	ethanol
FasL	fas ligand
FBS	fetal bovine serum
FN	fibronectin
GCL	germ-cell-less
GO	gene Ontology
GOAT	gene Ontology Annotation Tool
GT	granulation tissue
H&E	haematoxylin and Eosin
HaCaT	human keratinocyte
HDL	high-density lipoprotein
HEPES	N-(2-hydroxyethyl)piperazine-N'-2-ethanesulphonic acid
HMW	high molecular weight marker
HP1 $\beta$	heterochromatin protein 1 beta
HRP	horse peroxidase
IF	intermediate filament
INM	inner nuclear membrane
IPTG	isopropyl $\beta$ -D-thiogalactopyranoside
K14	keratin 14
KASH	Klarsicht ANC-1 SYNE homology
KD	knock down

kDa	kilodalton
KO	knock out
LAP	lamina associated proteins
LINC	linker of nucleoplasm and cytoplasm
LMW	low molecular weight marker
MAPK	mitogen-activated protein kinase
MCP1	monocyte chemoattract protein 1
MEFs	mouse embryonic fibroblasts
MOPS	3-(N-morpholino)propanesulfonic acid
MTOC	microtubule organizing center
NE	nuclear envelope
NETs	nuclear envelope transmembrane proteins
NPC	nuclear pore complexes
OCT	optimum cutting temperature
ONM	outer nuclear membrane
PBG	Phosphate buffer with fish gelatin
PBS	Phosphate buffer solution
PC	Panniculus carnosus
PDGF	platelet-derived growth factor
PFA	paraformaldehyde
PKC	Ca <sup>2+</sup> induced protein kinase C
PMSF	phenylmethylsulphonylfluoride
PPAR $\beta/\delta$ ,	Peroxisome proliferator-activator receptor $\beta/\delta$ ,
q-PCR	Quantitative polymerase chain reaction
RNA	Ribonucleic acid
SAA3	Serum Amyloid A3
SAFB	Scaffold attachment factor-B

SAM	Significance analysis of microarray
SDS	sodium dodecylsulfate
TAFII68	TATA Element-binding Protein-associated Factor
TBP	TATA box binding protein
TEMED	Tetramethylethylenediamine
TGF	transforming growth factor
TRAIL	TNF-related apoptosis-inducing ligand
WT	Wild type

# 1 Introduction

## 1.1 Nucleus and Nuclear envelope

The eukaryotic cell is enclosed by a plasma membrane and contains several membrane-bound organelles with specific functions. The nucleus is the largest membrane bound organelle encompassing about 10% of the cell volume. It is sometimes referred to as the control centre of the cell as it harbors most of the genetic material of the cell in the form of chromosomes formed as a result of condensation of the DNA in complex with histone proteins (Figure 1.1). The nucleus is physically separated from the cytoplasm by a membrane barrier called nuclear envelope (NE). The NE is a double lipid bilayer forming an inner (INM) and outer nuclear (ONM) membrane the latter of which is continuous with the endoplasmic reticulum (ER). Nuclear pore complexes (NPC) consisting of approximately 30 different proteins called nucleoporins are inserted into the NE and serve as channels for the trafficking of proteins, RNA and ribonucleoprotein complexes between nucleoplasm and cytoplasm (Hetzer et al., 2005; Tran and Went, 2006; D'Angelo and Hetzer, 2008). Nuclear pore channels typically have a  $\sim 100$  nm outer diameter and  $\sim 40$  nm as central transport channel (Beck et al., 2004; Beck et al., 2007; Teryy et al., 2007). The nuclear membranes contain specific proteins, the nuclear envelope proteins. Furthermore, certain proteins are specifically localized either to the INM or ONM. Some well known proteins residing in the INM are Lamina associated proteins (LAP1, LAP2), Emerin, SUN domain

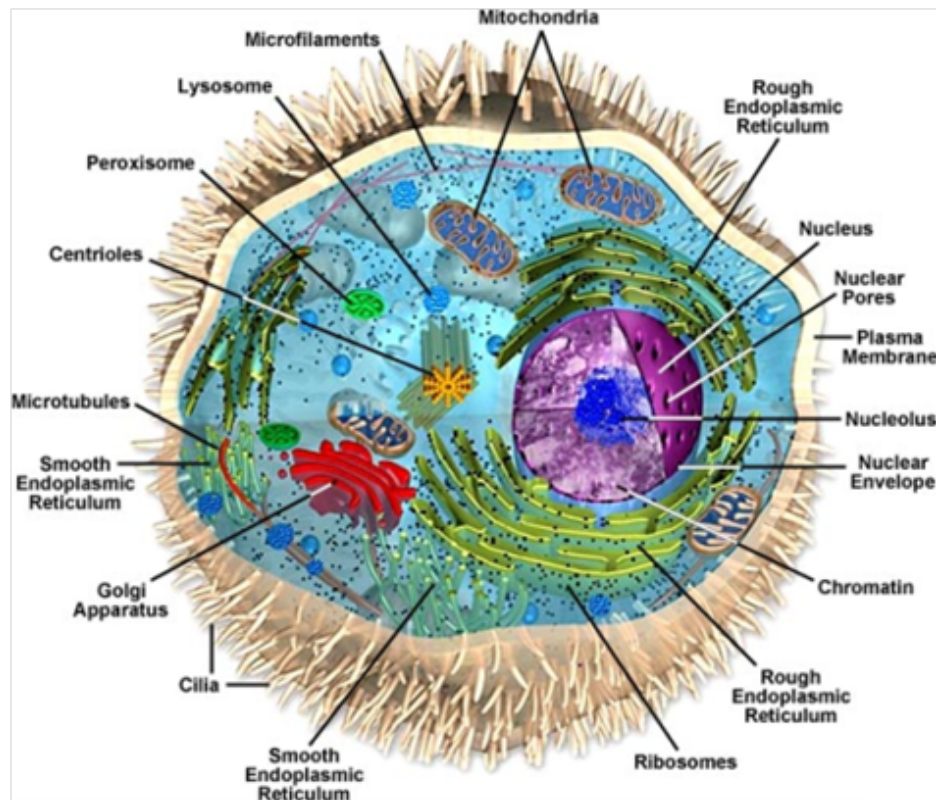


**Figure 1.1: Schematic representation of a eukaryotic cell.** Every cell is enclosed by a selectively permeable membrane called the plasma membrane. It contains ribosomes, centrioles, microtubules, microfilaments, and membrane bound organelles like the endoplasmic reticulum, Golgi apparatus, lysosomes, the nucleus and mitochondria. These organelles perform different functions within the cell. Figure adopted from Google image (Glogster beta).

containing proteins and MAN1 (Akhtar and Gasser, 2007; Dorner et al., 2007; Schirmer and Foisner, 2007) whereas Nesprin-1 and -2 are localized at the ONM and INM. INM specific proteins have important roles in gene expression, chromatin organization and DNA metabolism (Mattout et al., 2006; Heessen and Fornerod, 2007; Reddy et al., 2008), while ONM specific proteins are involved in nuclear positioning which is important for processes like cell polarization, pronuclear migration, and syncytia organization (Fridkin et al., 2009).

The inner nuclear membrane (INM) contains a subset of integral membrane proteins, termed nuclear envelope transmembrane proteins (NETs) (Schirmer et al., 2003). ONM and INM are separated by a luminal space of  $\sim 100$  nm in width

and are fused through NPCs. Beneath the INM towards the nucleoplasm the nuclear lamina is located, composed of type V intermediate filament (IF) proteins called lamins. The proteins of the lamina are A, C and B type Lamins (Fisher et al., 1986; McKeon et al., 1986). The nuclear lamina is thought to provide a frame work for organizing the NE structure and providing an anchoring site at the nuclear periphery for interphase chromatin (Gerace et al., 1978; Hancock et al., 1982; Lebkowski and Laemmli 1982). Mutations in lamina associated proteins lead to a variety of diseases known as Laminopathies, indicating the importance of the lamina in the development of different tissues.

## 1.2 Nesprins - their roles in human disease

Nesprins (Nuclear envelope spectrin repeat proteins) are ubiquitously expressed proteins. They contain an N-terminal F-actin binding domain (ABD), a long spectrin repeat containing region and a C-terminal transmembrane domain followed by a short region extending into the perinuclear space (KASH). Together with SUN domain containing proteins they form the LINC (**l**inker of **n**ucleoplasm and **c**ytoplasm) complex (Figure 1.2). Through alternative transcriptional initiation, termination and splicing, the two Nesprin genes *Syne1* (Nesprin-1) and *Syne2* (Nesprin-2) give rise to many isoforms, which vary markedly in size. The largest isoforms of Nesprins are Nesprin-1 Giant and Nesprin-2 Giant which are also called as ENAPTIN and NUANCE, respectively (Zhen et al., 2002; Padmakumar et al., 2004). Nesprin-1 (1.01 MDa) shares 46% sequence identity and 59% homology with the C-terminal region of Nesprin-2 (796 kDa) (Mislow et al., 2002). Nesprins have single giant orthologues in both *Drosophila* (MSP300) and *Caenorhabditis elegans* (ANC-1). MSP300 is a cytoskeleton protein that localizes to the Z-line in muscle and therefore mutation in MSP300 causes muscle defect (Zhang et al., 2002; Rosenberg-Hasson et al., 1996; Volk, 1992). The *C. elegans* protein ANC-1 is local-

ized in the ONM via its KLS/KASH domain (*klarsicht*/ANC-1 (anchorage 1)/SYNE homology). Its role in nuclear migration requires both the KLS/KASH domain and CH domain, which binds to F-actin (Starr and Han, 2002).

Nesprin-1 and Nesprin-2 interact with Lamin A/C of the nuclear lamina (Mislow et al., 2002; Libotte et al., 2005). Mutations in the Lamin A/C encoding gene LMNA resulted in a diverse range of clinical syndromes including partial lipodystrophy, Charcot-Marie-Tooth type 2 (CMT2) neuropathy, Hutchinson-Gilford progeria, an autosomal-dominant form of Emery-Dreifuss muscular dystrophy (EDMD) and many more, which are collectively referred to as Laminopathies (Broers et al., 2004; Burke et al., 2001; Gruenbaum et al., 2005; Lloyd et al., 2002).

A mutation in Nesprin-1 and Nesprin-2 can cause human diseases which are similar to Laminopathies. Patients with the R374H missense mutation in Nesprin-1 $\alpha$  developed dilated cardiomyopathy. Mice lacking the C-terminal KASH domain showed lethality with approximately half of the animals dying at or near birth from respiratory failure and surviving mice exhibited an EDMD like phenotype (Puckelwartz et al., 2009; 2010). Fibroblasts from patients with EDMD disease showed a disturbance of the Nesprin/Lamin/Emerin interaction. In Nesprin-2 KO fibroblasts Emerin failed to distribute properly along the NE and often formed aggregates in the deformed NE areas. This indicates the involvement of Nesprin-1 and Nesprin-2 in the pathogenesis of EDMD, which was earlier considered as a consequence of mutations in Emerin and Lamin A/C (Lüke et al., 2008; Wheeler et al., 2007; Zhang et al., 2007). Disruption of the endogenous LINC complex leads to mechanical stiffness, which is similar to the phenotype caused by a lack of LaminA/C (Hutchinson et al., 2008). Nesprin-2 knockout (KO) primary dermal fibroblasts and keratinocytes exhibit heavily misshapen nuclei displaying a significant similarity to nuclear deformations of Laminopathies. Furthermore Nesprin-2 was shown to act as a structural reinforcer at the NE by safeguarding its architecture in LMNA mutant (S143F) progeria cells (Lüke et al., 2008; Kandert et al., 2007).

These studies showed the possible involvement of Nesprins in diseases.

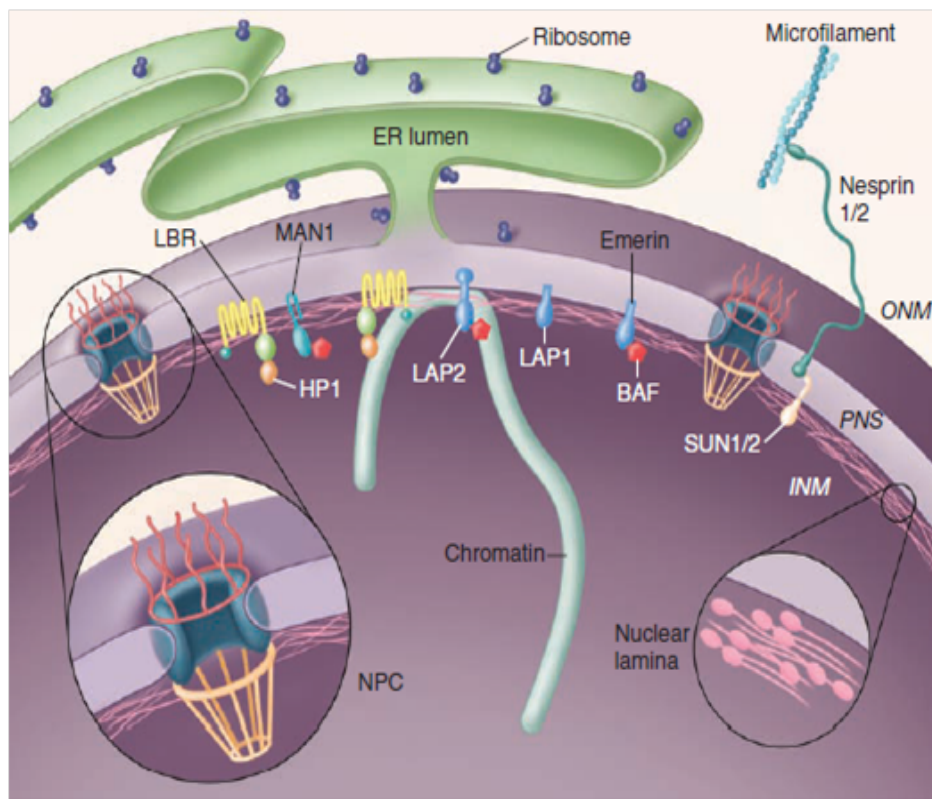


**Figure 1.2: Nesprin-2 localization and its interaction partners in mammalian cells.** Nesprins-2 present at the ONM binds to SUN domain containing proteins through which it connects with the nuclear lamina. Short isoforms of Nesprin-2 have been found in the nucleoplasm. At the cytoplasmic face of the nucleus, Nesprin-2 binds to actin filaments and acts as a Linker of nucleoplasm and cytoplasm (LINC) (Stewart et al.,2007).

### 1.2.1 Structural composition, binding partners and role of Nesprin-2 at the nuclear envelope

Nesprin-2 at the ONM connects the nucleoplasm with the cytoplasm. To execute this function it uses its C-terminal KASH domain and N-terminal actin binding domain (ABD). Nesprin-2 giant, the largest Nesprin-2 isoform, has a molecular weight of 796 kDa, its short C-terminal isoforms are ranging from 48 to 377 kDa. A Nesprin-2 Giant knock out (Nesprin-2  $\Delta$ ABD) mouse was generated by deleting

the calponin homology (CH1) domain 1 which together with the CH2 domain forms the functional ABD (Gimona et al., 2002; Figure 1.3). Sun proteins are highly conserved proteins present in yeast, *Dictyostelium* and *C. elegans* and human. They are essential components of the LINC complex. The mechanisms that keep Sun proteins at the NE vary. For example, UNC84 in *C. elegans* and mammalian Sun-2 require Lamin binding, whereas the Sun-1 association with the NE is Lamin independent (Lee et al., 2002; Padmakumar et al., 2005; Haque et al., 2010). For the *Dictyostelium* homolog a chromatin association is responsible for targeting Sun-1 to the INM (Xiong et al., 2008). Interactions with chromatin or chromatin associated proteins are also known for further NE proteins such as Lamin A/C or Emerin, which can affect gene expression (Heesen and Fornerod, 2007). For Lamin A, a direct interaction with transcription factor c-Fos was reported, whereas the lamina-associated protein 2 $\alpha$  (LAP2 $\alpha$ ) is involved in Retinoblastoma protein (Rb) activity (Dörner et al., 2006). LAP2 $\beta$  acts more indirectly and represses transcription through interaction with HDAC3 followed by histone deacetylation (Somech et al., 2005). Overall, the role of the NE in several of these processes may be one in which transcription factors are sequestered to the NE and by providing a surrounding, which may be inhibiting or activating gene expression (Towbin et al., 2009).

Previous data from Nesprin-2 knock out (KO) studies have shown that Nesprin-2 is an important scaffold protein in the maintenance of nuclear envelope architecture. The loss of Nesprin-2 in dermal fibroblasts and keratinocytes showed misshapen and blebbing nuclei and an increase in the size of the nuclei causing the thickening of the epidermis and indicating its key role in the maintenance of nuclear morphology. Loss of Nesprin-2 Giant also showed a requirement for Nesprin-2 in the migration of dermal fibroblasts as the KO fibroblasts exhibited a significantly lower migration speed compared to wild type cells after 20 hours of cells scratching. They exhibited also a defective cell polarity with respect to the Golgi complex and

microtubule organising center at the wound edge (Lüke et al., 2008). The role of Nesprin-2 Giant in other cell types of the skin tissue is not clear. Therefore we carried out experiments to analyse other cell types in the Nesprin-2 KO and test whether they are also impaired in migration. We conducted an in vivo wound healing assay and showed that Nesprin-2 is required for keratinocyte proliferation and differentiation and ultimately for healing of the wound.

Nesprin-2 Giant carries a F-actin binding site which was previously shown to be functional in vitro (Zhen et al., 2002). F-actin structures are involved in many cellular processes, including cell adhesion, migration and division. Reorganisation of the F-actin cytoskeleton is critical for different steps of cell migration, including those essential for cell protrusion, adhesion and shape change (Stricker et al., 2010). These studies have clear indication of potential role of F-actin during the wound healing process. During my PhD work, I also studied the F-actin cytoskeleton in Nesprin-2 KO fibroblast.

In general, the giant isoform of Nesprin-2 is thought to localize at the ONM whereas the shorter isoform Nesprin-2 $\alpha$  can enter the INM by diffusion through the nuclear pores (Worman and Gundersen, 2006). However, there are also reports, that Nesprin-2 Giant is present in the INM (Zhen et al., 2002; Libotte et al., 2005). The functional relevance of Nesprin-2 Giant localization in the INM has not been studied so far. Here I propose that Nesprin-2 Giant is associated with chromatin thereby regulating the transcription of genes involved in the wound healing process. I made an attempt to study the transcriptional regulation of genes related to wound healing by Nesprin-2 Giant using the corresponding knock out mice.

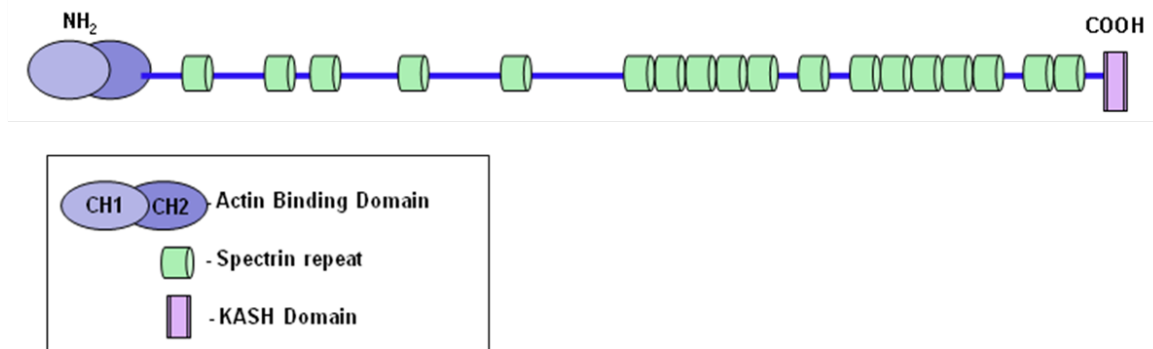


**Figure 1.3: Structural features of Nesprin-2 Giant .** Nesprin-2 Giant is composed of an N-terminal actin binding domain which is formed by two Calponin Homology domains, CH1 and CH2, followed by several spectrin. Not all of the 56 predicted spectrin repeats are indicated. At its C-terminal end it consists of the highly conserved KASH (**K**larsicht, **A**NC-1, **S**yne **H**omology) domain. This KASH domain anchors the protein at the NE (modified from Lüke et al., 2008).

## 1.3 Cell migration and wound healing

The process of healing is an immediate response to tissue injury, which involves different overlapping phases. During this process several cell types will become activated and act to heal the wound.

### 1.3.1 Phases of wound healing

The process of wound healing normally proceeds from coagulation and inflammation through fibroplasia, matrix deposition, angiogenesis, epithelialisation, collagen maturation and finally wound contraction. These processes are divided into three different but overlapping phases, namely the inflammatory phase, new tissue formation phase and finally tissue remodelling phase (Schäfer and Werner, 2008).

### **A. Inflammatory phase**

Following tissue injury, a wound must stop bleeding in order to heal and for the injured host to survive. Therefore cellular and molecular elements involved in haemostasis also signal tissue repair. Immediately after wounding or tissue damage the platelets activated by thrombin release insulin like growth factor  $\alpha$  (IGF- $\alpha$ ), transforming growth factor  $\beta$  (TGF- $\beta$ ) and platelet-derived growth factor (PDGF) which attract leukocytes, mainly macrophages and fibroblasts into the wound area. In response to tissue damage as a defence mechanism many inflammatory cells are activated and attracted to wound area. Among the inflammatory cells neutrophils enter first followed by mast cells and monocytes, which will subsequently differentiate into macrophages. Macrophages play a dominant role in the synthesis of wound healing molecules as coagulation-mediated tissue repair signals fall (Franz, 2009). Neutrophils and macrophages are essential for defence against invading bacteria through their phagocytic function and through their capacity to secrete toxic mediators. Macrophages and monocyte are the source for chemo attractants which are required for the late phase of the wound healing (Figure 1.4 A).

### **B. New tissue formation phase**

The new tissue formation phase is characterised by cellular proliferation and migration of different cell types. This begins with migration of keratinocytes from the epidermis at the wound edge and from injured appendages. Keratinocytes at the leading edge alter the expression of integrin receptors to allow attachment to new substrates and they express various proteases to allow the degradation of connective tissue (Martin, 1997). These keratinocytes migrate forward between fibrin and the dermis. The migration of keratinocytes is followed by their hyperproliferation. In the later part of this phase, fibroblasts, which are attracted from the wound edge or from the bone marrow, are stimulated by macrophages.

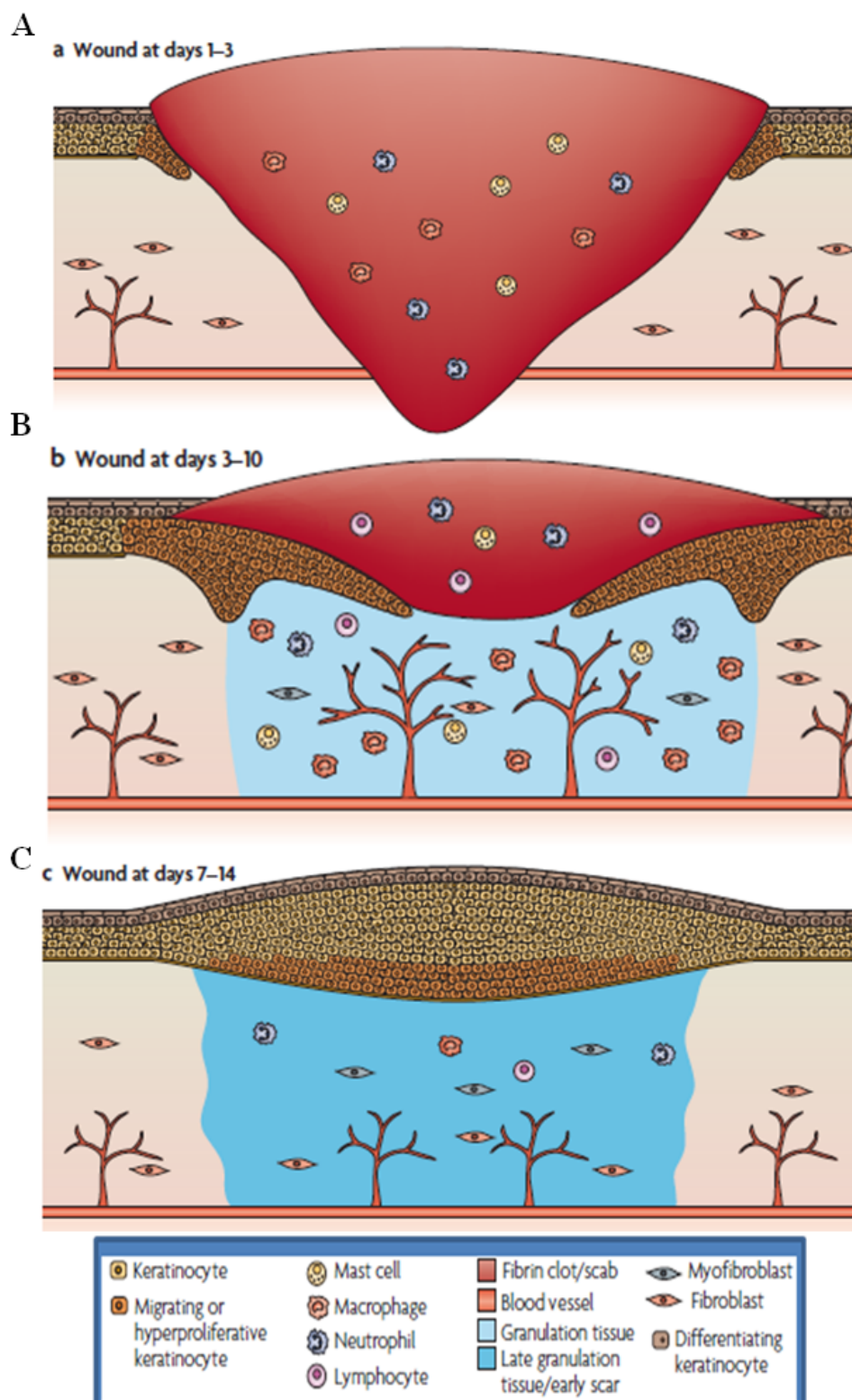


**Figure 1.4: Phases of wound healing.** In vivo wound healing occurs in three overlapping phases - (A) Inflammatory phase (B) New tissue formation phase and (C) Tissue remodelling phase (taken from Schäfer and Werner, 2008). (for a detailed description please see text).

Fibroblasts also migrate, proliferate and deposit extracellular matrix and some differentiate into myofibroblasts (Schäfer and Werner, 2008). Myofibroblasts are specialized contractile fibroblasts that play a critical role in generating the contractile force responsible for wound closure and pathological contractures (Tomasek et al., 2002; Hinz et al., 2003). They are characterized by the acquisition of a contractile phenotype and the expression of  $\alpha$ -smooth muscle actin ( $\alpha$ -SMA) (Skalli et al., 1986; Desmouliere et al., 1993), which correlates with the generation of contractile force (Hinz et al., 2001; Hinz et al., 2002). An understanding of the regulation of expression of  $\alpha$ -SMA in myofibroblasts will be important in controlling the formation and function of myofibroblasts in wound healing and pathological contractures (Figure 1.4 B).

### **C. Tissue remodeling phase**

During this phase wound re-epithelialization is complete and extracellular matrix is remodeled. Formation of the new blood vessels is essential for the supply of oxygen and nutrients. During this phase all of the processes initiated after tissue damage wind down and cease. Most of the endothelial cells, macrophages and myofibroblasts undergo apoptosis or exit from the wound area. Then matrix metalloproteases that are secreted by fibroblasts, macrophages and endothelial cells, help in strengthening the repaired tissue (Lovvorn et al., 1999). The remodeled extracellular matrix will result in scar formation. At this phase the wound will not have any appendages (Schäfer and Werner, 2008) (Figure 1.4 C).

## 1.4 Role of nuclear envelope proteins in transcription regulation and cell proliferation

The INM proteins engage in direct chromatin-independent interaction with transcription factors and the sequestering of transcription factors to the INM (Heessen and Fornerod, 2007). One important example which has been studied in detail with respect to sequestration of transcription factors to the NE is c-Fos by Lamin A/C. c-Fos together with c-Jun forms the activating protein 1 (AP1), which plays a role in several cellular processes including cell proliferation and differentiation. Lamin A/C is known to regulate the process of cell proliferation by sequestering c-Fos to the NE (Ivorra et al., 2006). The process of cell proliferation was shown to be enhanced in the absence of Lamin A/C. In human fibroblasts the expression of lamina-associated polypeptide 2  $\alpha$  (LAP2  $\alpha$ ) upon entry and exit from G0 is tightly correlated with phosphorylation and subnuclear localization of the retinoblastoma protein (Rb) (Pekovic et al., 2007). It is not only LaminA/C but also other NE proteins which are participating in the regulation of transcription factor and thereby in the process of cell proliferation.

Nearly 15 INM proteins were characterized in mammalian cells so far (Dreger et al., 2003). Among them is MAN1 which is an integral INM protein consisting of a LEM domain, two transmembrane domains at its N-terminus, and a RNA recognition motif at the C-terminus. Several groups showed an interaction of MAN1 and Smad transcription factors. Smads are crucial regulators of transforming growth factor- $\beta$  (TGF- $\beta$ ), bone morphogenic protein (BMP) and activin signalling. MAN1 acts as a nuclear scavenger, sequestering R-Smads that illegitimately enter the nucleus (Ishimura et al., 2006). MAN1 also interacts with several other transcriptional regulators including the transcription factor germ-cell-less (GCL), the BCL2 associated transcription factor (BTF) and the barrier to autointegration

factor (BAF) (Mansharamani and Wilson, 2005). The INM proteins Emerin and LAP2 $\beta$  were also found to associate with several transcription regulators. Furthermore, Lamin A/C as an important member of the nuclear lamina plays a crucial role in several cellular processes. Kandert et al., (2009) showed that LMNA mutation R545C impairs both the proliferation and differentiation capacities of myoblasts as part of the pathogenesis of AD-EDMD (Autosomal Dominant EDMD). Mutation in Lamin A/C negatively acts on the interaction between Emerin and LaminA/C, and skin fibroblasts carrying this mutation exhibited enhanced cell proliferation, collagen-dependent adhesion, larger number of filopodia and smaller cell spread size compared to control cells. Cell migration, speed and polarization were elevated in these cells too. The functional interaction between Emerin and Lamin A/C acts on cell spreading and proliferation through the ERK1/2 signalling pathway (Emerson et al., 2009). LaminA/C is involved in cellular processes under mechanical stress situation and affects cellular plasticity. Mouse embryonic fibroblasts (MEFs) deficient in Lamin A/C showed weak cytoplasmic mechanics. These MEFs also showed slower migration to cover the scratched area and the microtubule organizing center (MTOC) was localized away from the scratched area. In wild type cells they are present in the direction of the scratched area showing the importance of LaminA/C in the generation of cell polarity. The distance between MTOC and the nucleus was higher in Lamin A/C deficient cells as compared to wild type cells (Lee et al., 2007).

## **1.5 Aim of the research**

Loss of Nesprin-2 Giant resulted in a thickening of the epidermis as a consequence of increased epithelial nuclear size; emerin localization was altered and showed increased cytoplasmic staining; primary dermal knockout fibroblast and keratinocyte nuclei were heavily misshapen displaying a striking similarity to the nuclear defor-

mations characteristic for laminopathies. In vitro wound healing was impaired in mutant fibroblasts, furthermore, fibroblasts showed a polarization defect (Lüke et al., 2008). Studies by other groups revealed that mutations in the human Nesprin-1 or -2 genes can cause disease states that until now were considered to be a consequence of mutations in Lamin or in Emerin (Zhang et al., 2007). The mechanisms of disease involvement are however unclear. Similarly, a role of other NE proteins namely Lamin A/C, Emerin and SUN1 and SUN2 in cell migration and polarity was shown earlier (Lee et al., 2008). However the role of any of these proteins including Nesprin-2 during in vivo cell migration and tissue repair is not known so far. The first aim our of research is

- To reveal the role of Nesprin-2 in cell proliferation and differentiation during in vivo wound healing.

Based on its presence at the NE and its involvement in regulating nuclear shape, Nesprin-2 has the potential to be involved in regulation of gene expression.

- The next aim of our research is to study the role of Nesprin-2 in regulating the expression of genes which are involved in cell proliferation,
- To study the role of Nesprin-2 in chromatin association,
- To study the role of Nesprin-2 in regulating gene transcription using microarray analysis.

## 2 Results

### 2.1 Transcriptional profiling in Nesprin-2 knockout fibroblasts

A cDNA microarray analysis was carried out to study transcriptional changes in Nesprin-2 knockout fibroblasts. For this RNA from WT and Nesprin-2 KO dermal fibroblasts were isolated and synthesis and labelling of cDNA was done as described in Materials and Methods (Target preparation). For the microarray analysis a total of 6 slides with 3 different samples each from WT and Nesprin-2 KO were used for hybridization and scanning. The normalised data were imported to SAM (Significant Analysis of Microarray), which not only identifies the differentially regulated genes, but also predicts the number of false positives ( Figure 2.1). Without additional threshold SAM reported 57 genes as differentially regulated, of which 45 were up-regulated and 12 down-regulated (Table 2.1).

The list of differentially regulated genes was classified using the Gene Ontology Annotation Tool (GOAT). This tool classifies the genes based on their biological processes, the molecular functions in which they participate, and the cellular locations in which they are active (Figure 2.2 A-C). The left panel shows the enrichment ratio and hierarchy. The values in the right panel indicates information about those GO (Gene Ontology) node. The values in the **List** indicate number of genes in the target gene list which were found significantly regulated due the treatment (in my case due to knock out of Nesprin-2). The values in the **Total** indicate number

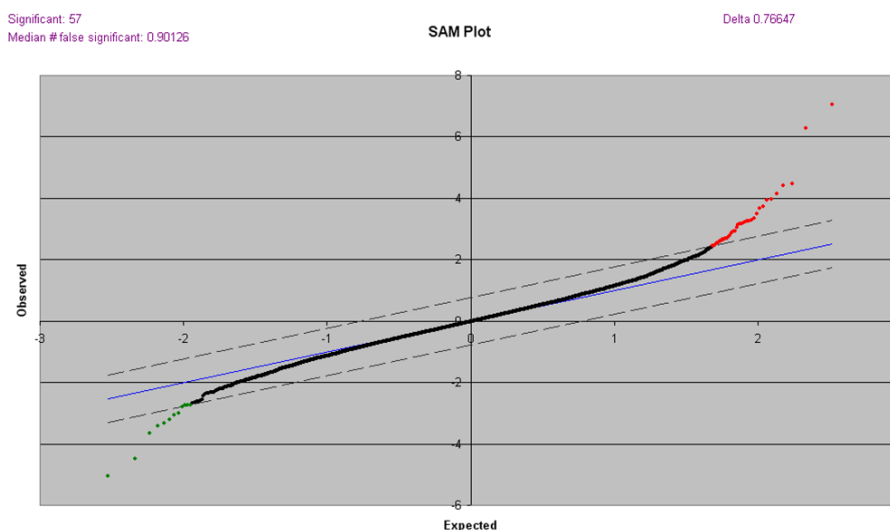


**Figure 2.1: Significance analysis of microarray (SAM) plot.** SAM identifies statistically significant genes by carrying out gene specific t-tests. This will adjust the threshold of number of genes which are referred as significant and estimates False Discovery Rate for multiple testing.

of genes in the reference gene list means number of genes in the mouse genome sequence. The multiple-testing corrected p-value (p-value) and the GO term (Annotation). For example from Figure 2.2 A among total of 742 genes which belongs to the category (Annotation) response to stress, there were 5 genes found significantly regulated with  $p = 0.01$ .

**Table 2.1: List of differentially regulated genes from microarray analysis**

GENE NAME	UP REGULATED GENES	FOLD CHANGE
AK010675	SAA 3	1.841
X67799	Clone C1-2H(DNAfor Eg variable region-heavy chain)	1.622
L07051	Aggrecan	1.612
NM_009141	chemokine (C-X-Cmotif)ligand 5	1.293
AF087578	antisense product of high-affinity glutamate transporter EAAC1 and EAAC2 (ASEC1)	1.259
NM_024183	FIP 1 like 1(S.cerevisiae)	1.222
BC006914	rogdi homolog -Drosophila	1.281

<b>GENE NAME</b>	<b>UP REGULATED GENES</b>	<b>FOLD CHANGE</b>
AK004319	ELOVL family member 5,elongation of long chain fatty acid-Yeast	1.247
NM_009640	angiopoietin 1(Angpt 1)	1.358
NM_011333	chemokine (C-C motif) ligand 2	1.268
AK009960	RIKEN Cdna	1.304
AK007604	RIKEN cDNA 1810026B05	1.425
AK015050	RIKEN cDNA 4930402H24	1.349
AK003208	Impad 1 inositol monophosphatase domain containing 1	1.269
BC011531	expressed sequence AI447318 and RNA binding motif protein 26	1.64
AK014710	RIKEN cDNA 4833416J08 gene	1.241
NM_009315	TAF6 RNA polymerase II,TATA box binding protein(TBP)associated factor	1.215
NM_017367	cyclin(Ccni)	1.272
AK017327	Mus musculus 6 days neonate head cDNA, RIKEN full-length enriched library	1.221
AK005760	sperm acrosome associated 4(Spaca 4)	1.273
U96635	neural precursor cell expressed,developmentally down regulated gene 4(Nedd4)	1.271
AK006699	RIKEN cDNA 1700045 I 11 gene	1.391
M25572	Mouse Ig active H-chain mRNA,V-region,subgroup IIC,clone L10	1.26
AK008226	adult male small intestine cDNA, RIKEN full-length enriched library SIMILAR TO 5' NUCLEOTIDASE, MITOCHONDRIAL homolog [Mus musculus], full insert sequence	1.171
U43512	dystroglycan(Dag1)	1.234
AK008096	adult male small intestine cDNA, RIKEN2010004I09 product:similar to CYTOCHROME C OXIDASE ASSEMBLY PROTEIN COX11,MITOCHONDRIAL PRECURSOR [Homo sapiens],	1.194
NM_013884	chondroitin sulfate proteoglycan 5 (Cspg5)	1.191
BC002235	tetratricopeptide repeat domain 15	1.164

<b>GENE NAME</b>	<b>UP REGULATED GENES</b>	<b>FOLD CHANGE</b>
NM_007743	collagen,type 1,alpha 2	1.26
AK014179	platelet endothelial aggregation receptor 1	1.243
NM_016892	copper chaperone for superoxide dismutase (Ccs),	1.126
NM_011330	small chemokine (C-C motif) ligand 11 (Ccl11),	1.307
AK013752	adult male hippocampus cDNA, RIKEN2900064P18	1.24
NM_016906	Sec61 alpha 1 subunits (S.cerevisiae)	1.181
NM_007833	decorin(Dcn)	1.229
NM_008524	lumican (Lum)	1.142
NM_011341	stromal cell derived factor 4	1.202
AK021285	RIKEN cDNA D330022H12 gene	1.233
AK008001	RIKEN cDNA 2010109N18	1.196
NM_008422	potassium voltage gated channel,shaw-related sub- family,member3 (Kcnc3)	1.118
NM_024198	glutathione peroxidase 7 (Gpx7)	1.159
AK016999	RIKEN cDNA 4933430M04	1.148
AK007533	motile sperm domain containing 1	1.26
NM_013591	mucosal vascular addressin cell adhesion molecule 1(Madcam1)	1.179
AK004919	adult male liver cDNA,RIKEN clone:1300006N24	1.373
<b>GENE NAME</b>	<b>DOWN REGULATED GENES</b>	<b>FOLD CHANGE</b>
NM_026423	RIKEN cDNA 2410018C20	0.760
M16356	major urinary protein 2(Mup2)	0.813
AK018008	Rap guanine nucleotide exchange factor 2(Rapgef2)	0.840
Z25851	immunoglobulin kappa chain variable region	0.784
AK020567	RIKEN cDNA9530022L04	0.821
AK020454	RIKEN cDNA 9430032L10	0.771
AK016502	RIKEN cDNA 4931433A01	0.813
M55561	phosphatidylinositol-linked antigen(pB7) (Cd52)	0.803
L10894	guanylate cyclase activator 2b (Guca2b)	0.809
NM_010425	forkhead box D3	0.833
AK017960	RIKEN cDNA 5830431M20 gene	0.804
NM_007561	bone morphogenin protein receptor, type II (ser- ine/threonine)( Bmpr2)	0.845

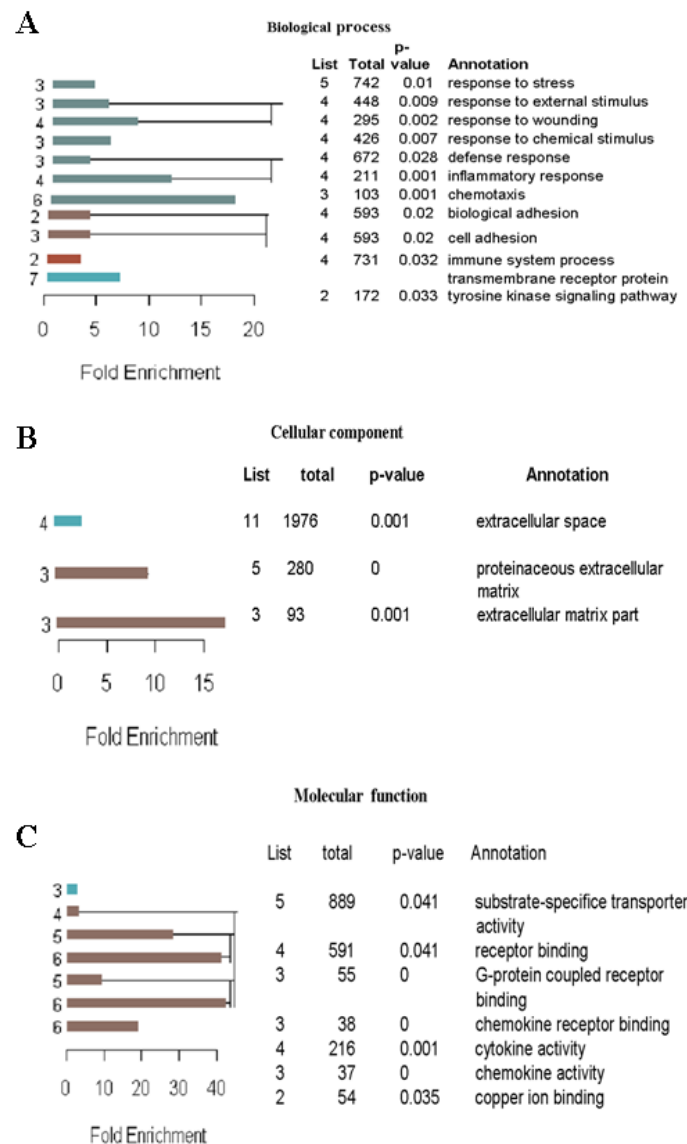


**Figure 2.2: Classification of differentially regulated genes based on GOAT.** Differentially regulated genes were classified based on GOAT as (A) Biological process, based on their involvement in different processes, (B) Cellular components, based on their locations and these genes were classified based on their role in different molecular process in Molecular function (C). In A-C the left panel shows the enrichment ratio and hierarchy. The numbers on the left of the bars are GO (Gene Ontology) node levels. The right panel shows information about those GO nodes: number of gene in the target gene list (list), number of genes in the reference gene list (total), the multiple-testing corrected p-value (p-value) and the GO term (Annotation).

## **2.2 In vivo wound healing study in Nesprin-2 knock out mice**

### **2.2.1 Macroscopic observation showed a delay in wound healing in Nesprin-2 KO mice as compared to wild type**

In vivo wound healing is a complex process involving three main overlapping phases. When tissues get damaged there will be an immediate response to the damage by flowing of blood as there will be damage of blood vessels. Immediately after the blood flow blood coagulates and at the cellular level inflammatory cells are activated and act on the wound area as a defence mechanism against bacteria. These cells act during the initial phase of wound healing which is called the inflammatory phase followed by the new tissue formation and tissue remodeling phase. We studied the process of wound healing and analysed the different phases in detail.

At first a macroscopic analysis was carried out by taking photographs of all wounds from day 0 until day 10. Each mouse carries four circular wounds on its dorsal side. From each mouse two wounds were considered for macroscopic observation. The open area of the wound was measured using Image J. From the open wound area the percentage (%) of wound closure was calculated by taking the wound area of zero day as 100% (Figure 2.3 A). At 1day after wounding (1DAW or 1D ), Nesprin-2 KO mice showed 60% of wound closing as compared to WT wounds which showed 50% of wound closing. At 3DAW Nesprin-2 KO mice showed 68% of wound closing while WT mice showed 62% of wound closure. The faster closing of the wound in Nesprin-2 KO mice continued until 5DAW. At 5DAW Nesprin-2 KO wounds were healed by nearly 71% leaving 29% of open wound area as against 67% closure of wound area in WT mice. Although the wound healing was faster in Nesprin-2 KO mice than in WT mice at 1, 3 and 5 DAW the difference in the recovery rate was not significant as reflected by the t-test with p values of 0.064, 0.176 and

0.061 respectively (Figure 2.3 B). We conclude that the wound healing process is accelerated in Nesprin-2 KO mice during the inflammatory phase which normally takes place between 1 to 5 DAW as compared to WT.

However at later stages from 7 to 10DAW the process of wound healing is faster in WT compared to KO. In KO mice 86 % of the wound was healed with 14% of open wound area whereas WT wounds were healed by almost 88% with 12% of open wound area. Similarly at 10DAW, the KO wounds are delayed in closing the wounds where they showed 92% wound closure in comparison to KO wounds that closed to an extent of 95%. The fast rate of wound healing in WT mice compared to KO mice at 7 and 10DAW was statistically significant ( $p= 0.038$  and  $p=0.013$  respectively) (Figure 2.3 B). This indicates that, although not significant, the wound healing process is faster in Nesprin-2 KO mice as compared to WT at the inflammatory phase (1-5DAW), but this trend is reversed during later phases from 7-10DAW when the new tissue formation and tissue remodeling phase has started and thereby leading to a significantly faster recovery in WT compared to the KO. This observation showed that Nesprin-2 absence from the mouse skin affects the in vivo wound healing process when compared to WT mice skin. The delay in the wound healing process was further confirmed and factors that might be responsible for this delay were studied.

### **2.2.2 The distance between the epidermal tips is altered in Nesprin- 2 KO wounds**

The process of wound healing in WT and Nesprin-2 KO mice which was observed macroscopically was confirmed by measuring the distance between the migrating epidermal tips. The wound samples were collected at the indicated time points (1, 3, 5, 7 and 10DAW). Among four circular wounds two wounds were used for sectioning (paraffin and cryo sectioning) and the remaining two wounds were stored at  $-80^{\circ}\text{C}$  for RNA and protein isolation. For further analysis the circular

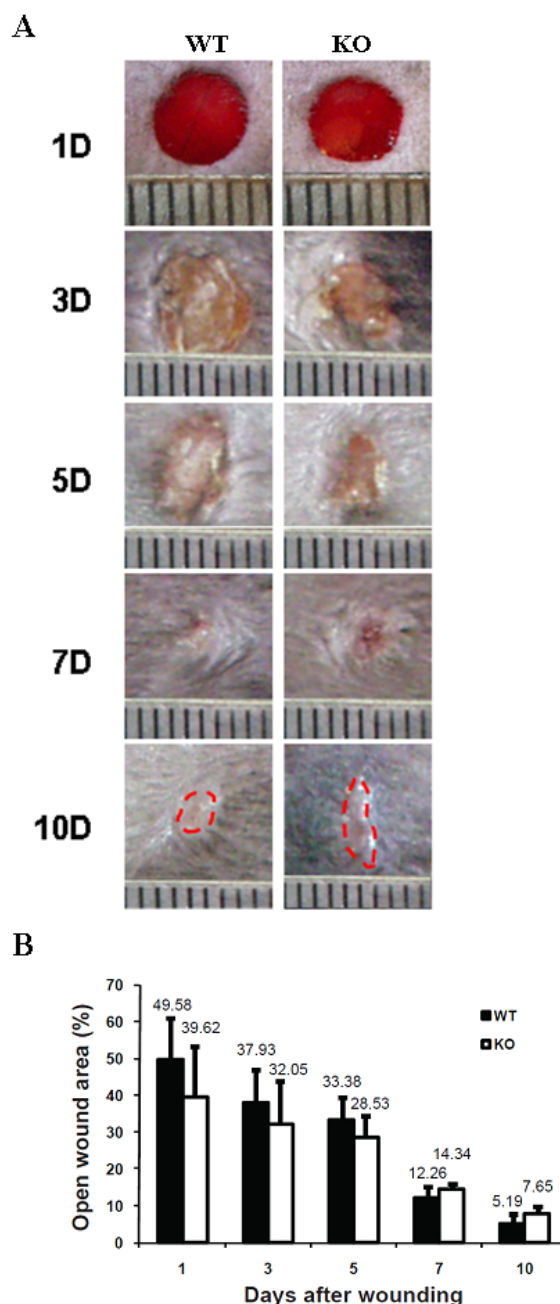


**Figure 2.3: Wound closure is changed in Nesprin-2 Giant knockout mice as macroscopically analysed.** (A) Four circular wounds were made on the dorsal side of WT and Nesprin-2 KO mice. Wounds were photographed at regular time intervals-1, 3, 5, 7 and 10 days after wounding (DAW). The red dotted line indicates the wound area left open at day 10. (B) The wound area was measured and the percentage (%) of open wound area calculated. At each time point wounds (2 wounds / mouse) from six WT and KO mice each were analysed. Graph showing the wound healing in WT and Nesprin-2 KO mice. \* $p=0.038$  (7DAW) and  $0.013$  (10DAW).

wounds were harvested together with some skin around the wound. Then the wounds were cut caudocranially (tail to head or head to tail) and fixed in paraffin blocks (Figure 2.4 A). The paraffin block, which contained skin tissue was sectioned with section size of 6 $\mu$ m. The sections were further used for staining with H&E (Haematoxylin and Eosin) and also with antibodies. The H&E stained sections were used for measuring the distance between the migrating epidermal tips. The distance between the epidermal tips gives the diameter of the wound (mm) (Figure 2.4 B black arrows). Again the wounds from all the time points were used for measuring the distance between the epidermal tips. This measurement was consistent with and supported the macroscopic observation. At 1DAW Nesprin-2 KO and WT wounds showed almost the same distance between the migrating epidermal tips (4.94 mm and 5.02 mm, respectively). This trend continued further at 3 and 5DAW. The distance for Nesprin-2 KO and WT mice was 4.87 mm and 4.98 mm, respectively, at 3DAW and 3.60 mm and 3.91 mm, respectively, at 5DAW. Nesprin-2 KO wounds showed a reduced distance between the epidermal tips (diameter of the wound) as was the case with macroscopic observations suggesting that these KO wounds showed a faster healing as compared to WT at the inflammatory phase from 1 to 5DAW, but this difference was statistically not significant ( $p= 0.62, 0.73$  and  $0.41$  for 1, 3 and 5DAW, respectively). Then the healing process was accelerated in WT from 7DAW onward as determined by the decreased distance between the migrating epidermal tips in these wounds compared to Nesprin-2 KO wounds. At 7DAW Nesprin-2 KO mice showed a value of 2.7 mm as the distance between the epidermal tips which was significantly different from the 2.55 mm in WT ( $p= 0.04$ ). At 10DAW the wound healing process continued to be faster in the WT mice and 2.08 mm were measured as compared to 2.55 mm in the KO mouse ( $p= 0.0092$ ) (Figure 2.4 C). This pattern of wound healing agreed with our macroscopic observations.

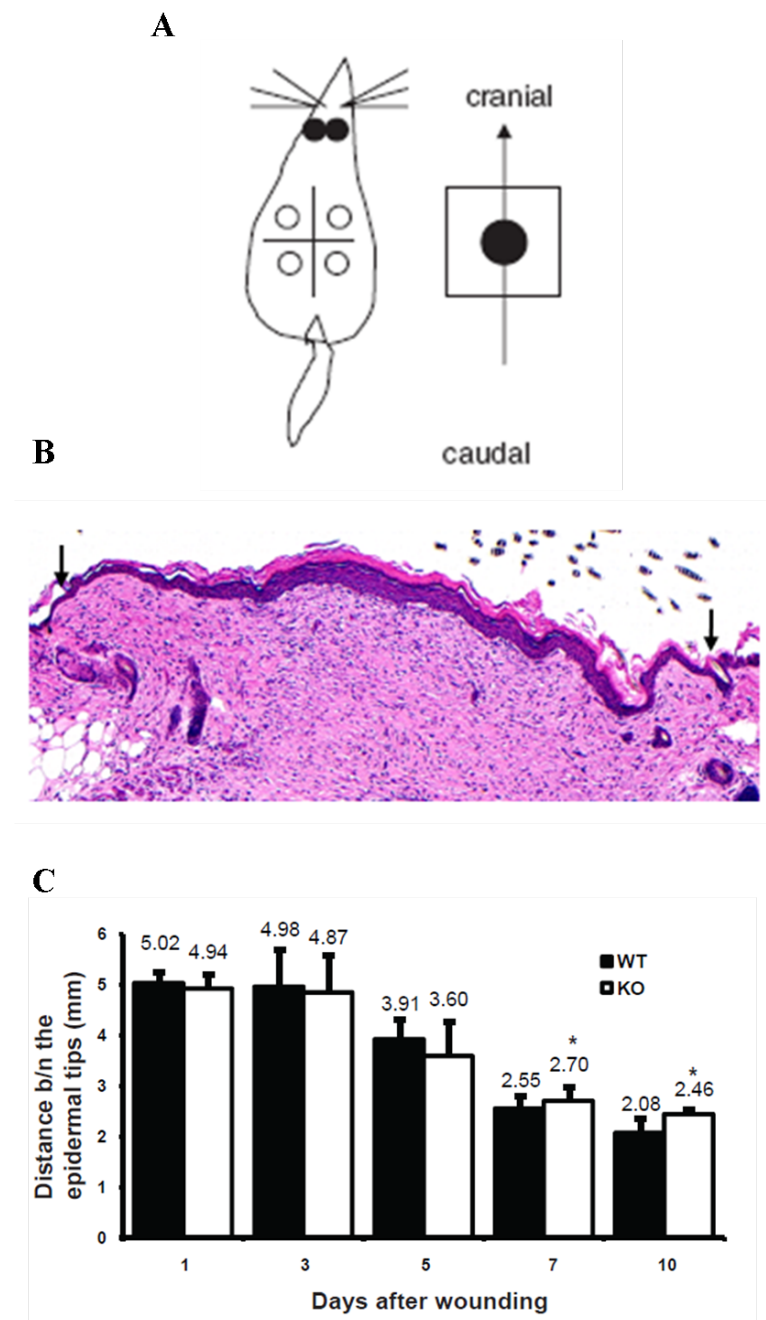


**Figure 2.4: The distance between the two migrating epidermal tips showed a reduced healing in wounds from Nesprin-2 KO from 7 DAW to 10DAW compared to WT wounds.** (A) Four circular wounds were made on the dorsal side of the mice and the entire wound harvested along with surrounding normal skin. Then this skin is cut caudo cranially and fixed in paraffin blocks (Figure from Gerharz et al., 2006).(B) Skin sections from WT and KO were stained with H & E and the distance between the migrating epidermal tips (black arrows) from day 1 to day 10 was measured using the Diskus programme (n= 3-5 sections per wound).(C) At day 7 and 10 the distance between epidermal tips of WT and KO is significantly different (\*  $p=0.044$  and  $p=0.0092$ , respectively; student's t-test).

### 2.2.3 Inflammatory phase

#### **Higher influx of macrophages into the wound area causes faster wound healing in Nesprin-2 KO during the early phase.**

To study the earliest phase of the wound healing process, inflammatory phase wound sections from Nesprin-2 KO and WT were stained with the macrophage specific antigen F4/80 (Eming et al., 2007). The F4/80 monoclonal antibody has been used widely to identify and study macrophages in the mouse under normal and pathological conditions. The F4/80 antigen is a 160 kDa cell surface glycoprotein that is a member of the EGF 7 transmembrane (7TM) protein family of proteins which shares 68% overall amino acid identity with the human EGF module containing mucin like hormone receptor 1 (EMR1). Expression of F4/80 is heterogeneous and varies during macrophage maturation and activation (Van den Berg and Kraal, 2005). Though the inflammatory phase occurs between 1 and 3DAW some of the inflammatory cells are still present at 5DAW. Therefore the F4/80 antibody was used to stain the sections of Nesprin-2 KO and WT wounds from 1, 3 and 5DAW. The sections were subjected to immunohistochemistry with F4/80 antibody, and Hematoxylin was used as a co-stain for the nucleus. The macrophages stained with F4/80 are brown in colour while the nucleus looks blue. The Nesprin-2 KO wounds showed a dense brown staining deposited at the wound area in the sections from all 1, 3 and 5DAW compared to WT. This indicates that in Nesprin-2 KO wounds there was an increased influx of macrophages (Figure 2.5). This could be an indication that Nesprin-2 regulates the inflammatory cells which act during initial phase of the healing process.

Nesprin-2 might play a role in regulating the expression of some inflammatory genes. Interestingly this is supported by the data of our microarray study where we found among the differentially regulated genes some that are involved in the

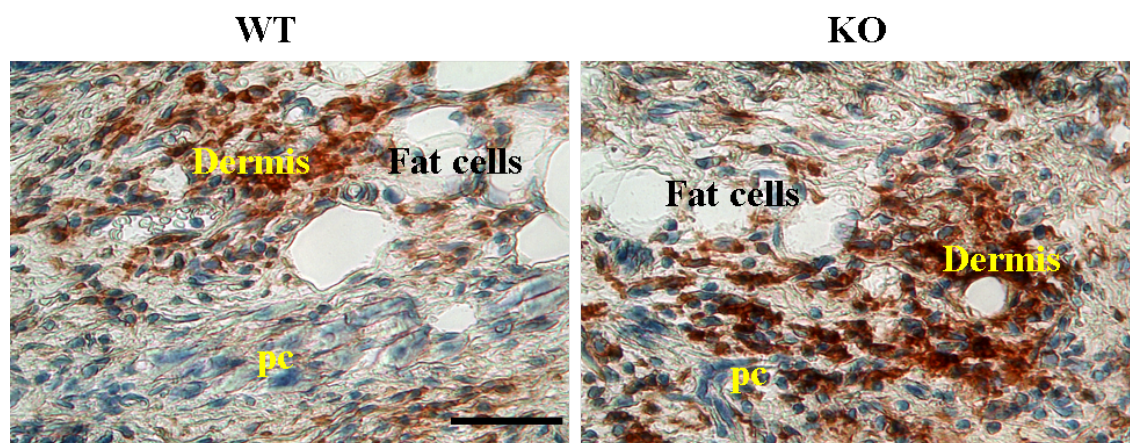


**Figure 2.5: The macrophage population is increased in the wound area in Nesprin-2KO mice.** (A) Skin sections were stained for macrophages with the F4/80 antibody and photographed using the Diskus software. Nesprin-2 KO wounds showed an increased staining of F4/80 compared to WT at 1, 3 and 5 days after wounding. In the figure brown staining indicates F4/80 stained cells (shown for day 5) and blue staining from Haematoxylin indicates nuclear staining. Comparable areas in the dermis of the wounds are shown. (pc -Panniculus carnosus) Scale bar, 50  $\mu$ m.

inflammatory process namely Serum Amyloid A3 (SAA3), Chemokine (C-X-C motif) ligand 5, Chemokine ligand 2 or MCP1 (Monocyte chemoattract protein 1) and Small Chemokine (C-C) ligand 11 (Table 2.2). Serum amyloid (SAA) proteins are

**Table 2.2: List of up-regulated inflammation related genes from microarray analysis.** Genes involved in the inflammatory process were found up-regulated in microarray analysis.

Significantly regulated genes	Fold changes
SAA3	1.84
Aggrecan	1.61
Chemokine(C-X-Cmotif) ligand5	1.3
Chemokine ligand2-MCP1	1.27
Small Chemokine(C-C) ligand11	1.31
Cyclin (Ccn1)	1.27
TAF6	1.22
Collagen type1, alpha2	1.2

a family of apolipoproteins associated with high-density lipoprotein (HDL). Different isoforms of SAA are expressed constitutively (constitutive SAAs) at different

levels or in response to inflammatory stimuli (acute phase SAAs). Three acute phase SAA isoforms have been reported in mice, called SAA1, SAA2 and SAA3. Acute phase serum amyloid A proteins (A-SAAs) are multifunctional apolipoproteins produced in large amounts during the acute phase of an inflammation and also during the development of chronic inflammatory diseases (Zhang et al., 2005). The expression of SAA3 was found upregulated in Nesprin-2 KO fibroblasts (Table 2). Next we studied the expression of the SAA3 in wound samples. The RNA from wounds of Nesprin-2 KO and WT was isolated from 1, 3 and 5DAW samples and cDNA was synthesised from these RNA samples and used for the study of expression of SAA3 by q-PCR. The q-PCR results clearly showed that the expression of SAA3 was enhanced in Nesprin-2 KO wounds at 1 and 3DAW while its expression is significantly reduced after 5 days of wounding compared to WT (Figure 2.6).

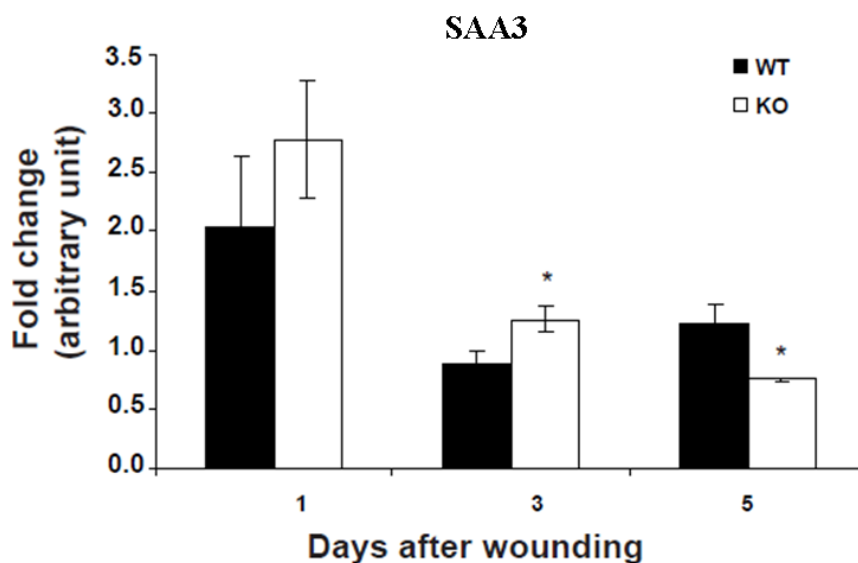


**Figure 2.6: The expression of the inflammation related gene SAA3 is increased in Nesprin-2 KO wounds.** The expression of SAA3 was up-regulated in Nesprin-2 KO fibroblast and this was confirmed in wound samples from 1, 3 and 5DAW (\*  $p=0.016$  and  $0.008$  at 3 and 5DAW, respectively).

Monocytes and macrophages are a source of several chemoattractants during the inflammatory phase which are required for the later phase of the healing

process. To check for chemoattractant production at the transcriptional level in wound samples, cDNA of Nesprin-2 KO and WT mice from 1, 3 and 5DAW was used in q-PCR experiments. We checked for MCP1 (CCL2), a monocyte specific chemoattractant protein, which is a member of the small inducible gene (SIG) family. MCP1 plays a role in the recruitment of monocytes to the sites of injury and infection. The expression of MCP1 in the wounds should correlate with the macrophages population. This was indeed the case in our analysis. The macrophage staining was increased in the KO wounds and in parallel the expression of MCP1 was significantly up-regulated in Nesprin-2 KO mice at 1, 3 and 5DAW. The expression of MCP1 was increased in Nesprin-2 KO wounds at 1DAW (4 fold), nearly 2 fold at 3DAW and more than 1 fold at 5DAW as compared to WT. The expression of MCP1 gradually decreased in both Nesprin-2 KO and WT wounds from 1 to 5DAW as the population of macrophages also decreased from the inflammatory phase to the new tissue formation phase (Figure 2.7).

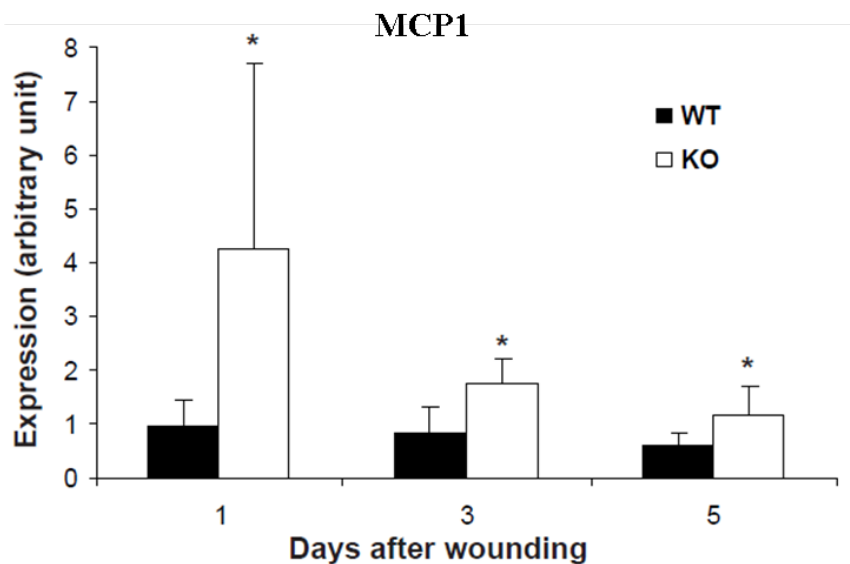


**Figure 2.7: Quantitative PCR (q-PCR) data showed a significant upregulation of the chemokine MCP1 (CCL2) in the wounds of Nesprin-2 KO.** The expression of the macrophage specific chemoattractant was found upregulated in Nesprin-2 KO wounds by q-PCR. (\*p=0.042, 0.0026 and 0.027, respectively, for 1, 3 and 5DAW).

## **2.2.4 New tissue formation and tissue remodelling phase**

Migration of keratinocytes towards the wound area occurs during the new tissue formation phase followed by hyper proliferation of the keratinocytes. In the dermis, fibroblasts from the neighbouring dermis migrate also towards the wound area and proliferate and some of them will differentiate into myofibroblasts. These fibroblasts deposit extracellular matrix and the tissue which is formed by these cells is called granulation tissue area. For this keratinocyte migration and proliferation and fibroblast proliferation was studied.

### **I - The keratinocyte migration pattern is altered in Nesprin-2 KO wounds and neo epidermis is lost in the KO wounds**

Two models have been proposed to describe the epidermal migration process during wound healing: the “sliding” model and the “rolling” model (Usui et al., 2005). Which model represents the actual migratory event best remains controversial. The “sliding” model focuses on the newly exposed basal keratinocytes at the leading edge. Upon wounding, changes in hemidesmosomal attachments enable basal keratinocytes to retract from the basement membrane zone, degrade dermal matrix, deposit new basement membrane components such as laminin 5, and migrate laterally over the provisional wound matrix. By virtue of the strong desmosomal attachments of migratory basal cells to adjacent basal and suprabasal keratinocytes, the entire epidermis then moves as a sheet or column to eventually close the wound. Evidence in support of the “sliding” model comes from extensive *in vitro* studies.

For the complex stratified epidermis, the “rolling” model of epithelialization may reflect epidermal wound healing more accurately even though it is less widely accepted as a possible mechanism for the epidermal repair process. In this “rolling” model, the primary keratinocytes participating in wound closure are suprabasal. Suprabasal keratinocytes exposed to the wound environment upon injury are

thought to undergo cell shape change, reduce their desmosomal attachments, and tumble over basal keratinocytes that remain strongly attached to the basement membrane. In the unwounded epidermis, Keratin 14 (K14), a marker for migrating keratinocytes was shown to be localized only in basal keratinocytes and at 1DAW K14 was found in suprabasal keratinocytes along with basal keratinocytes. From 3 D onwards its expression was found throughout the epidermis or all the layers of the epidermis (Usui et al., 2005).

I studied the keratinocyte migration pattern by staining the sections from 5, 7 and 10DAW sample with a K14 specific antibody (Figure 2.8). The red staining shows the presence of K14 which stains the keratinocytes in the epidermis (Epi) and blue is nuclear staining from DAPI. The keratinocytes are migrating from the neighboring epidermis towards the wound area and migrate further between the Fibrin clot and the dermis (Derm) by forming a sharp edge (dotted line in Figure 2.8 insets) also called neo epidermis in case of WT wounds from 5DAW and 7DAW. Whereas in Nesprin-2 KO, keratinocytes are migrating with no sharp edge which means that they have lost the neo epidermis in both 5 and 7DAW (Figure 2.8 insets). The epidermis with neo epidermis or with a sharp edge may speed up the migration of keratinocytes. This could be one of the reasons for faster closing of wounds in WT than in Nesprin-2 KO mice from 7DAW onwards. At 10DAW, WT wounds showed reduced wound area compared to Nesprin-2 KO wounds. This is shown by drawing a line indicating the distance between the migrating epidermal tips. The white arrow heads in the inset indicates that red staining (K14 staining) is reducing in WT as there is DAPI staining at the basal keratinocytes. The wound in WT at 10DAW is recovering from wound to normal skin. While in KO wounds at 10DAW, distance between the migrating tips is high as compared to WT and also we could see the K14 staining in the all the layers of the epidermis. The wound in KO at 10DAW is not completely recovered from the wound to normal skin.

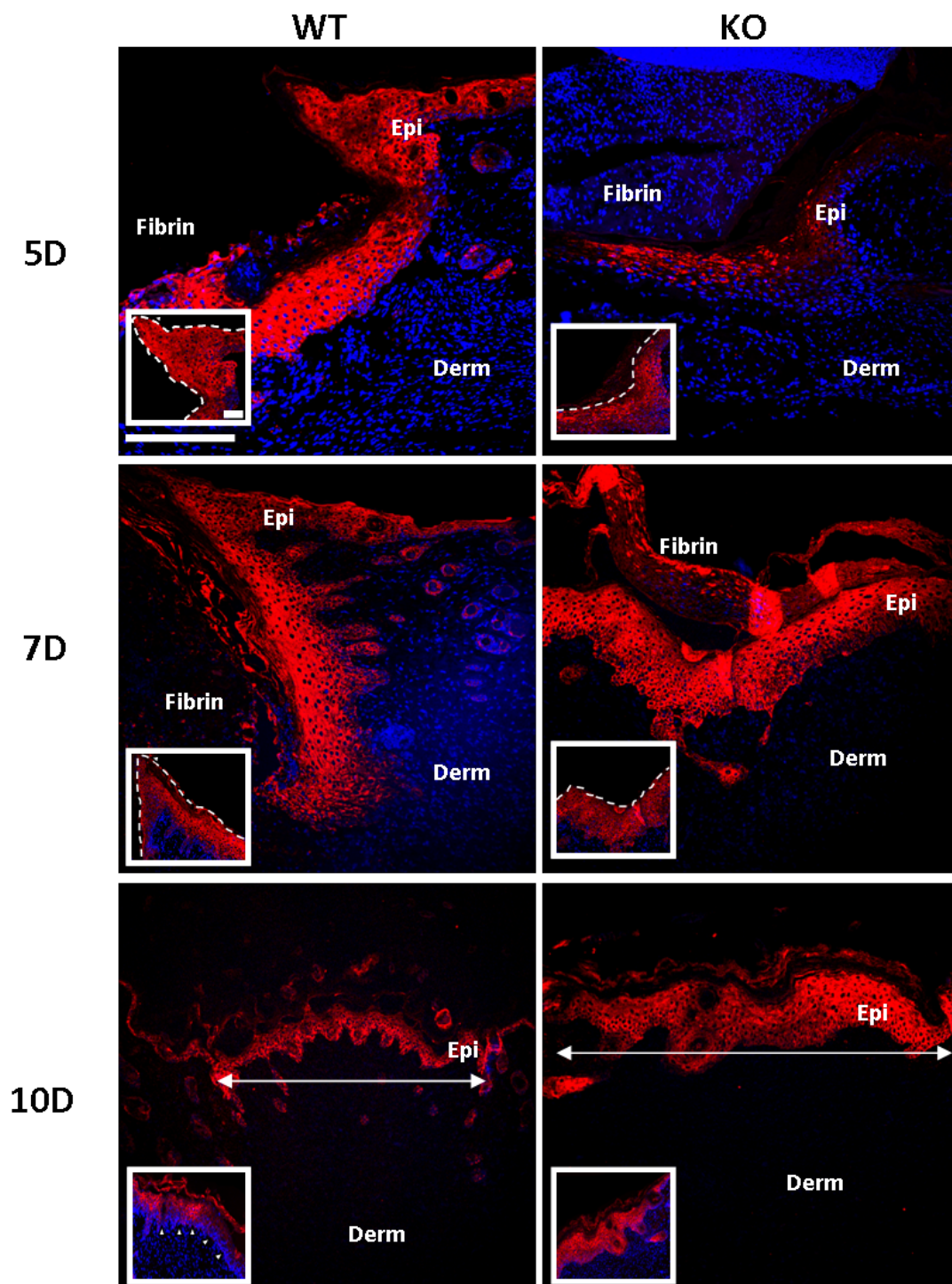


**Figure 2.8: The keratinocyte migration pattern is altered in Nesprin-2 KO mice.** Keratinocyte migration over the wound area between fibrin and the dermis was studied with a Keratin 14 specific antibody. Red staining is from K14 which stains the keratinocytes in the epidermis and blue staining is from DAPI, a nuclear stain. Scale bar for 200 $\mu$ m. Inset showing sharp migrating tips. Line in the 10D indicates distance between the migrating tips. The white arrow heads in the inset at 10D indicates that red staining (K14 staining) is reducing in WT which is replaced by DAPI staining at the basal keratinocytes. Scale bar, 50 $\mu$ m.

## **II - Proliferation of keratinocytes is reduced in Nesprin-2 KO wounds**

Migration of keratinocytes from the nearby epidermis towards the wound area is followed by their hyperproliferation. The expression of Ki67, a marker of cell proliferation, was restricted to basal and immediate suprabasal layers at the wound edge. In normal skin, expression of Ki67 is observed in very few nuclei along the basal cell layer, whereas during epidermal wound healing an increased expression in basal and immediate suprabasal cells is seen (Usui et al., 2005; Patel et al., 2006). Ki67 staining had been earlier assessed in unwounded skin of Nesprin-2 KO and WT and was found to be nearly identical and restricted to the basal layer (Lüke et al., 2008).

When I carried out the analysis in skin sections of Nesprin-2 KO and WT from 5, 7 and 10DAW the expression of Ki 67 was observed both in the basal and suprabasal layer of the epidermis. However the number of proliferating keratinocytes was reduced in Nesprin-2 KO wounds (Figure 2.9 A). In order to determine the proliferation rate of keratinocytes in the wounded epidermis, I counted the number of Ki67 positive cells in the wounds from three time points, 5, 7 and 10DAW. Nesprin-2 KO wounds showed an average of 9 cells per unit area which is significantly less as compared to WT (~30 cells per unit area) at 5DAW. Similarly, at 7DAW the number of Ki67 positive cells was significantly reduced in Nesprin-2 KO wounds (22 cells per unit area) as compared to WT wounds (~41 cells per unit area) and at 10DAW Nesprin-2 KO wounds contained approximately 10 Ki67 positive cells per unit area whereas WT wounds had nearly 18 cells per unit area (Figure 2.9 B). The reduction in keratinocyte proliferation in Nesprin-2 KO wounds may be one of the reasons for the delay in wound healing observed at 7 and 10DAW.

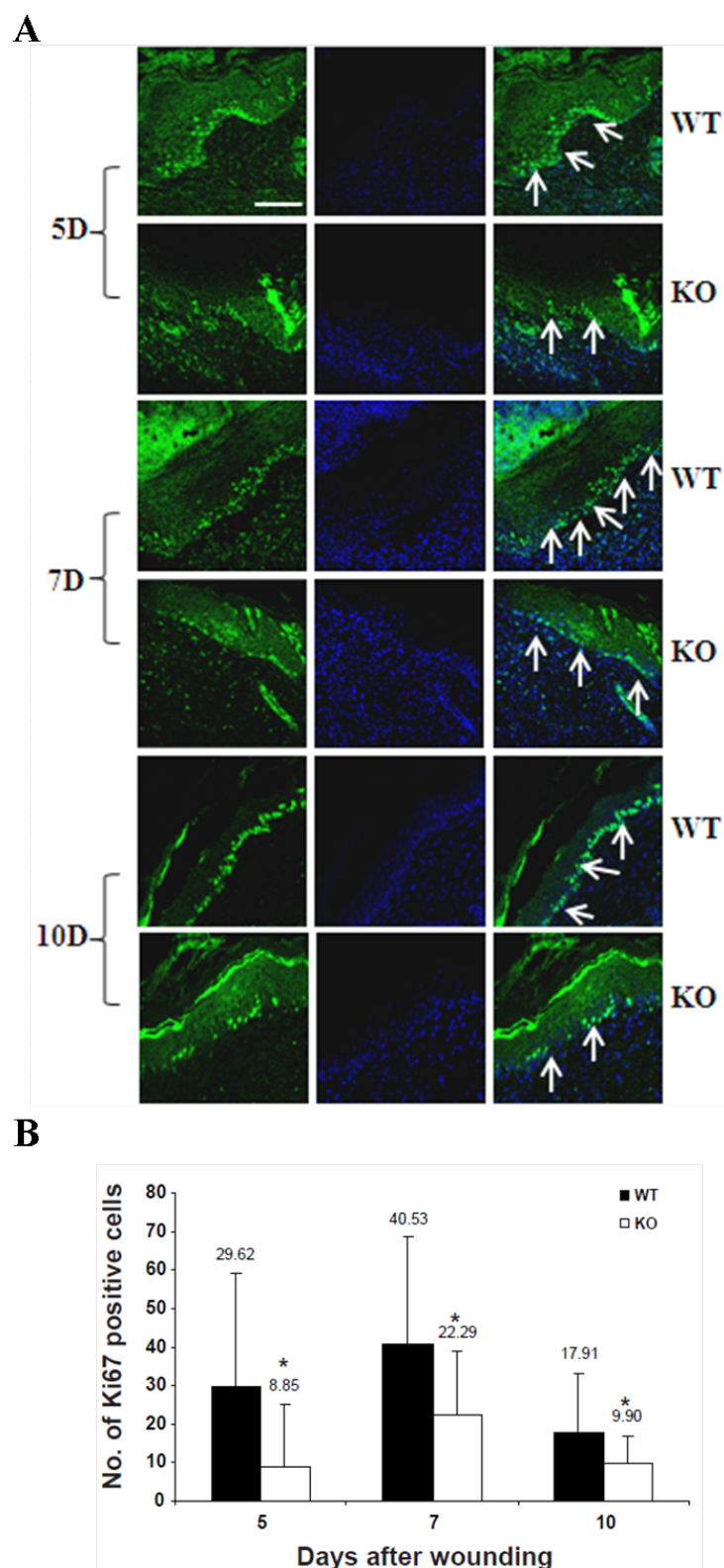


**Figure 2.9: Keratinocyte proliferation is slowed down in Nesprin-2 KO wounds.** (A) Proliferation of keratinocytes is studied by staining the sections with the proliferation marker Ki67. The expression of Ki67 at the basal and suprabasal layer of the epidermis is indicated by white arrows. Scale bar, 100 $\mu$ m. (B) The average number of Ki67 positive cells in Nesprin-2 KO and WT wounds per unit area was determined (\* $p=0.027$ ,  $0.029$  and  $0.031$  at 5, 7 and 10DAW).

### **III - Differentiation of fibroblasts into myofibroblasts in the granulation tissue area is reduced in Nesprin-2 KO wounds**

During healing of an open wound, resident dermal fibroblasts proliferate from the wound margin and migrate into the provisional matrix composed of a fibrin clot. About 1 week after wounding, the provisional matrix is replaced by newly formed connective tissue known as granulation tissue which is essentially composed of small vessels, extracellular matrix, and fibroblastic cells that become activated and differentiate into myofibroblasts. The main feature of myofibroblasts is their contractile apparatus which is similar to that of smooth muscle and in particular the expression of  $\alpha$ -smooth muscle actin ( $\alpha$ -SMA). Myofibroblasts play a central role in closing the wound tissue through their capacity to produce a strong contractile force possibly generated within stress fibers, similar to those present in cultured fibroblasts (Skalli et al., 1986; Serini and Gabbiani, 1999). Because wound contraction takes place when de novo expressed  $\alpha$ -SMA is incorporated in stress fibers, it has been suggested that this actin isoform plays an important role in granulation tissue contraction (Hinz et al., 2001).

Based on the fact that Nesprin-2 Giant is an actin binding protein, it might well be involved in regulating myofibroblast differentiation. Because the expression of alpha smooth muscle actin ( $\alpha$ -SMA) is considered as the most reliable marker for differentiated myofibroblasts I stained the sections from Nesprin-2 KO and WT wounds with an  $\alpha$ -SMA specific antibody in order to study myofibroblast differentiation. The staining for  $\alpha$ -SMA was strong in the dermis where the granulation tissue (GT) is present (Figure 2.10 A).

The visual comparison of the expression of  $\alpha$ -SMA in the wounds of KO and WT mice was followed by a quantification of the intensity of staining per unit area using the Leica confocal software. Although the staining intensity of  $\alpha$ -SMA appeared higher in WT wounds as compared to Nesprin-2 KO wounds, the

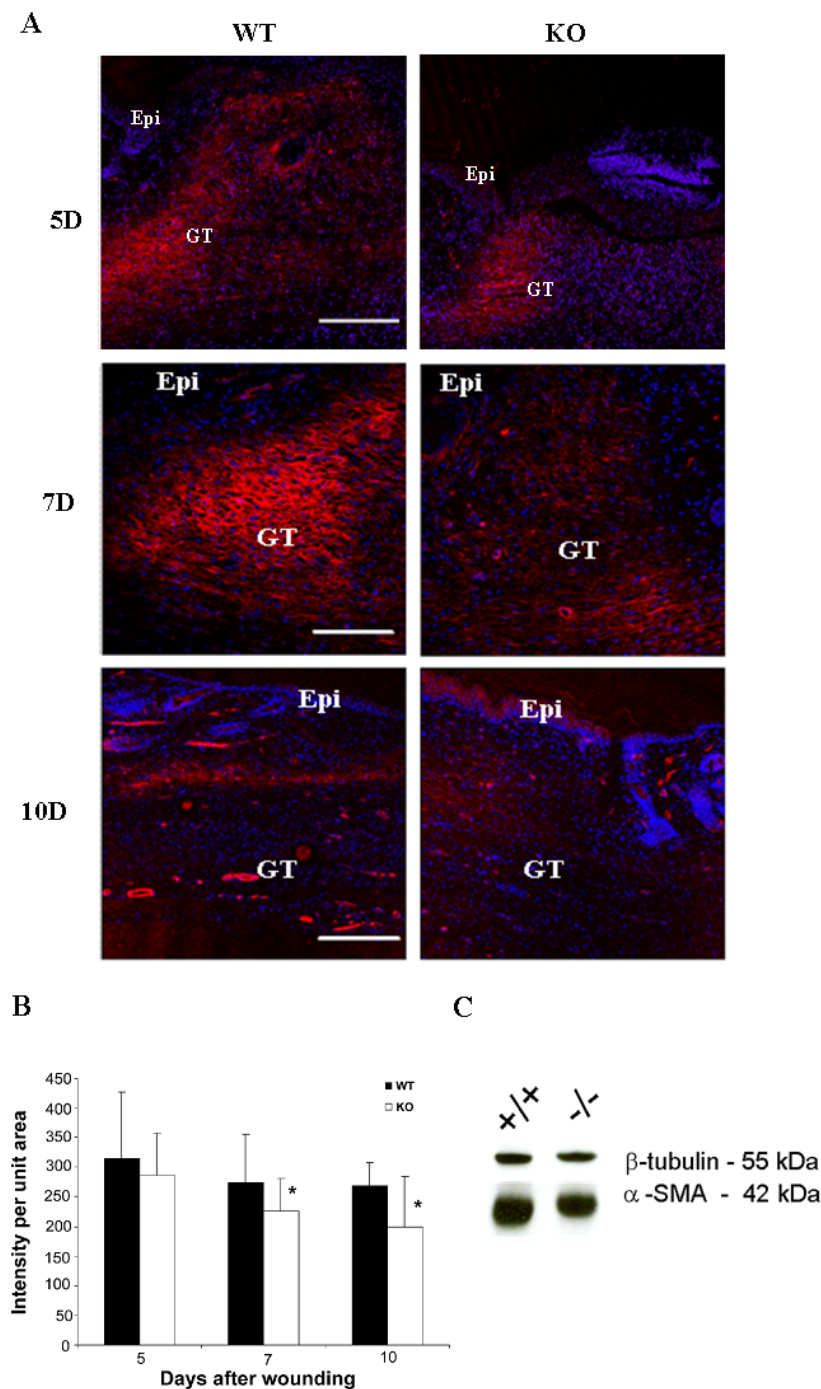


**Figure 2.10: Differentiation of fibroblasts into myofibroblasts is reduced during the wound healing process in Nesprin-2 KO mice.** (A) Differentiated myofibroblasts were studied in wounds from 5, 7 and 10DAW. Alpha smooth muscle actin ( $\alpha$ -SMA) was taken as a marker. Epi-epidermis and GT-granulation tissue. Scale bar, 100 $\mu$ m. (B) The intensity of  $\alpha$ -SMA staining was quantified as intensity per unit area using Leica Confocal Software. The intensity per unit area at 7 and 10DAW differed significantly (7DAW,  $p=0.04$ ; 10DAW,  $p=0.04$ ). (C) Western blot analysis of homogenates using  $\alpha$ -SMA antibody and  $\beta$ -tubulin as a loading control. Samples from 7DAW are shown.

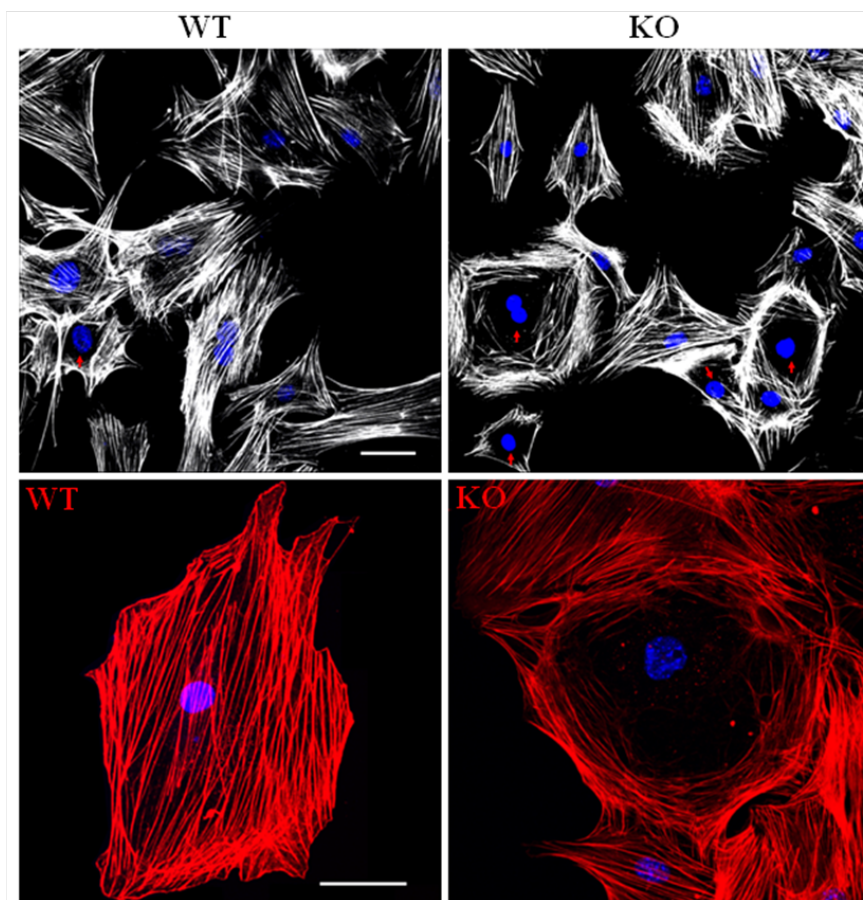
intensity per unit area did not reveal a significant difference in the staining intensity at 5DAW between Nesprin-2 KO and WT wounds. However, there was a significantly higher intensity of  $\alpha$ -SMA staining per unit wound area in WT at 7 and 10DAW (7DAW,  $p=0.04$ ; 10DAW,  $p=0.04$ ; Student's t-test) indicating that more fibroblasts had differentiated into myofibroblasts in WT compared to Nesprin-2 KO wounds (Figure 2.10 B). The western blot analysis also showed an increased expression of  $\alpha$ -SMA in WT as compared to KO (Figure 2.10 C). This can be further important reason for the faster wound closure in WT mice compared to KO.

### **III A. F-actin fibers were disturbed around the nucleus in Nesprin-2 KO fibroblasts**

Induction of transforming growth factor- $\beta$ 1 (TGF- $\beta$ 1) in fibroblasts enhances the formation of “structural element”, bundles of actin filaments or stress fibers, vinculin-containing fibronexus adhesion complexes and fibronectin fibrils, and increases the expression of  $\alpha$ -SMA. The formation of these structural elements is thought to serve as a prerequisite for TGF- $\beta$ 1 induced expression of  $\alpha$ -SMA. They are also important for generating contractile force in myofibroblasts which is associated with wound contraction. Formation of stress fibres therefore directly correlates with the expression of  $\alpha$ -SMA and a reduction in  $\alpha$ -SMA is equivalent to a reduction in F-actin content (Vaughan et al., 2000).

We stained fibroblasts from Nesprin-2 KO and WT with TRITC-phalloidin for F-actin detection we found that the F-actin network was disrupted around the nucleus (red arrow) in many Nesprin-2 KO fibroblasts (Figure 2.11 A). To verify this observation I determined the number of fibroblasts for Nesprin-2 KO and WT which showed a disturbed or disrupted F-actin network around the nucleus. In the Nesprin-2 KO  $\sim 22\%$  of fibroblasts had an altered F-actin staining around the nucleus. In WT fibroblasts similar changes were seen in only  $\sim 12\%$  of cells (Figure 2.11 B).

A



B

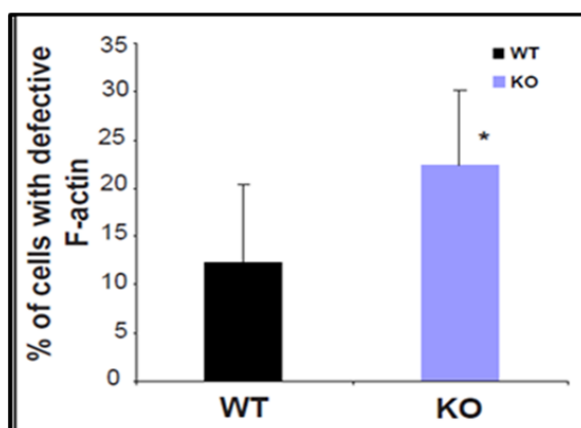


**Figure 2.11: Nesprin-2 absence led to disturbed actin fibers around the nucleus in primary fibroblasts.** (A) Wild type fibroblasts and Nesprin-2 knock out fibroblasts were stained for F-actin with TRITC Phalloidin. Fibroblasts with disrupted actin fibers (arrow) were counted and used for calculating the percentage. Scale bar, 50 $\mu$ m. The lower panel shows a single wild type and Nesprin-2 KO fibroblast at higher magnification. DAPI is used for staining the nucleus. Scale bar, 100 $\mu$ m. (B) Cells with defective F-actin fibers were counted and used for calculating the percentage (%). The KO fibroblasts showed a significantly higher percentage (%) of cells with a defective actin cytoskeleton than wild type ( $p= 8.96^{-9}$ ).

The fibroblasts from Nesprin-2 KO and WT were also stained with a  $\beta$ -actin specific antibody, the nucleus was stained with DAPI (blue) and Nesprin-2 was determined by polyclonal antibodies pAbK1. pAbK1 is directed against the C-terminus of Nesprin-2 and recognises all C-terminal isoforms of which a 50 kDa protein is still present in the KO mouse which is presumably derived from an internal promoter (Lüke et al., 2008; Zhang et al., 2005). WT fibroblasts showed a proper distribution of actin fibers throughout the cell compartment in contrast to the Nesprin-2 KO fibroblasts which exhibited a dense unusual staining of  $\beta$ -actin deposited in spots around the nucleus (arrows), indicating that Nesprin-2 is necessary for proper formation of actin fibers (Figure 2.12). We reasoned that Nesprin-2 Giant might be required in a chain which signals to the F-actin network required for TGF- $\beta$ 1 dependent myofibroblast differentiation, and its absence might lead to reduced fibroblast differentiation into myofibroblasts under a mechanical stress situation.

### **III B. Nesprin-2 acts on the F-actin network in human keratinocyte (HaCaT) cells**

Cell locomotion and adhesion play key roles during embryonic development, tissue regeneration, immune responses, and wound healing in multicellular organisms. Cell migration, changes in cell shape, and adhesive properties are regulated by a continuous remodelling of the actin cytoskeleton (Hotulainen and Lappalainen 2006).

The actin network was studied in Nesprin-2 Giant deficient human keratinocytes. Nesprin-2 was knocked down (KD) in a human keratinocyte cell line (HaCaT). The cells were then stained with Nesprin-2 specific antibody K20-478 to check the Knockdown (KD) efficiency and FITC-Phalloidin for F-actin (Figure 2.13). In control cells F-actin localizes along the NE (white arrow head) and also at the cell junctions (arrows). The inset shows the NE localization of F-actin. In Nesprin-2

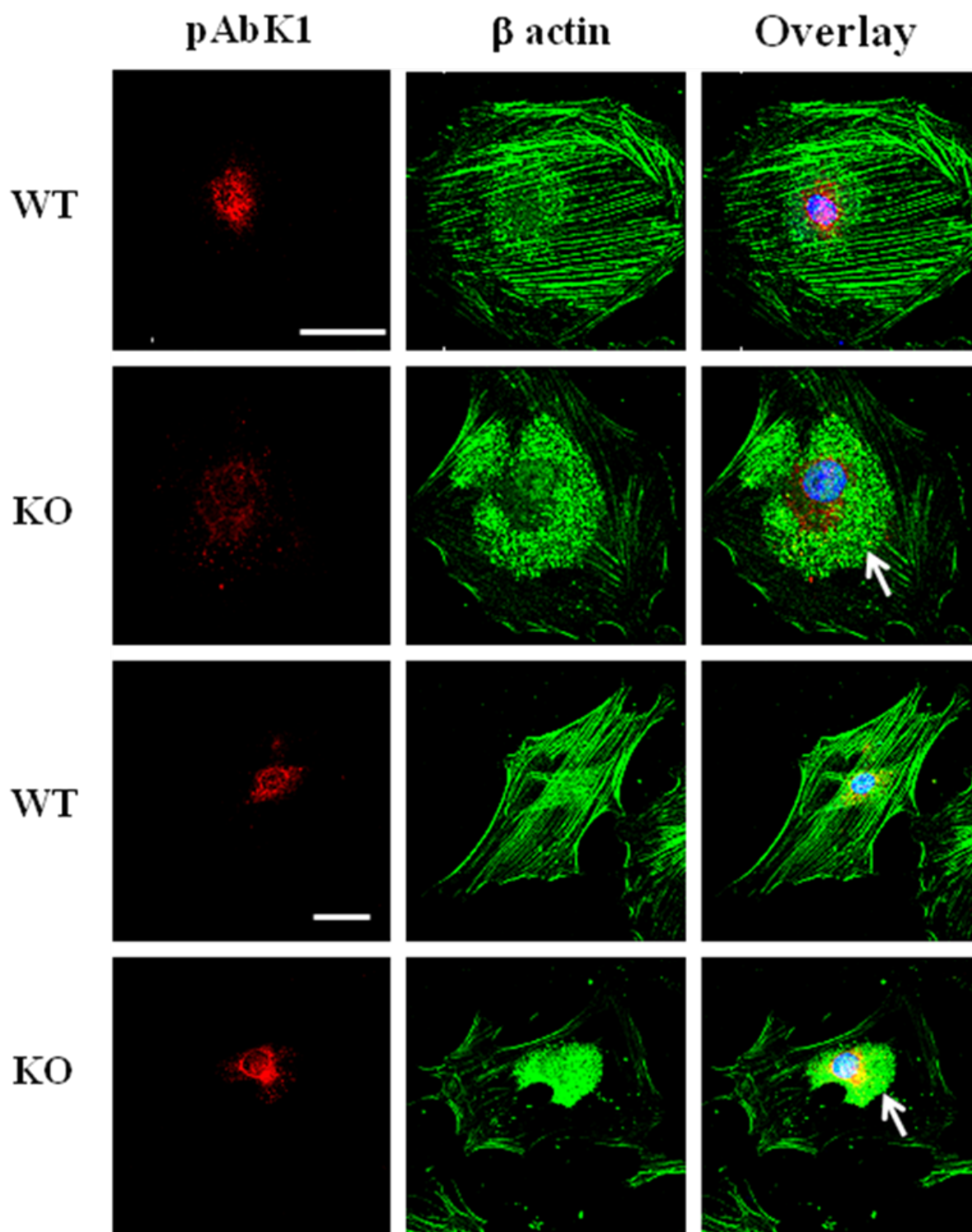


**Figure 2.12: Nesprin-2 Giant maintains actin fibers around the nucleus in primary fibroblasts.** Actin fibers are detected with  $\beta$ -actin monoclonal antibody (green) and Nesprin-2 with pAbK1, a polyclonal C-terminus specific antibody (red) and nucleus with DAPI (blue). White arrows showing disorganized distribution of  $\beta$ -actin in Nesprin-2 KO fibroblasts. Scale bar 50 $\mu$ m.

KD cells the NE localization of F-actin is lost (inset white arrow head) and also the cell-cell junctions appear to be affected as revealed by Phalloidin staining.

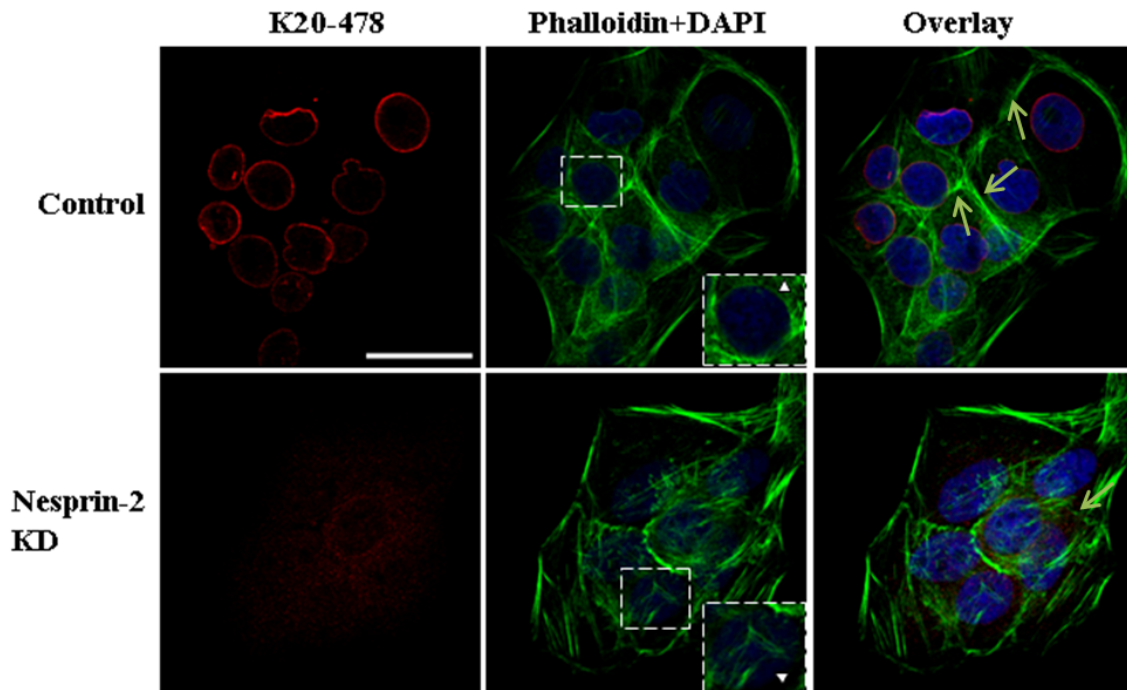


**Figure 2.13: F-actin distribution and localization is disturbed in Nesprin-2 knock down HaCaT cells.** HaCaT cells transfected with control and Nesprin-2 knock down ShRNA were stained with Nesprin-2 specific K20-478 antibody (red) and FITC-Phalloidin for F-actin (green) and DAPI for the nucleus (blue). The inset shows the presence (WT) and absence (KD) of F-actin at the NE (white arrow head). Scale bar, 25 $\mu$ m.

### III C. The granulation tissue area is reduced in Nesprin-2 KO wounds

To get further evidence for the reduced myfibroblast differentiation in Nesprin-2 KO wounds, the area of the granulation tissue (GT) was measured (Figure 2.14 A). In WT wounds significantly more granulation tissue (GT) area was observed at 7DAW (0.78 mm<sup>2</sup>) and 10DAW (0.55 mm<sup>2</sup>) which corresponds to increased myfibroblast differentiation. In Nesprin-2 KO the granulation tissue area was 1.00 mm<sup>2</sup> at 7DAW and 0.77 mm<sup>2</sup> at 10DAW after wounding leading to reduced myfibroblast differentiation (Figure 2.14 B). The contraction ability of

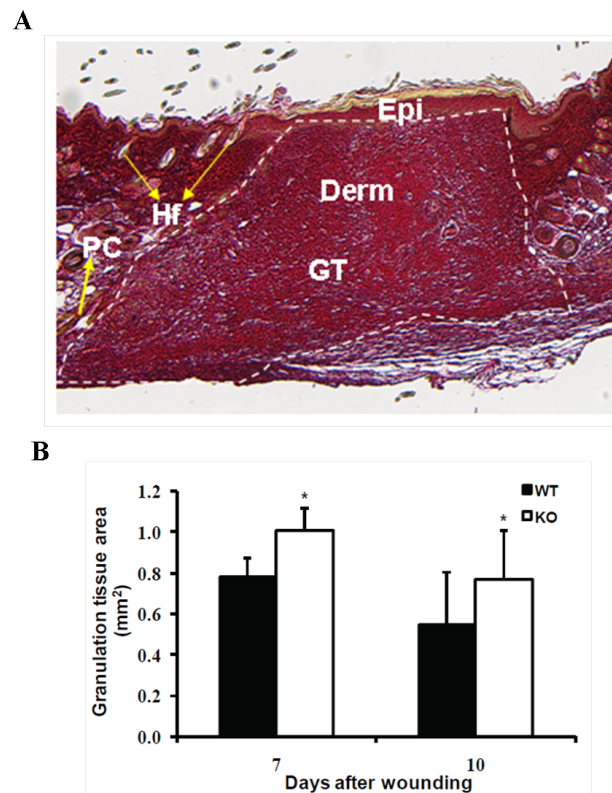


**Figure 2.14: Sirius red staining showing the granulation tissue area.** (A) Figure showing the wound area stained with Sirius red. The Figure represents an example from 7DAW WT wounds. Epi-Epidermis, Derm-Dermis, GT-Granulation Tissue, Hf-Hair follicles and PC-Panniculus Carnosus. (B) Quantification of granulation tissue area at 7 and 10DAW in WT and Nesprin-2 KO. (\* $p=1.6 \times 10^{-10}$  at 7DAW and 0.000384 at 10DAW).

myofibroblasts enables the shrinkage of a wound and closes its edges. Increased myofibroblast differentiation is equivalent to faster contraction or healing of the wounds.

### 2.3 The transcriptional regulation of genes involved in wound healing is altered in Nespin-2 Giant knock out mice

Based on its presence at the NE and its role in regulating the shape of the nucleus Nesprin-2 has the potential to be involved in controlling gene expression (Heesen and Fornerod, 2007). Hence we tested the expression of transcription fac-

tors PPAR  $\beta/\delta$  (Peroxisome proliferator-activator receptor  $\beta/\delta$ ), Egr-1 (Early growth response factor 1) and E2F1 by q-PCR. The PPAR  $\beta/\delta$  is one of the targets of activator protein-1 (AP-1) and a member of the PPAR family, which also includes PPAR $\alpha$  and PPAR $\gamma$ . PPAR  $\beta/\delta$  is a ligand-induced transcription factors of nuclear hormone receptor superfamily. AP-1 induces PPAR  $\beta/\delta$  gene expression by binding to its promoter (Tan et al., 2001).

I observed that the expression of PPAR $\beta/\delta$  was down regulated in wounds from Nesprin-2 KO compared to the respective time points from WT (1, 3 and 5DAW). Though the difference in the expression of PPAR  $\beta/\delta$  between Nesprin-2 KO and WT is not significant, the tendency of expression is notable (Figure 2.15 A). The expression of PPAR  $\beta/\delta$  is increased at 3DAW in both Nesprin-2 KO and WT indicating the start of wound reepithelialisation at this point. In general, PPAR  $\beta/\delta$  expression is enhanced in keratinocytes during skin injury (Tan et al., 2001).

Egr-1 is a member of the Egr family of zinc-finger transcription factors, which also includes Egr-2 (Krox-20), Egr-3 and Egr-4. Upon wounding of mouse embryos (E11.5), a strong induction of Egr-1 and Egr-2 expression was observed in epithelial and mesenchymal cells at the wound edge (Grose et al., 2002) where Egr-1 enhances angiogenesis in the wound, collagen deposition and re-epithelialization. Here I found down regulation in the expression of Egr-1 in Nesprin-2 KO wounds whereas in WT Egr-1 expression was upregulated (Figure 2.15 B).

E2F1 acts as a regulator of inflammation and reepithelialisation in wounded skin (Schäfer and Werner, 2007). E2F transcription factors regulate proliferation, differentiation, DNA repair and apoptosis. Tight E2F regulation is crucial for epidermal formation and regeneration. E2F1 downregulation is necessary for proper keratinocyte differentiation, as exogenous E2F1 expression in differentiating cultured keratinocytes prevents exit from the cell cycle, causes apoptosis and interferes with expression of differentiation markers, such as transglutaminase 1 and keratin 10 (Dicker et al., 2000; D'Souza et al., 2001). An earlier study reported that deregulation

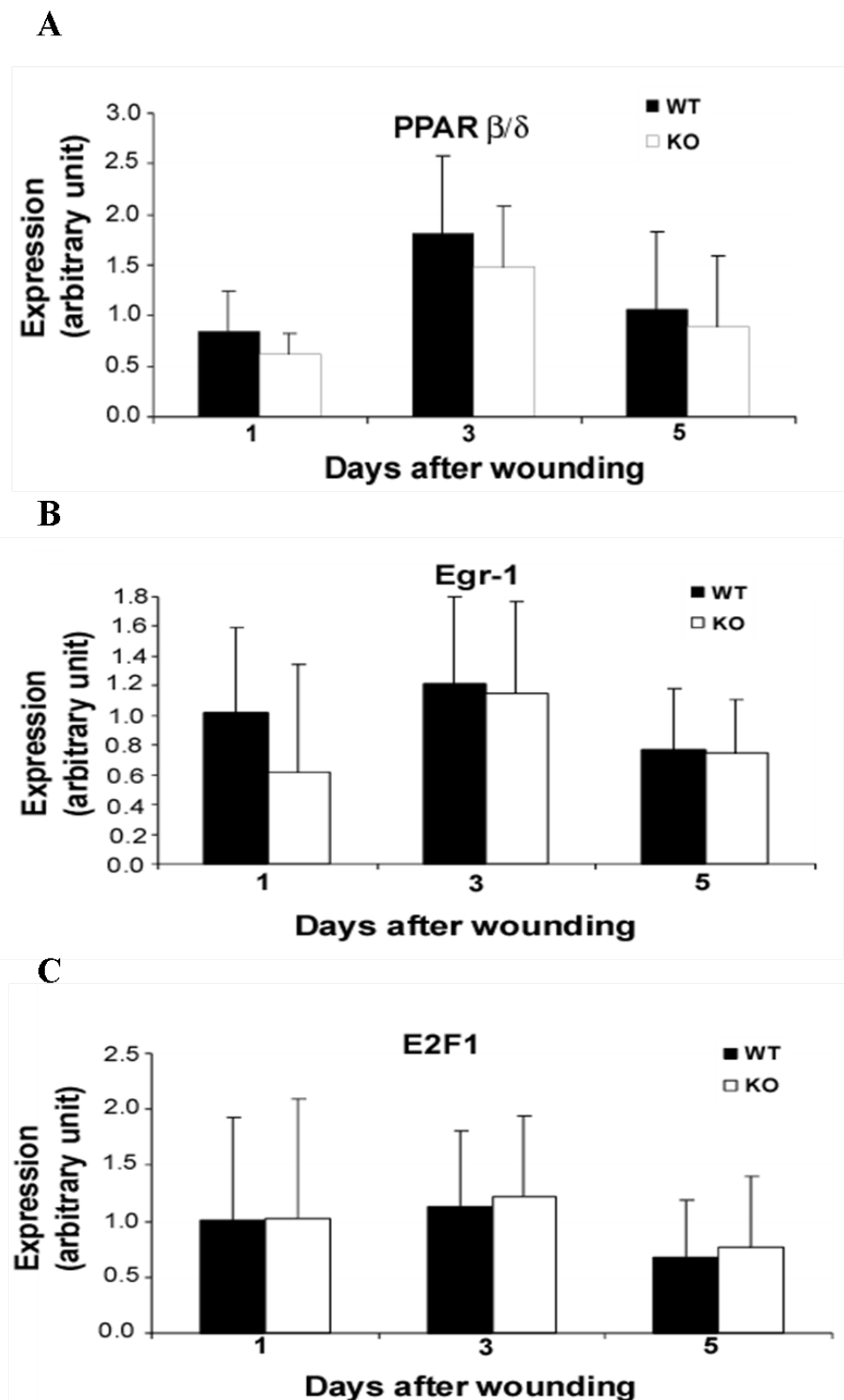


**Figure 2.15: Transcription factors are differentially regulated in Nesprin-2 KO wounds.** Expression of transcription factors known to be induced during mechanical stress condition was studied. Quantitative PCR (q-PCR) was carried out using RNA from wounds harvested at 1, 3 and 5DAW and the levels of mRNA of transcription factors PPAR $\beta/\delta$  Egr-1 (B) and E2F1 (C) were determined.

lated expression of E2F-1 in the mouse epidermis induced hyperplasia and hyperproliferation but did not inhibit terminal differentiation (Pierce et al., 1998). E2F1 expression was slightly up-regulated in Nesprin-2 KO wounds at 1 and 3DAW (Figure 2.15 C). Overall, the expression of transcription factors PPAR $\beta/\delta$  and Egr-1 is down-regulated in Nesprin-2 KO wounds at 1, 3 and 5DAW compared to WT wounds whereas the expression of E2F1 is up-regulated in Nesprin-2 KO wounds. Though the difference in the expression of these transcription factors is not significant, the observed changes are interesting as they match the expression pattern from earlier studies.

## **2.4 c-Fos localization in Nesprin-2 KO and WT epidermis**

The reduced keratinocyte proliferation in Nesprin-2 KO wounds and the presence of Nesprin-2 at the NE suggest that Nesprin-2 might be involved in regulating the transcription factors which are involved in the cell proliferation process. We further studied c-Fos, a transcription factor of the Activator protein-1 (AP-1) family of transcription factors regulating cell proliferation by indirect immunofluorescence (Eferl and Wagner, 2003). c-Fos belongs to the activator protein-1 (AP-1) leucine zipper transcription factors, which are composed of hetero- or homodimers of the Fos (c-Fos, FosB, Fra-1, and Fra-2), Jun (c-Jun, JunB, and JunD), and CREB/ATF (ATF2, ATF3, ATF4, and ATFa) protein families. The AP-1 transcription factors regulate the expression of various genes involved in the wound healing process (Schäfer and Werner, 2007). Strong immunostaining of c-Fos and c-Jun was also seen during the inflammatory and proliferative phases of wound healing in humans (Kondo and Yonezawa, 2000).

Keratinocytes near and away from the wound area in both WT and Nesprin-2 KO showed nuclear localization of c-Fos at 1DAW. In Figure 2.16 nuclear staining of

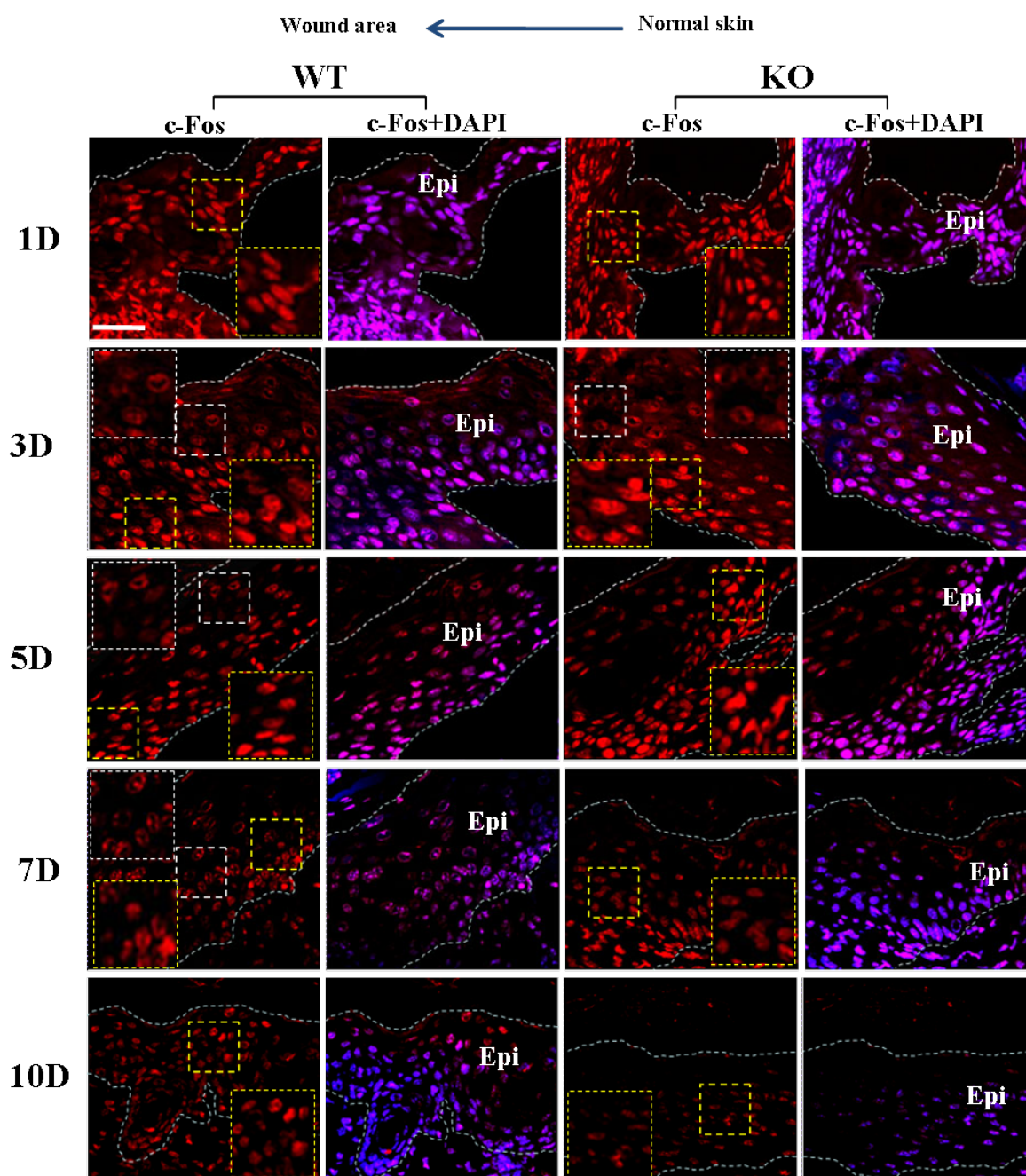


**Figure 2.16: c-Fos localization at various stages of wound healing in Nesprin-2 KO and WT mice.** c-Fos was detected with polyclonal c-Fos antibody (red) and DAPI was used for nuclear staining (blue). Nuclear localization of c-Fos is indicated by insets with yellow dotted lines and cytoplasmic localization is indicated by insets with white dotted lines. Scale bar 40 $\mu$ m.

c-Fos is indicated by yellow dotted line and cytoplasmic localization by white dotted line. At 3DAW, c-Fos nuclear staining is confined to basal keratinocytes in WT, and most of the keratinocytes in the upper layer of the epidermis have lost clear nuclear staining and showed cytoplasmic (inset with white dotted lines). In KO wounds at 3DAW c-Fos is localised within the nucleus in some of the keratinocytes, other cells have lost the nuclear localization and c-Fos is cytoplasmic. In Nesprin-2 KO wounds the majority of the cells retain nuclear staining for c-Fos compared to WT at this time point. At 5DAW c-Fos is found within the nucleus in WT and some cells still showed cytoplasmic localization of c-Fos, while Nesprin-2 KO wounds at this time point showed completely nuclear localization of c-Fos. A similar localization is observed at 7DAW where WT wounds showed both nuclear and cytoplasmic (most of the keratinocytes) localization, while Nesprin-2 KO wounds showed completely nuclear localization of c-Fos. At 10DAW WT regain the c-Fos nuclear localization in all layers and Nesprin-2 KO continued its nuclear localization of c-Fos similar to earlier time points. However the staining intensity of c-Fos is reduced in Nesprin-2 KO wounds. Taken together, Nesprin-2 KO wounds showed nuclear localization of c-Fos in most of the keratinocytes whereas WT showed both nuclear and cytoplasmic localization. At 10DAW c-Fos staining is seen in the nucleus of the keratinocytes in all layers of the epidermis in WT and KO; however the staining intensity is higher in WT than in the KO (Figure 2.16).

## **2.5 Nesprin-2 regulates the localization of c-Fos in human keratinocytes**

To further study a possible dependence of c-Fos on Nesprin-2 Giant, human keratinocytes (HaCaT) were transfected with shRNA plasmids to knock down Nesprin-2 Giant (KD) expression or with control plasmids (Lüke et al., 2008). In control cells c-Fos is present in the nucleus whereas in KD cells we observe

it in the nucleus and in the cytoplasm. Also, overall staining in the KD is more intense compared to control cells (Figure 2.17 A). To further check whether the c-Fos expression is increased in Nesprin-2 KD cells, quantitative PCR (q-PCR) was done by using RNA from control and Nesprin-2 KD HaCaT cells which showed that the expression of c-Fos was significantly increased in KD cells compared to control HaCaT cells (Figure 2.17 B). Western blot analysis also confirmed the increased expression of c-Fos in Nesprin-2 KD cells compared to control cells. Tubulin detected by mAb WA3 was used as a loading control (Figure 2.17 C).

## **2.6 Control HaCaT cells showed a gradient localization of c-Fos in in vitro cell scratch assays which was lost in Nesprin-2 KD cells**

To mimic in vivo wound healing, a cell scratch assay was done in KD and control HaCaT cells. HaCaT cells were scratched on the cover slips and the c-Fos localization one hour and six hours after scratching analysed by immunostaining (Figure 2.18). One hour after scratching control cells still showed nuclear staining for c-Fos (inset with yellow dotted lines) but we observed a gradient in the intensity, i.e. the intensity of c-Fos in cells near the scratched area was reduced (inset with white dotted line) as compared to cells away from the scratch. Many of the Nesprin-2 KD cells showed nuclear localization (inset with yellow dotted lines) and some showed cytoplasmic staining (inset white dotted line) of c-Fos at one hour after scratching. However we did not find a difference in intensity between cells near the scratched area and cells away from scratched area. Also, here we did not notice a gradient in intensity for c-Fos as in control cells. At six hours after wounding c-Fos is lost from the nucleus in control cells (inset), whereas in KD cells c-Fos localization is more nuclear (inset). c-Fos localization in Nesprin-2 KO wounds and Nesprin-2 KD scratched cells is always the same and shows no changes under

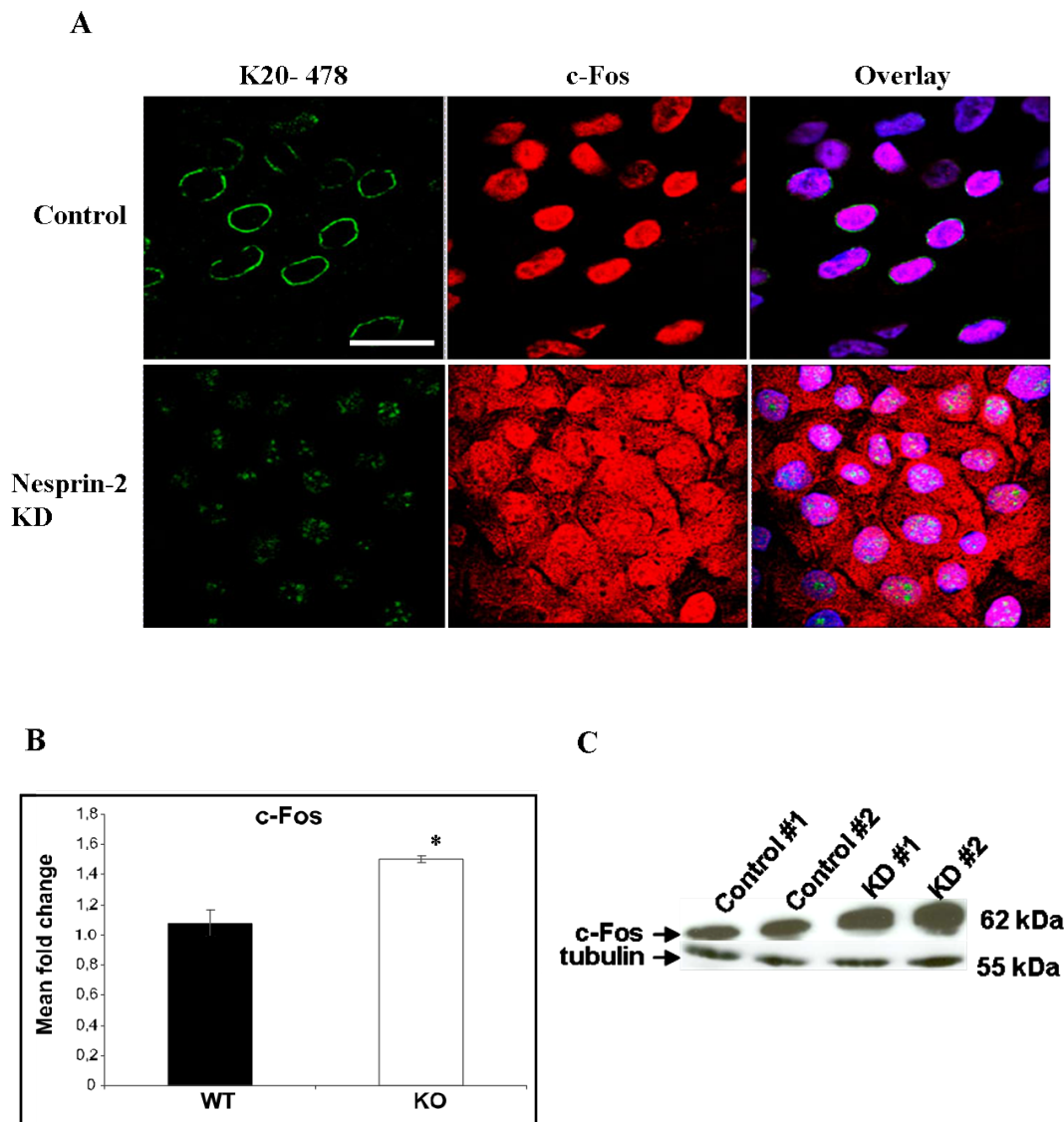


**Figure 2.17: The localization and expression of c-Fos has changed in Nesprin-2 knock down cells.** (A) c-Fos localization was studied in control and Nesprin-2 knock down (KD) human keratinocyte (HaCaT) cell line. The efficiency of the knock down was checked with mAb K20-478 recognizing Nesprin-2 Giant. Scale bar, 100 $\mu$ m. (B) c-Fos expression is studied by q-PCR by using the RNA from control and Nesprin-2 KD cells. (C) Western blot analysis showed increased expression of c-Fos in KD.

different conditions, while the localization of c-Fos is shuttling between the nucleus and cytoplasm in WT (in vivo wound) and control (in vitro scratch).

## 2.7 Apoptosis in Nesprin-2 KO cultured fibroblasts

In Nesprin-2 KO fibroblasts the nuclei are mishappen, showed blebbing and often a honeycomb shaped nucleus. Based on the observed changes in nuclear architecture which was reminiscent of apoptotic cells, we studied apoptosis in Nesprin-2 KO fibroblasts. Apoptosis initiation involves either death receptor (DR) stimulation at the plasma membrane by members of the TNF family, i.e. TNF- $\alpha$  Fas ligand (FasL) and TNF-related apoptosis-inducing ligand (TRAIL), or a perturbation of mitochondria in response to stresses generated by damages occurring in different organelles such as the nucleus and the endoplasmic reticulum (ER) (Boyce and Yuan, 2006). A possible apoptotic nature of fibroblasts was addressed by dual staining with acridine orange (AO) and ethidium bromide (EB). Apoptotic cells are characterised by degradation of their chromatin early in the process, and damaged DNA and nuclear collapse are seen while the plasma membrane is still intact. Both AO/EB intercalate into DNA, and preferentially stain cell nuclei. Acridine orange is a cell-permeant, allowing visualization of nuclear structures in living cells. Nuclei stained with AO appear yellow-green; red fluorescence may also be seen in the cytoplasm of normal cells (e.g. from RNA, mitochondrial DNA, or various granules). EB does not penetrate intact cells; in contrast, when a cell dies and its plasma membrane ruptures, EB reaches the nucleus and, overwhelming the AO effect, stains the nucleus orange-red (Margaret et al., 2001). I counted the cells with orange red staining as dead or apoptotic cells (Figure 2.19 A) in WT and Nesprin-2 KO fibroblasts and found that about 22% of WT and 30% of Nesprin-2 KO fibroblasts undergo apoptosis. This difference is not significant. However there are more cells present in Nesprin-2 KO fibroblast cultures which appear to

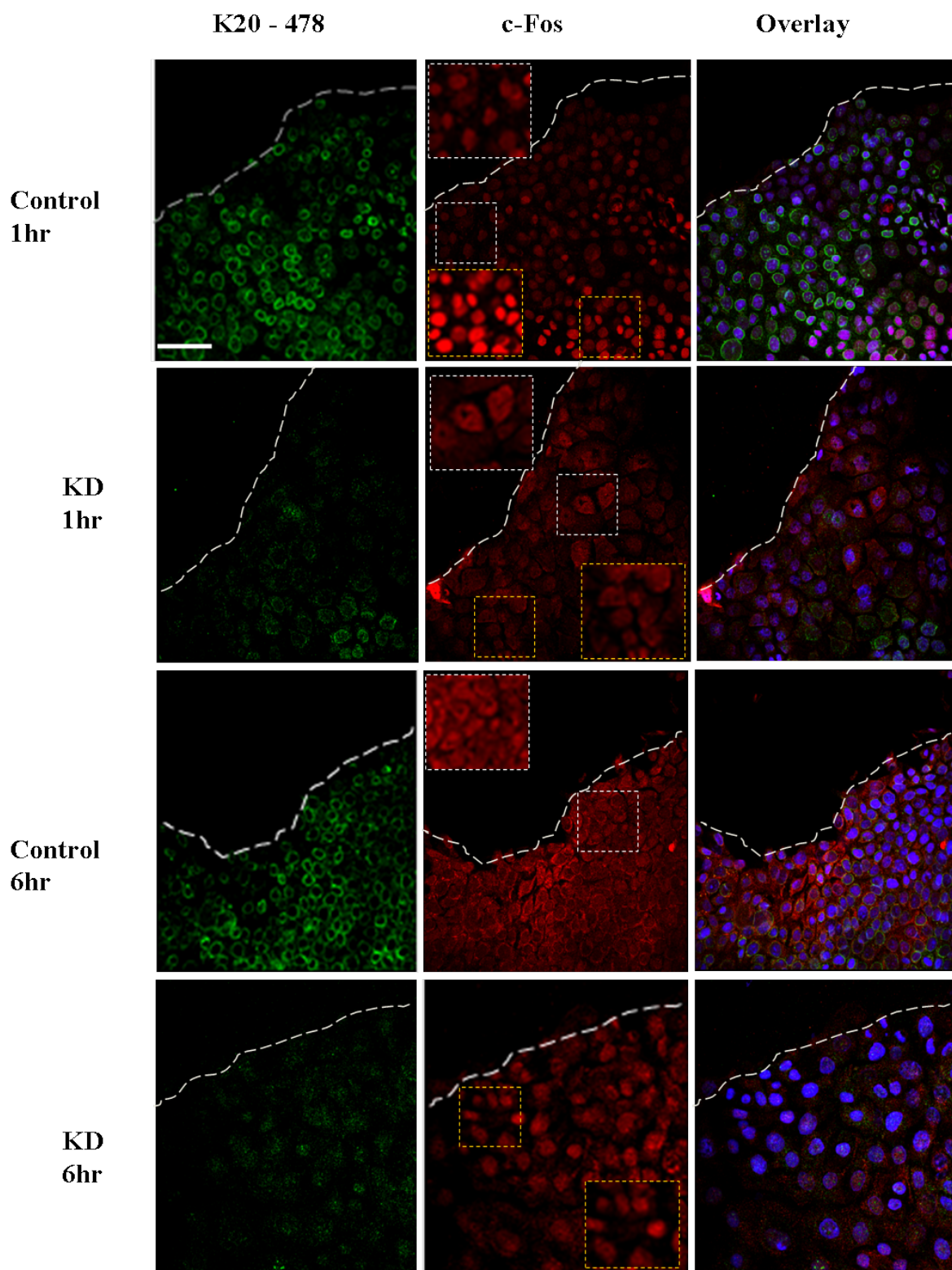


**Figure 2.18: c-Fos localization in control and Nesprin-2 KD HaCaT cells after scratching.** c-Fos localization was studied in control and Nesprin-2 KD cells by in vitro cell scratching, 1 hour and 6 hours after scratching. Nesprin-2 was detected by mAb K20-478, c-Fos was detected c-Fos polyclonal antibody, and nuclei were stained with DAPI. Inset with white dotted line indicates cytoplasmic (at the top corner) and yellow dotted line indicates nuclear localization (at the bottom corner) of c-Fos. Scale bar, 50 $\mu$ m

be in the early stage of apoptosis than in WT (yellow stained cells, indicated by red arrows) (Figure 2.19 B). Fibroblasts which lack Nesprin-2 may undergo apoptosis more frequently than WT fibroblasts which express good amounts of Nesprin-2. Nesprin-2 may be essential for the cells to perform proper functions. Once the nuclear morphology has changed like in Nesprin-2 KO cells, then these cells may undergo programmed cell death.

## **2.8 Caspase-3 in Nesprin-2 KO fibroblasts**

To confirm this data fibroblasts from WT and Nesprin-2 KO were stained with a Caspase-3 specific antibody. Caspases are crucial mediators of programmed cell death (apoptosis) and among them caspase-3 is a frequently activated death protease, catalyzing the specific cleavage of many key cellular proteins (Porter and Jänicke, 1999). The fibroblasts from Nesprin-2 KO and WT which were stained with Caspase-3 showed no difference with respect to staining. An analysis with acridine orange and ethidium bromide and also with Caspase-3 point to an increase in the number of apoptotic cells in Nesprin-2 KO compared to WT fibroblasts but the difference is not significant (Figure 2.20).

## **2.9 The Localization of SAFB1 has changed in Nesprin-2 KO fibroblasts**

Scaffold attachment factor-B1 (SAFB1) is a nuclear matrix protein that has been proposed to couple chromatin structure, transcription, and RNA processing. SAFB1 was shown to interact with TAFII68 (TATA Element-binding Protein-associated Factor), a member of the basal transcription machinery. Peroxisome proliferator activated receptors (PPARs) are members of nuclear hormone receptor family and functioning in transcription factors by regulating the expression of genes. PPARs they play several important roles in regulation of several cellular processes in-

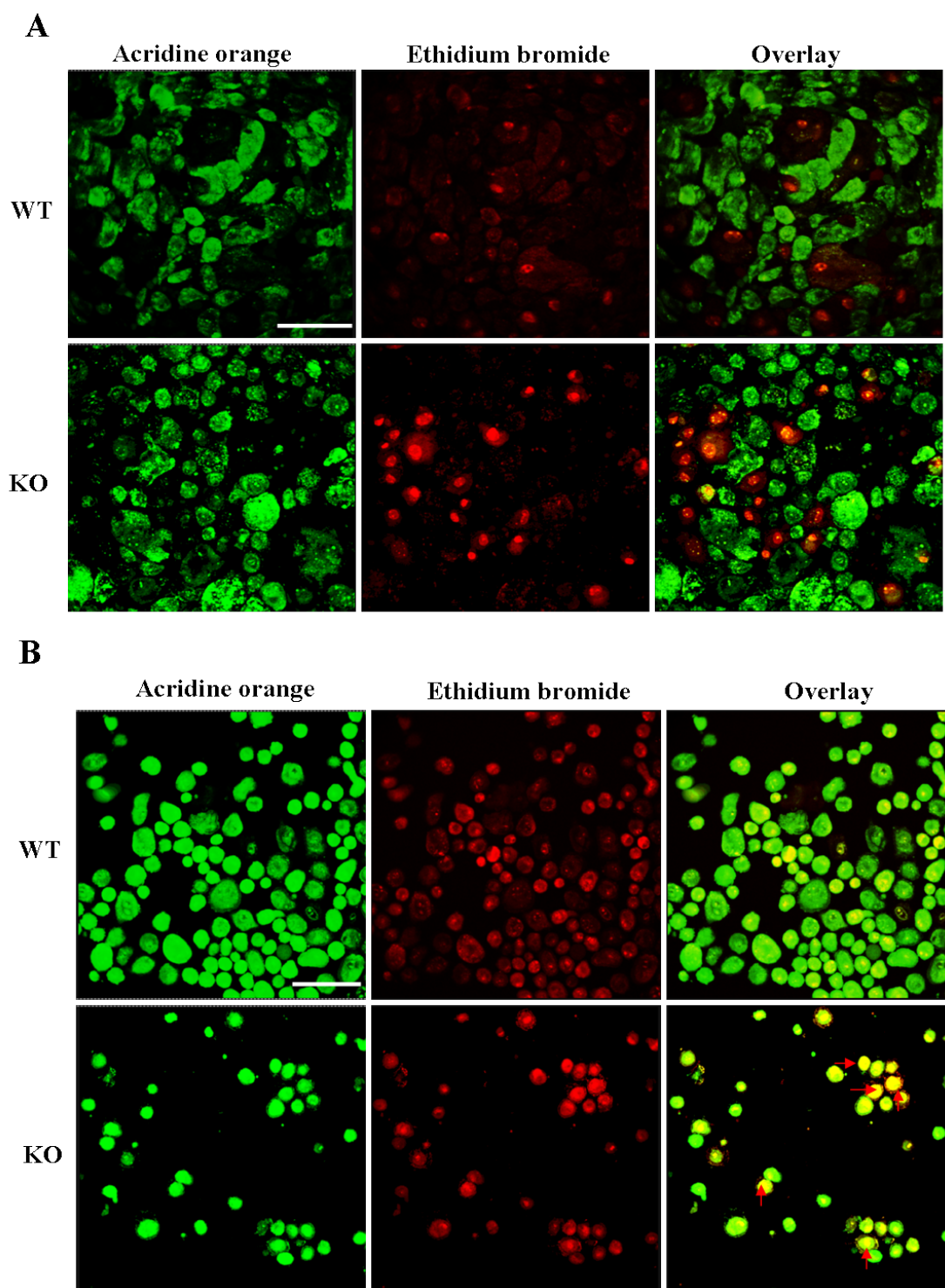


**Figure 2.19: Apoptosis in Nesprin-2 KO and WT fibroblasts.** (A) Apoptosis in Nesprin-2 KO and WT fibroblasts was studied by staining with acridine orange and ethidium bromide. Scale bar, 100 $\mu$ m. (B) Nesprin-2 KO fibroblasts show a higher number of cells in early stages of apoptosis (red arrows) than WT. Scale bar, 100 $\mu$ m.

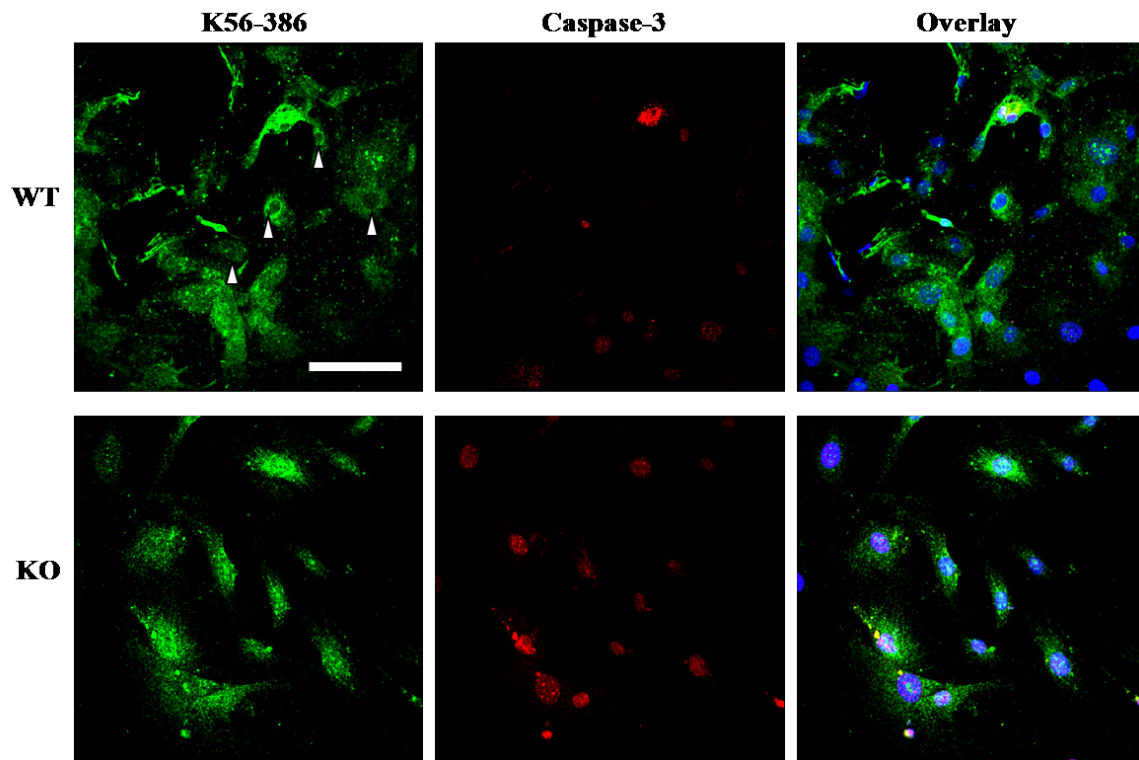


**Figure 2.20: Caspase-3 in WT and Nesprin-2 KO fibroblasts.** Fibroblasts from WT and Nesprin-2 KO were stained for the apoptosis marker Caspase-3 with Active Caspase-3 antibody (red). K56-386 antibody (green) detects Nesprin-2 at the NE (white arrow heads) and the nucleus is stained with DAPI (blue). Scale bar, 100 $\mu$ m.

cluding cell cycle, cell differentiation, proliferation and development (Fajas et al., 2003). Most of these nuclear receptors were regulated by SAFB1. SAFB (scaffold attachment factors) has at least two family members, SAFB1 and SAFB2 (Jiang et al., 2006). SAFB1 represses ER $\alpha$  activity via indirect association with histone deacetylase and interaction with the basal transcription machinery (Townson et al., 2004; Garee and Oesterreich, 2010). These function as estrogen receptor corepressor and play a role in cell proliferation. SAFB1 is exclusively nuclear while SAFB2 was detected in cytoplasm as well as the nucleus (Townson et al., 2003). SAFB1 is a nuclear protein which binds to DNA and the C-terminal domain of RNA polymerase II (Nayler et al., 1998). This binds to multiple nuclear receptors, mostly in a ligand-independent manner and inhibits their transcriptional activity.

In this way SAFB1 acts as a co repressor for nuclear receptors (Debril et al., 2005) I tested the expression and localization of SAFB1 in fibroblasts from WT and Nesprin-2 KO. The expression (intensity of staining) of SAFB1 showed no difference while the localization of SAFB1 has changed in Nesprin-2 KO fibroblasts to some extent. SAFB1 was found in the nucleus in WT, in Nesprin-2 KO fibroblast it was also found in the cytoplasm (white arrow heads) together with the nucleus (Figure 2.21).

The Activator protein-1(AP-1) complex members Fos and Jun are target genes of SAFB1 which are repressed by SAFB1 (Hammerich-Hille et al., 2010). Here our hypothesis is that SAFB1 regulates the activity of transcription factors PPAR  $\beta/\delta$  and c-Fos in WT cells. In Nesprin-2 KO cells, the activity of SAFB1 to regulate these transcription factors may be reduced because it is mislocalized to cytoplasm as well. The residual SAFB1 in the nucleus of KO cells may not be enough to regulate the transcription factors. This can be one of the reasons which cause a mislocalization of c-Fos in Nesprin-2 KD cells

## **2.10 Nesprin-2 Giant binds to heterochromatic DNA**

So far we have shown that the transcription of specific transcription factor genes and the subcellular localization of transcription factors are altered during wound healing in Nesprin-2 deficient mice and in KD HaCAT cells. Two mechanisms can be envisioned how Nesprin-2 affects gene expression. First, it could be involved in chromatin organization and generate a surrounding for genes which affects their transcription. The second possibility is that Nesprin-2 influences the activity and localization of transcription factors through a direct interaction or through its interaction with components of the NE such as lamin or emerin which have been shown to interact with several transcription factors (Dorner et al., 2007).

To test chromatin association directly we carried out chromatin immunoprecipita-

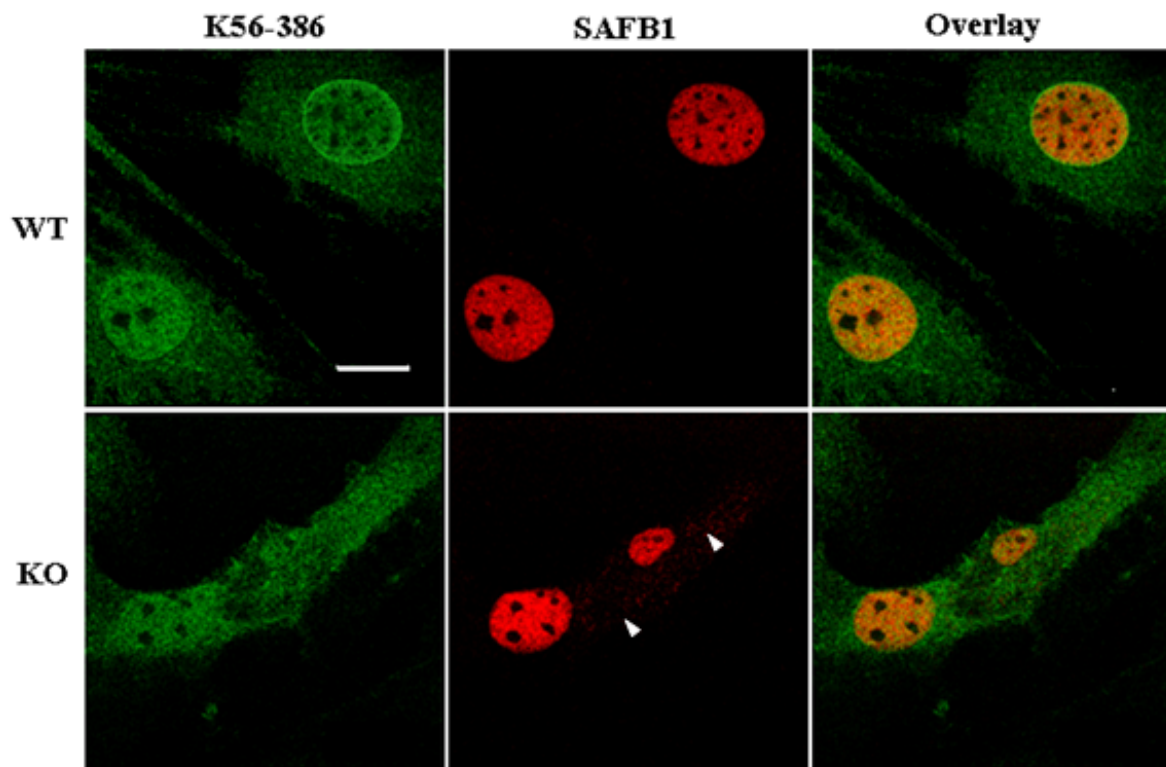


**Figure 2.21: Scaffold attachment factor-B1 (SAFB1) in WT and Nesprin-2 KO fibroblasts.** Nesprin-2 Giant was detected with mAb K56-386 (green) and SAFB1 with SAFB1 polyclonal antibodies. The arrows pointing the cytoplasmic presence of the SAFB1 in KO fibroblast. Scale bar, 20 $\mu$ m.

tion (ChIP) experiments with mAb K20-478-4 using HaCAT cells. The precipitated DNA was subsequently purified and processed for sequencing. The ChIP-Seq data were analysed and mapped onto the human genome. We found in repeated experiments that the majority of the sequences that could be uniquely mapped to the human genome (Mar. 2006 (NCBI36/hg18) assembly) represented centromere and other heterochromatic sequences derived from almost all chromosomes (71.64% and 81% heterochromatic sequences, respectively, Table 2.3). Since heterochromatic regions of most chromosomes are underrepresented in the hg18 assembly due to their repetitive nature we think that our mapping approach revealed only a part of all reads assignable to such regions. Significantly fewer reads were derived from coding sequences. Furthermore, the coding sequences were not identical

among the independent experiments whereas centromere and heterochromatic sequences were consistently observed. In experiments carried out in parallel with different antibodies no centromere and heterochromatin sequences were identified.

To get further evidence for a heterochromatin interaction we stained Nesprin-2 Giant deficient and WT fibroblasts with antibodies recognizing HP1 $\beta$  (Heterochromatin protein 1 $\beta$ ) (Figure 2.22). HP1 $\beta$  and the variant HP1 $\alpha$  are predominantly found in foci of constitutive heterochromatin (Dialynas et al., 2007). Staining with antibodies gives a speckled pattern overlaying a diffuse fluorescence. The number of speckles can vary depending on the cell type. A speckled pattern was obtained in wild type and mutant primary fibroblast, however the number of speckles varied. In wild type fibroblasts we counted  $10.2 \pm 7$  speckles per nucleus, in the KO fibroblasts the number was significantly reduced to  $7.6 \pm 6.8$  speckles (Table 2.4). The altered HP1 $\beta$  staining in the Nesprin-2 Giant deficient cells supports changes in heterochromatin.

Our data indicate that Nesprin-2 Giant associates primarily with heterochromatin and through this interaction it can affect the nuclear landscape and the transcriptional activity in the nucleus, whereas a mechanism in which Nesprin-2 Giant binds specifically to genes regulating cell proliferation and differentiation is less likely. Also, Nesprin-2 Giant may not act as a scavenger for c-Fos at the NE as we did not detect c-Fos in immunoprecipitates obtained with Nesprin-2 Giant specific antibodies. These results do however not exclude the possibility that Nesprin-2 Giant through interactions with its binding partners lamin or emerin which are known transcription regulators affects c-Fos and c-Fos mediated transcription indirectly.

Table 2.3: Chip-assay data showing the presence of centromere sequences in the ChIP carried out with mAb K20-478.

	ChromosomeTotal		Total reads per chromo- some Exp.1	Satellite		Satellite		Centromere		Centromere		Gene	
	reads	per chro- some		repeats Exp.1	repeats Exp.2	reads Exp.1	reads Exp.2	reads Exp.1	reads Exp.2	reads Exp.1	reads Exp.2	Gene	reads Exp.1
1	143057	59237	7068	6061	117062	41986	18927	11622					
2	47676	25093	9464	5870	23505	6322	15175	13369					
3	20927	11658	9820	2920	1332	504	10207	8234					
4	47671	17127	17542	7144	20856	7551	9273	3368					
5	18493	8235	4234	4186	2146	0	11609	4013					
6	64419	34602	5904	3082	52339	27550	6176	4712					
7	50061	24465	37875	2978	4176	16096	8010	5391					
8	66135	6593	3461	3210	53906	1858	8768	2525					
9	13259	5176	6676	3094	0	0	6583	2082					
10	142640	40650	1671	3401	132876	33001	6392	4752					
11	19515	6817	5204	1556	5131	0	8761	5261					
12	16449	9008	4062	2052	3597	972	8790	5975					
13	7872	4580	5406	1270	0	0	2934	4662					
14	12755	4069	6879	1260	1495	0	4381	3745					
15	8593	5161	3216	4789	0	0	5377	708					
16	37583	11073	35985	6933	0	0	1598	4140					
17	6495	8639	2332	1607	0	540	4130	6492					
18	49007	16408	3976	6040	35821	7843	4933	2525					
19	41319	15126	39059	12125	0	0	2260	3001					
20	5939	7949	1884	3233	1692	540	2363	4644					
21	2774	2095	0	1263	1874	0	900	832					
22	1953	2831	555	1296	0	0	1398	1535					
x	22136	6601	6469	2950	10466	2727	4735	924					
y	25005	12360	2683	5042	20954	6778	1368	0					
Sum	871733	345553	221425	93362	489228	154268	155048	104512					
% of total reads			25.40%	27.01%	56.12%	44.64%	17.78%	30.24%					

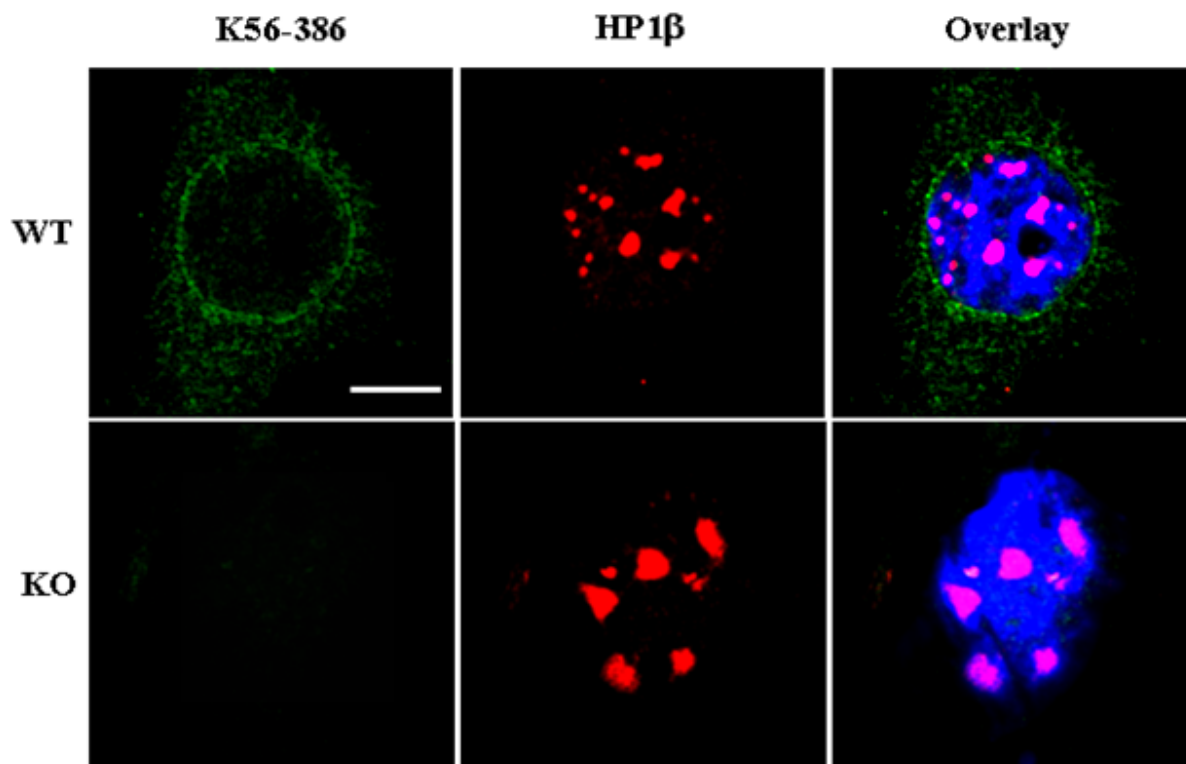


**Figure 2.22: Heterochromatin HP1 $\beta$  distribution in WT and Nesprin-2 KO fibroblasts.** Wild type and Nesprin-2 KO fibroblasts are stained with HP1 $\beta$  specific polyclonal antibodies to visualize constitutive heterochromatin accumulation. Scale bar, 10 $\mu$ m.

**Table 2.4: Quantification of the number of HP1  $\beta$  stained speckles.**

	No. of speckles/cell $\pm$ SD	No. of cells without Speckles $\pm$ SD
WT	10.24 $\pm$ 7.0	19.07 $\pm$ 21.67
KO	7.59 $\pm$ 6.8*	36.46 $\pm$ 23.94*

## **3 Discussion**

### **3.1 Transcriptional profiling in Nesprin-2 KO and WT fibroblasts**

To reveal further consequences of a loss of Nesprin-2 Giant in mice a transcription profiling was done using an Oligonucleotide microarray. We found that more than 50 genes were differentially regulated in Nesprin-2 KO fibroblasts. Among them were genes relating to the inflammatory process (SAA3, CCL2, Cxcl5, Ccl11 and angiopoietin 1), matrix associated and signal transduction genes (aggrecan, dystroglycan, chondroitin sulfate proteoglycan 5, collagen type 1 alpha 2, Decorin, guanylate cyclase activator 2b, lumican and Rap guanine nucleotide exchange factor 2 (RAPGEF2), cell cycle related and transcription regulation factors (cyclin-Ccni, TAF6 RNA polymerase II, TATA box binding protein(TBP) associated factor and bone morphogenin protein receptor, type II. It appears that Nesprin-2 affects the transcription of the genes which are involved in a variety of processes showing its functional diversity. Mouse primary dermal fibroblasts and keratinocytes lacking Nesprin-2 Giant had nuclei that were heavily misshapen displaying a striking similarity to nuclear deformations characteristic for laminopathies. Studies by other groups revealed that mutations in the human Nesprin-1 or -2 genes can cause disease states that until now were considered to be a consequence of mutations in lamin or in emerin (Zhang et al., 2007). Accumulating data suggest that the periphery of the nucleus provides a platform for sequestering transcription

factors away from chromatin. The principle of sequestering transcription factor c-Fos to the nuclear envelope by lamin A/C was shown earlier (Ivorra et al., 2006). Not only lamin A/C but also other INM proteins including emerin and MAN1 were shown to interact with transcription factors. Important for our work are the findings that several transcriptional regulators operating in different signal-transduction pathways physically interact with components of the inner nuclear membrane which bind directly to Nesprin-2 like Emerin and Lamin A/C. Furthermore, and the presence of Nesprin-2 at the NE is essential for proper localization of Emerin (Libotte et al., 2005; Lüke et. al 2008)

### **3.2 The wound healing process is accelerated during the early phase but showed a delay in the later phase in Nesprin-2 KO mice**

The LINC complex forms a connection between the nuclear lamina and cytoskeletal elements in the cytosol. Its importance is highlighted by the findings that mutations in LINC complex components can cause a variety of human diseases called laminopathies. From these findings the concept emerged that lamin A/C and its associated nuclear envelope proteins regulate gene expression through interactions with signaling processes, transcription factors and chromatin-associated proteins (Boban et al., 2009). Furthermore, defects in the LINC complex lead to adverse effects on actin mediated cellular functions including cell adhesion, cell migration and cell mechanics in laminopathic models (Hale et al., 2008). We could show that in migrating fibroblasts obtained from Nesprin-2 Giant KO mice the microtubule organizing center (MTOC) failed to reorient to a position between the leading edge and the nucleus (Lüke et al., 2008). As directional cell migration is essential for development, wound healing and immune function we carried out an in vivo analysis to test whether components of the LINC complex also control cell migration

in vivo i.e. in the wound healing process and to study the impact of these proteins during mechanical stress. Such experiments have not been done so far.

We observed a delay in wound healing at day 7 and day 10 in Nesprin-2 KO mice, whereas the early response was not affected. In fact, the Nesprin-2 KO mice showed faster closing of the wounds in the earlier phase of wound healing, the inflammatory phase. During this phase four signs of inflammation occur that include redness, swelling, heat and pain. The pain is caused by distension of tissue spaces due to swelling and pressure. These events attract inflammatory cells including neutrophils, mast cells and macrophages to the wound area (Gillitzer and Goebeler, 2001). These cells help in the wound healing process by acting as precursors for new tissue formation. We found more macrophages in wounds of Nesprin-2 KO mice and an up-regulation of the chemokine MCP1. Influx of macrophages to the wound site plays a critical role in the wound healing process. They promote the recruitment and proliferation of fibroblasts and express some of the key growth factors that stimulate angiogenesis (Lai et al., 2009). Enhancement of macrophages could explain the faster healing of the wound in Nesprin-2 KO mice in the inflammatory phase. Nesprin-2 might act indirectly in this process through other NE proteins like LBR or its binding partner emerin, which are involved in neutrophil development and activation (Squarzoni et al., 2000; Gainnes et al., 2008). Neutrophils are the first cells which arrive at the wound area in response to any mechanical damage followed by mast cells and monocytes that will subsequently differentiate into macrophages. The increase in the inflammatory cell population (mainly macrophages) immediately after tissue damage may cause the enhanced healing of the wounds during the early phases in Nesprin-2 KO mice.

### **3.3 Nesprin-2 regulates the cell proliferation and differentiation under the wound healing situation by affecting transcription factors**

Nesprin-2 KO skin did not show changes with respect to keratinocyte proliferation and differentiation when compared to WT skin in healthy mice (Lüke et al., 2008). However, under the wound healing situation keratinocyte proliferation declined in the KO mice. To test for a possible proliferation and differentiation defect we focused on transcription factors regulating these processes, namely Egr-1, PPAR $\beta/\delta$ , E2F1 and c-Fos, and observed slight alterations in the accumulation of the PPAR $\beta/\delta$ , Egr-1 and E2F1 transcripts in mutant wounded skin. Egr-1 expression was reduced at day 1, 3 and 5 as compared to WT and PPAR $\beta/\delta$  was also reduced at these time points in the Nesprin-2 KO wound. PPAR $\beta/\delta$  is one of the targets of Activator protein-1 (AP-1) and in the WT situation its expression is strongly enhanced in keratinocytes after skin injury. This upregulation in the expression of PPAR $\beta/\delta$  in WT wounds or its downregulation in Nesprin-2 wounds is of functional importance because heterozygous and in particular homozygous ppar $\beta/\delta$  knockout animals showed a significantly reduced rate of reepithelialisation. The enhanced expression of PPAR  $\beta/\delta$  might be a critical factor required for wound reepithelialisation (Michalik et al., 2001; Tan et al., 2005). The observed delayed wound healing or reepithelialisation in Nesprin-2 KO mice could be a result of reduced expression of PPAR $\beta/\delta$ .

The early growth response transcription factor-1 (Egr-1) is a member of the Egr family of zinc-finger transcription factors. The upregulation of Egr-1 in excisional mouse and rat wounds, resulted in the upregulation of platelet-derived growth factor, VEGF and TGF- $\beta$ 1 and this was accompanied by enhanced wound angiogenesis, reepithelialization, collagen deposition and wound contraction (Bryant et al., 2000). Therefore, Egr-1 seems to enhance different aspects of wound healing. The

down regulation of Egr-1 in Nesprin-2 KO mice might be responsible for a reduced rate of reepithelialization and in turn to reduced wound healing.

Among the E2F transcription family members, E2F1 is unique in its ability to regulate a number of key genes that participate in both cell cycle progression and apoptosis, providing a potential link with its role in tumorigenesis (Fang and Han, 2006). There is several studies showing that E2F1 behaves as both an oncogene and a tumor suppressor gene. On one hand, enhancement of E2F1 activity in tissue culture cells can stimulate cell proliferation and be oncogenic. On the other hand, E2F-1 has been demonstrated as a tumor suppressor by spontaneous development of multiple tumors in mice lacking E2F1. Overexpression of E2F-1 suppressed the expression of differentiation markers (transglutaminase type 1 and keratin 10) in differentiated keratinocytes (Dyson, 1998; Bell and Ryan, 2004).

The expression of transcription factor E2F1 was found increased in Nesprin-2 KO wounds as compared to WT wounds. Some of the earlier work demonstrated that E2F family members, particularly E2F-1 may play a dual role as both a regulator of proliferation and a suppressor of differentiation in keratinocytes. In this study Dicker et al., (2000) showed that overexpression of E2F-1 in human keratinocytes can inhibit the induction of differentiation specific genes.

E2F1 transcript levels are slightly increased in Nesprin-2 KO compared to WT. E2F1 activity is essential for proper epidermal morphogenesis and keratinocyte proliferation. In differentiating keratinocytes, Ca<sup>2+</sup> induced protein kinase C (PKC) activation downregulates E2F1 by activating p38 $\beta$  mitogen-activated protein kinase (MAPK) (Ivanova et al., 2006). Murine keratinocyte differentiation is associated with loss of E2F1/pRb DNA-binding complexes (D'Souza et al., 2001). E2F1 downregulation may be a prerequisite for proper differentiation of various cell types as exogenous E2F1 expression prevents terminal differentiation in various cells (Scheijen et al., 2003; Porse et al., 2001; Paramio et al., 2000). Together, a decrease in PPAR $\beta/\delta$  Egr-1, an increase in E2F1 expression and re-localization of

c-Fos to the cytoplasm may cause the slowing down of proliferation in Nesprin-2 KO mice. It is possible that this line of events is caused by a loss of some cellular signal which is normally transduced from the cell surface to the nucleus through the LINC complex with Nesprin-2 as one of its components or in response to mechanical damage (Figure 3.1. model).

c-Fos together with c-Jun forms the transcription factor AP-1. AP-1 binds to DNA at AP-1 sites which are present in the promoter regions of many genes including collagen-encoding genes and collagenase (Setoyama et al., 1986; Schonthal et al., 1988). The Fos and Jun gene families of proto-oncogenes encode nuclear proteins that are associated with a number of transcriptional complexes and proliferative processes (Angel and Karin, 1991). In non scratched control human keratinocytes (HaCaT) c-Fos localized clearly in the nuclear compartment. c-Fos, c-Jun and their family members are activated following various kinds of extracellular stimuli such as mitogens, growth factors or mechanical stimuli (Greenberg and Ziff, 1984; Okada et al., 1988; Wang and Johnson, 1994, Nogami et al., 1999). Localization of c-Fos and Jun members (B-Jun, c-Jun and D-Jun) are restricted to nuclei in unwounded epidermis.

When we studied c-Fos in the wounded tissue we found that c-Fos localized to the nucleus in both WT and KO at 1DAW. c-Fos cycles between nucleus and cytoplasm in the subsequent time points in keratinocytes in WT wounds. In contrast, in Nesprin-2 KO wounds, c-Fos is confined more to nucleus than the cytoplasm. Also, keratinocytes in Nesprin-2 KO wounds did not show much variation with respect to c-Fos localization as it shows nuclear staining in many of the cells. At day 10 c-Fos intensity was reduced in the KO compared to WT. Similar results were obtained for HaCaT cells in which Nesprin-2 expression was reduced by shRNA knockdown and which were scratched to mimic the in vivo wound healing situation. In control HaCaT cells we found a gradient type of localization of c-Fos. In the cells 1 hour after scratching it is localized to nucleus and 6 hours after scratching it moved to

the cytoplasm. In Nesprin-2 KD cells c-Fos is localized more in the nuclear compartment (both 1 hour and 6 hours after scratching). Earlier studies support our findings for the localization of c-Fos in control and Nesprin-2 KD cells. From our observation we hypothesize that a distinct localization of c-Fos in WT wounds and control scratched cells leads to proper functioning of c-Fos. c-Fos in Nesprin-2 KO wounds and KD scratched cells did not shuttle between the nucleus and the cytoplasm to the same extent as in wild type which can restrict its functioning in cell proliferation. This was observed mainly in keratinocytes.

There are two hypotheses through which lamins regulate the cell structure and gene expression and cause various disease phenotypes. The 'structural' hypothesis proposes that mutations in A-type lamins or emerin give rise to a weakened nuclear envelope, which is predisposed to damage. In striated muscle particularly damage to the nucleus is thought to promote myocyte death and cause replacement with fatty and fibrotic tissue (Gotzmann and Foisner, 2005). The 'gene expression' hypothesis proposes that, as A-type lamins are important regulators of gene expression, mutations in these proteins will alter their interactions with various gene regulatory proteins and thereby promote disease in different tissues (Cohen et al., 2001; Wilson et al., 2001; Hutchison and Worman, 2004). There is evidence to support each hypothesis, with a consensus emerging that structural weakness and altered gene expression both contribute to pathogenesis. Nesprin-2 also functions in these pathways and contributes to the structural and gene expression hypothesis either by interacting with Lamin A/C or with other INM proteins. Assuming the 'structural hypothesis' to be functional Nesprin-2 regulates the morphology of the nucleus. Nesprin-2 is one of the factors which are essential for maintaining the proper shape and the size of the nucleus. Considering a functioning of Nesprin-2 in the context of the 'gene expression hypothesis', it may regulate the expression of transcription factors c-Fos, PPAR  $\beta/\delta$  Egr-1 and E2F1 which are associated with

cell proliferation. Nesprin-2 functioning under these hypotheses may not be independent, instead it may act together with further interaction partners.

### **3.4 A disturbed F-actin network can cause the impaired myofibroblast differentiation in Nesprin-2 KO mice**

The new tissue formation and tissue remodeling phase of wound healing is characterized by wound contraction due to the action of fibroblasts. Fibroblasts which migrate to the wound area and differentiate into myofibroblasts were also reduced in Nesprin-2 KO wounds which led to reduced granulation tissue area. The granulation tissue helps to generate a contraction in the wound area mainly in the dermis. Myofibroblasts are the specialized fibroblasts that develop the contractile property and contribute to tissue contraction. With the development of a contractile property, the myofibroblasts acquire specific structural features associated with the generation and transmission of contractile force: bundles of actin microfilaments (called actin stress fibers), vinculin-containing fibronexus adhesion complexes and fibronectin (FN) fibrils (Singer et al., 1984; Welch et al., 1990). The actin cytoskeleton is important in processes that are fundamental to wound healing, cell migration, contraction, adhesion and proliferation. It is dynamic and remodelled in response to a variety of stimuli to generate the mechanical forces necessary for changes in cell contraction, adhesion and motility that underpin tissue repair (Cowin et al., 2006). Myofibroblast differentiation was studied by alpha smooth muscle actin ( $\alpha$ -SMA) where we found that the staining intensity was reduced in Nesprin-2 KO wounds. Reorganization of the actin cytoskeleton is a fundamental process during wound remodeling. Nesprin-2 as an actin binding protein regulates the formation and stability of F-actin filaments and through this activity it might be involved in regulation of fibroblasts

differentiation. To observe F-actin distribution and stress fiber development WT and Nesprin-2 KO fibroblasts were cultured in vitro and stained with TRITC phalloidin. We found extensive arrays of F-actin stress fibers in WT primary dermal fibroblasts, while F-actin fiber formation was diminished in Nesprin-2 KO fibroblasts. The actin filaments were completely absent around the nucleus in the majority of the KO fibroblasts. When probed with a  $\beta$ -actin specific antibody we detected a dotted staining around the nucleus. This impairment in the formation of stress fibers in the Nesprin-2 KO fibroblast may be the major cause for reduced fibroblast differentiation. Reduced fibroblast differentiation into myofibroblast again resulted in reduced wound contraction and delay in wound healing.

### **3.5 Fate of the cells which showed nuclear deformation in Nesprin-2 KO mice (an apoptotic approach)**

Nesprin-2 Giant being a member of LINC complex (Linker of Nucleoskeleton and Cytoskeleton) and present at the nuclear envelop, connects the nuclear material to cytoskeleton through the interaction with the actin cytoskeleton. Nesprin-2 was also found to regulate the shape of the nucleus, as Nesprin-2 absence in primary mouse fibroblasts and keratinocytes showed blebbing and a honey comb structure instead of a round nucleus (Lüke et al., 2008). The nucleus regulates the integrity of genes and gene expression, being referred to as the control center of a cell. When such an important structure is impaired in the cell in terms of its shape, what would be fate of those cells? Important would be to know whether these cells undergo programmed cell death, i.e. apoptosis. To study the fate of the cells, mouse primary fibroblasts were treated with acridine orange and ethidium bromide. Ethidium bromide which stains nucleic acid can penetrate through the damaged cell membrane of dead cells and bind to DNA. When the cells treated with ethidium

bromide are exposed to ultraviolet light will fluoresce with an orange colour. In this experiment we noted a slightly higher number of dead cells for Nesprin-2 KO cells. Apoptosis was also assessed by immunofluorescence detection of the active form of Caspase-3, a key member of the caspase family involved in cellular self-destruction (Marcotte et al., 2004) in fibroblasts. There are many cells which showed early stages of apoptosis in case of Nesprin-2 KO fibroblasts. Nesprin-2 which regulates nuclear morphology might have an impact on the programmed cell death as the number of apoptotic cells in Nesprin-2 KO increased (though not significant) compared to WT.

### **3.6 Nesprin-2 interacts with heterochromatin and associates with chromatin**

There has been considerable interest in the way in which chromatin is spatially organised within the nucleus and how that may relate to gene expression and its control. From our study we propose that Nesprin-2 Giant has two important roles in wound healing (A) through its capacity as actin-binding protein and (B) through its interaction with chromatin. (A) At the ONM it interacts with F-actin and is responsible for the correct formation of the actin cytoskeleton around the nucleus. Through this interaction it may also be connected to the plasma membrane and the extracellular matrix. At the NE it interacts with SUN proteins located in the INM and the underlying nuclear lamina. The nuclear lamina components themselves can interact with transcription factors and through this chain of interactions Nesprin-2 may affect transcription. Loss of Nesprin-2 Giant leads to a loss of F-actin around the nucleus and signals from the extracellular matrix are no longer transmitted through the actin cytoskeleton to the NE and the nuclear lamina. (B) Heterochromatin is mainly located near the nuclear envelope where it interacts with Nesprin-2 Giant. The DNA which we could map onto the

human chromosomes was derived to a large part from human centrosomes and heterochromatin. We propose from these findings that Nesprin-2 Giant is involved in organising the chromatin and providing an anchor for mainly heterochromatic DNA. In general heterochromatic DNA is considered transcriptionally inactive although results from several studies showed the involvement of heterochromatin protein (HP 1) in DNA repair and other cellular processes (Ball and Yokomori, 2009). Loss of Nesprin-2 Giant from the NE leads to rearrangements of the chromatin affecting transcription. As the changes in the Nesprin-2 Giant KO mice were only observed under physiological stress conditions, there must be other proteins which ensure a correct arrangement of the chromatin and functioning of the cell. Such a mechanism is vital for a cell to survive adverse conditions as during mechanical stress.

### **3.7 Model for Nesprin-2 Giant function in wound healing**

In the wild type situation Nesprin-2 interacts with F-actin and regulates its distribution around the nucleus. In the nucleoplasm it binds with and regulates the functioning of extracellular signal-regulated kinases (ERK or MAPK 1/2) (Warren et al., 2010). It further interacts with SUN domain proteins, Lamin and also with centromeric and heterochromatin DNA. Through these interactions Nesprin-2 might be one of the main linkers which transduce the signal from TGF  $\beta$ 1 at the focal adhesion to the transcription factor on the chromosome to perform proper cellular functions. We concentrated mainly on those transcription factors (c-Fos, PPAR  $\beta/\delta$ , Egr-1 and E2F1) which play a role in cell proliferation and differentiation.

When Nesprin-2 is absent in the cell, there will be loss of actin filaments around the nucleus. Nesprin-2 also acts on the nuclear landscape as we found reduced

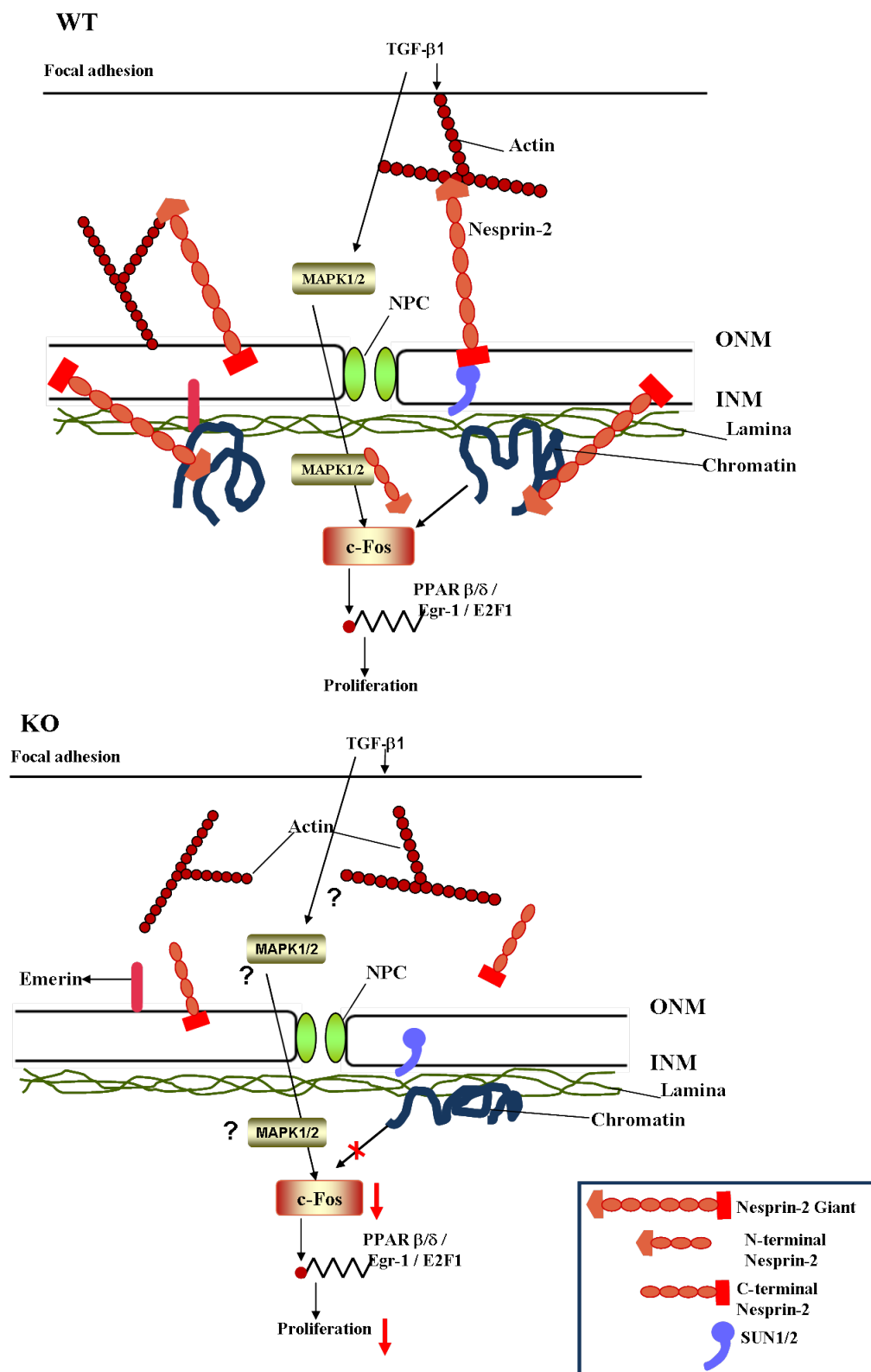


**Figure 3.1: Model for Nesprin-2 Giant function in wound healing.** WT- Nesprin-2 binds to actin in the cytoplasm and to heterochromatin in the nucleoplasm. This arrangement mediates the transduction of the signal from extracellular matrix to the nuclear compartment.

KO- Nesprin-2 binding to F-actin is lost along with the localization of F-actin around the NE. The absence of Nesprin-2 disturbs the signal transduction.

heterochromatin protein (HP1 $\beta$ ) speckles. In the WT situation Nesprin-2 mediates the signal transduction from focal adhesion to the nuclear compartment. Once Nesprin-2 is lost, transcription factors may fail to get signals from focal adhesions to perform normal cellular functions and fail to respond to mechanical stress. When cells and tissue are mechanically damaged as in wound healing, they undergo different kinds of stress like change in cell shape, loss of connection with neighbouring cells. Then cells need to overcome this stress to perform normal functioning. During this process cells migrate, proliferate and try to connect neighbouring cells to fill the gap caused by mechanical damage. All of these functions occur within the cell nucleus. The nucleus needs a signal from outside; such a signal is believed to be mediated by Nesprin-2. Once this link is lost due to the absence of Nesprin-2 then cell functions, proliferation and differentiation are delayed, though not completely lost. It is possible that other Nesprin-2 isoforms may take over some of these functions.

We found that Nesprin-2 Giant binds to heterochromatin which gives a strong evidence for the localization of Nesprin-2 in the nuclear compartment. Many of the models from earlier work showed that small isoforms of Nesprin-2 may localize within the nucleus and that the Giant isoform is restricted to the ONM (Zhang et al., 2005; Warren et al., 2005; Haque et al., 2010; for an alternate view: Libotte et al., 2005). These assumptions should be reconsidered in the view of our findings.

# 4 Materials and Methods

## 4.1 Kits and Reagents

Details regarding the following procedures are not included in this section: Standard molecular biological techniques were carried out as described (Sambrook et al., 1989). Instruments used were from the departmental facility.

### Kits

FairPlay Microarray Labeling kit	Stratagene
RNeasy Mini kit	Qiagen
RNeasy Midi kit	Qiagen
Cell Line Nucleofector Kit V	Amaxa
Immunohistochemical staining	DAKO

### Reagents

(2-ethansulfonic acid)]	Sigma-Aldrich
(Low/LMW and high/HMW)	GE Health care
1 kb DNA-marker	Bioline
4,6-Diamidino-2-phenylindol (DAPI)	Sigma
Acetic acid	Riedel-de-Haen
Acridine Orange	Sigma-Aldrich
Acrylamide (Protogel: 30: 0.8 AA/Bis-AA)	National Diagnostics

Agarose	Biozym
APS (Ammoniumperoxodisulfate)	Fluka
Benzamidine	Sigma-Aldrich
Boric acid	Merck
Bromophenol blue	Serva
Bromophenol blue (Na-salt)	Serva
BSA	Roth
Chloroform	Riedel-de-Haen
Coomassie-brilliant-blue R250	Serva
Cyanin3 and Cyanin5	Amersham
DEPC	Sigma
Dispase II	Roche
DMSO (Dimethyl sulfoxide)	Merck
DTT (1, 4-dithiothreitol)	Gerbu
EDTA (Ethylenediaminetetraacetic acid)	Merck
EGTA	Sigma
Eosine	Fluka
Ethanol	Riedel-de-Haen
Ethidium bromide	Sigma-Aldrich
Ethidium bromide	Sigma
FBS (fetal bovine serum)	Sigma-Aldrich
Fish DNA	Roche
Formaldehyde	Sigma-Aldrich
Formamide	Merck
Glucose	Sigma-Aldrich
Glycerol	Oxoid
Glycine	Degussa

Haematoxyline	Merck
HEPES	Biomol
High molecular weight protein marker	Amersham Biosciences
Immumount	Thermo Life Science
IPTG (isopropyl $\beta$ -D-thiogalactopyranoside)	Sigma-Aldrich
isopropanol	Merck
Ketavet	Pharmacia & Upjohn BGA
Low molecular weight protein marker	Amersham Biosciences
Methanol	Riedel-de-Haen
MOPS	Gerbu
MOPS (g-[Morpholino] propanesulfonic acid	Gerbu
N, N, N', N'-tetraacetic acid]	Sigma-Aldrich
Nonidet-P40 (Nonylphenyl-polyethylenglycerine)	Fluka
Paraformaldehyde	Sigma-Aldrich
Paramount	Fisher Scientific
p-coumaric acid	Fluka
Phalloidin FITC-conjugated	Sigma-Aldrich
Phalloidin TRITC-conjugated	Sigma-Aldrich
Ponceau S-concentrate	Sigma-Aldrich
Prestained marker	Fermentas
Protein marker	GE Healthcare
Quantitect SYBR® green real time PCR kit	Qiagen
Rompun	Bayer
SDS	Serva
SDS (sodium dodecylsulfate)	Serva
Sodium acetate	Merck
Sodium azide	Merck

Sodium hydroxide	Riedel-de Haen
Sucrose	Fluka
TEMED (tetramethylethylenediamine)	Merck
Tris (hydroxymethyl) aminomethane	Sigma-Aldrich
Triton-X-100 (t-octylphenoxypolyethoxyethanol)	Merck
TRIZOL	Gibco
Tween 20 (Polyoxyethylensorbitanmonolaurate)	Sigma-Aldrich
$\beta$ -mercaptoethanol	Sigma-Aldrich

## 4.2 Oligonucleotides

Oligonucleotide primers used for PCR were designed from <http://frodo.wi.mit.edu/primer3/>

### List of Oligonucleotides used

Oligo name	Sequence
SAA3 F	5' GCTGGTCAAGGGTCTAGAGAC 3'
SAA3 R	5' GGACCCGACGATTTTCAGTAGTC 3'
MCP1 F	5' GAAGCTGTAGTTTTTGTCCACCAAGC 3'
MCP1 R	5' GCATTTAGACTTCGATTACGTAGGTGA 3'
PPAR $\beta/\delta$ F	5' CACAACGCACCCTTTGTCATCCAC 3'
PPAR $\beta/\delta$ R	5' CTGGTCCACTGGGAGGAGTTCATACC 3'
Egr 1 F	5' GCACCTGACCACAGAGTCCTTTTC 3'
Egr 1 R	5' TTAGGAGGCTGGAGAAAGTAGGAGC 3'
E2F1 F	5' CCACCCAGGGAAAGGTGTGAAATC 3'
E2F1 R	5' GGTTCTTAGTATAGGTCACCGATCC 3'
c-Fos F	5' CCGAGCCCTTTGATGACTTCCTG 3'
c-Fos R	5' GGCCACCAGTGGACATGAGGGTC 3'
c-Jun F	5' GAGCAGGAGGGCTTCGCCG 3'
c-Jun R	5' GGTTGGAGTCGTTGAAGTTGG 3'

## 4.3 Enzymes and Antibodies

### List of Enzymes used

Enzymes	Suppliers
Pfu DNA polymerase	Promega
Proteinase K	Sigma
RNasin Ribonuclease Inhibitor	Promega
StrataScript Reverse Transcriptase	Stratagene
T4 DNA ligase	Boehringer
Taq-polymerase	Boehringer

### Primary antibodies

Name	Host and reactivity	Catalog No.	Supplier/reference
F4/80	Rat anti mouse monoclonal	MCA497R	Serotec
K14	Mouse anti mouse polyclonal	PRB-155P	Covance
Ki67	Rat anti mouse monoclonal	M7249	Dako
$\alpha$ SMA- Cy3 con- jugated	Mouse anti huma, mouse, rat	A5228	Sigma
c-Fos	Rabbit anti mouse polyclonal	sc-52	Santa Cruz Biotechnology
$\beta$ -actin	Mouse anti mouse, human	A5316	Sigma Aldrich
SAFB1	Rabbit anti mouse,human polyclonal	NB100-2593	NOVUS Biologicals
K20-478	Mouse anti human monoclonal	BiochemistryI	Zhen et al., 2002
K56-386	Mouse anti mouse monoclonal	Biochemistry	Lüke et al., 2008
pAbK1	Rabbit polyclonal	BiochemistryI	Libotte et al., 2005
Active Caspase 3	Rabbit monoclonal anti mouse,human and rat	8G10	Cell Signaling

## Secondary antibodies

<b>Name</b>	<b>Supplier</b>
Alexa 568 (goat anti mouse)	Sigma Aldrich
Alexa 488 (goat anti rat)	Sigma Aldrich
Alexa 488 (goat anti mouse)	Sigma Aldrich
Alexa 568 (goat anti rabbit)	Sigma Aldrich
Alexa 488 (goat anti rabbit)	Sigma Aldrich
Peroxidase conjugated (goat anti rabbit)	Sigma Aldrich

## 4.4 Media, Buffers and solutions

### Media and Buffers

All media and buffers were prepared with deionized water, filtered through an ion exchange unit (Membra Pure). The media and buffers were sterilized by autoclaving at 120°C and antibiotics were added to the media after cooling to approx. 50°C.

### 10x MOPS, pH 7.0/pH 8.0 (adjusted with NaOH)

41.9 g MOPS, 7 ml 3 M sodium acetate, 20 ml 0.5 M EDTA, add H<sub>2</sub>O to make 1 liter

### 10x NCP buffer, pH 8.0

12.1 g TrisHCl, pH 8.0, 87.0 g NaCl, 5.0 ml Tween 20, 2.0 g sodium azid, add H<sub>2</sub>O to make 1 liter

### 1x PBS, pH 7.4

8.0 g NaCl, 0.2 g KH<sub>2</sub>PO<sub>4</sub>, 1.15 g Na<sub>2</sub>HPO<sub>4</sub>, 0.2 g KCl dissolved in 900 ml deionized H<sub>2</sub>O, adjust to pH 7.4, add H<sub>2</sub>O to make 1 liter, autoclave

**20x SSC, pH 7.0**

3 M NaCl, 0.3 M sodium citrate

**PBG, pH 7.4**

0.5% bovine serum albumin, 0.1% fish gelatin in 1x PBS, pH 7.4

**Towbin buffer**

Glycin (39 mM)

Tri/HCl pH 8.3 (48 mM)

SDS (0.0375%)

EtOH (20%)

**Gel drying buffer**

EtOH (50%)

Glycerin (5%)

Water (45%)

**Destainig solution**

EtOH (5%)

Acetic acid (7%)

Water (88%)

**Lysis buffer**

Tri/HCl, pH 7.5 (50 mM)

NaCl (150 mM)

Nonidet P-40 (1%)

Na-desoxycholate (0.5%)

SDS (1%)

Protase inhibitor cocktail (1 mM)

**5 x SDS-Sample buffer**

Tris/HCl, pH 6.5 (0.5 M)

SDS (4%)

Glycerol (20%)

$\beta$ -Mercapto ethanol (1.43 M)

Bromophenol blue

**10 x SDS-PAGE running buffer**

Tris (0.25 M)

Glycine (1.9 M)

SDS (1%)

ECL (enhanced chemiluminescence)

Tris/HCl, pH 8.5, 2ml

Luminol 200  $\mu$ l

p-Cumaric acid 89  $\mu$ l

H<sub>2</sub>O-6 $\mu$ l

## **4.5 Nesprin-2 Giant knock out mice**

The Nesprin-2 Giant knock out mice generation has been described (Lüke et al., 2008). Animals were backcrossed into the C57Bl6 background for seven generations. All animals used in the wound healing studies were females between 4 and 6 months of age; age and sex-matched littermates were used as controls. Animals were housed in specific-pathogen-free facilities and all animal protocols were approved by the local veterinary authorities. For fibroblast isolation 2-4 days old new born mice were used.

## **4.6 Isolation of primary fibroblasts**

New born mice were killed by decapitation and disinfected the body in ethanol and then with 1X PBS. Transfer the body to a sterile dish and made two lengthwise incisions on dorsal side from head end and then widen the skin with a blunt end scissor towards tail. Cut the skin and rinse with ice cold PBS. Fat was removed from the skin carefully. Stored this skin in 4<sup>0</sup>C overnight with Dispase (10mg/ml), which helps to separate dermis from epidermis by cleaving fibronectin and collagen. Then next morning dermis was peeled off from epidermis under sterile condition. Fibroblasts were isolated from the dermis by culturing in DMEM medium.

## **4.7 Wounding**

Mice were anesthetized by intraperitoneal injection of Ketavet (Pharmacia Upjohn BGA Reg.Nr.8994) + 250 l Rompun, 2%, (Bayer Nr.1061). Four 5mm circular full-thickness wounds were created on the dorsal side of the mouse by excising skin and the subcutaneous muscle panniculus carnosus using CellSafe Biopsy kapseln. Wounds were left uncovered, photographed at the indicated time points and harvested at 1, 3, 5, 7 and 10 days after wounding. At each time point 6 mice were sacrificed from WT and Nesprin-2 KO. Macroscopic wound closure was determined using Image J programme (NIH) measuring open wound area.

## **4.8 Wound tissue harvesting and sectioning**

At each time point mice were sacrificed and complete wounds were removed including a small area of normal skin around the wound. The tissue was either frozen for protein lysate preparation, RNA isolation, or embedded in paraffin and optimum

cutting temperature (OCT). Before embedding in the paraffin the wound skin was fixed in 4% paraformaldehyde solution for 4 hours. Circular wounds were bisected caudocranially at the midpoint of the wound and fixed in paraformaldehyde separately. Sixµm sections were generated using Thermo Scientific microm hm 355 S and collected on MENZEL-GLÄZER SUPERFROST PLUS slides and further used for immunohistochemistry and immunofluorescence.

## **4.9 Histological staining**

To measure distance between the epidermal migrating tips and granulation tissue area sections were stained with Haematoxylin and Eosin (HE) and Sirius red respectively. Before staining any paraffin sections, they were treated as follows

### **Deparaffination**

Incubate the sections in xylene 3 times for 5 minutes

Treat in different concentration of alcohol- 96%, 90%, 80%, 70%, 50% and 30% for 5 minutes

Then dehydrate the sections with deionised water

Incubation in Haematoxylin for 5 minutes

Wash with HCL and then with water

Incubate in Eosin for 2-4 minutes

### **Differentiation**

70% ethanol

96% ethanol

Isopropanol

Xylene

### **Mounting**

Mount the sections with paramount

## **4.10 Immunohistochemistry and Immunofluorescence**

For Immunohistochemistry and Immunofluorescence with antibody each section was deparafinized with xylene and different dilution of ethanol as mentioned before. Additionally antigen retrieval is done by boiling the section in Citrate buffer or in Dako Target retrieval solution. Then incubate with primary antibody and after several wash with PBS buffer sections were incubated with secondary antibody. Then sections were mounted in Immumount. For immunohistochemistry Haematoxylin was used for counterstaining nucleus.

## **4.11 Western blotting**

The proteins resolved by SDS-PAGE were electrophoretically transferred from the gel to the nitrocellulose membrane at 15 V for 45 minutes. The membrane had been pre wet with water followed by Towbin buffer. After transferring the proteins, membrane was blocked with 5% milk solution in 1 x NCP and probed with different dilutions of the respective primary antibodies and horse radish peroxidase (POD) conjugated secondary antibodies. Antigens were detected by enhanced chemiluminescence (ECL).

### **Preparation of protein lysis from tissue and cells**

Fully confluent HaCaT KD and control cells were washed with PBS and the cells scraped off using PBS with protease inhibitor. Cells were pelleted by centrifugation at 1500 rpm for 5 minutes. Pellets were dissolved in lysis buffer and homogenize the pellet by drawing through 0.4mm syringe. Incubated on the ice for 15 minutes and then sonicated to shear genomic DNA with 50% permanent sonication. Then the sample was boiled at 95°C for 5 minutes for denaturation of proteins.

To prepare protein lysate from skin tissue- weight of the skin tissue was measured and then shock freezed in liquid N<sub>2</sub> or dry ice. Homogenize with pestle and mortar with liquid N<sub>2</sub>. Then homogenize in presence of 400µl lysis buffer using ULTRA TURRAX. Sonicate the homogenized sample and 5xSDS sample buffer was added and denatured the secondary structure by boiling at 95<sup>0</sup>C for 5minutes.

### **SDS-polyacrylamide gel electrophoresis**

Protein lysis were prepared from cells and tissues and then analysed with SDS-PAGE electrophoresis (Laemmli et al., 1970).

## **4.12 RNA isolation and RT-PCR analysis**

Total RNA was extracted from the wounds of WT and Nesprin-2 KO skin tissues with TRIZOL reagent (Invitrogen LifeTechnologies, Carlsbad, CA), following the manuals instructions. The RNA was also isolated from mice dermal primary fibroblast in similar way (TRIZOL method).The concentration of the total RNA was measured using Agilent Bioanalyser with RNA 6000 Nano Assay kit. From this Bioanalyser quantity and quality of RNA was measured.

The first strand cDNA was synthesised using Strata Script reverse transcriptase from Stratagene. For cDNA synthesis 5µg of total RNA was first incubated at 65<sup>0</sup>C for 5 minutes together with Oligo (dT) and DEPC water and cool down to anneal the primers to RNA. Then this mixture is again incubated at 42<sup>0</sup>C for 1 hour with StrataScript buffer, RNase block Ribonuclease Inhibitor, Reverse transcriptase and dNTP mix. The finally the reaction was inactivated by incubating at 90<sup>0</sup>C for 5 minutes.

For quantitative PCR (q-RT-PCR) 1µl cDNA was used from control and experimental sample. Two sets of primers were designed using Primer3output software at exon-exon junction to avoid genomic DNA contamination. Real time PCR was

carried out with the Opticon III instrument (MJ Research) using the Quantitect SYBR® green PCR kit (Qiagen, Hilden, Germany) according to Farbrother et al., (2006). Gene-specific primers of 22-28 bases in length directed against the 3' region of the corresponding genes for product sizes of 200-300 bases. PCR was performed using the following programme-

1. Incubate at 95<sup>0</sup>C for 15 min
2. Incubate at 95<sup>0</sup>C for 30 sec
3. Incubate at 60<sup>0</sup>C \* for 45 sec
4. Incubate at 68<sup>0</sup>C for 1min
5. Plate read
6. Goto line 2 for 50 times
7. Incubate at 12<sup>0</sup>C forever
8. End

\* Annealing temperature designed based on the primer melting temperature As a quantification standard defined concentrations of the annexin VII gene (Doring et al., 1995) cloned into the pT7-7 vector (Tabor, 1990) were used for amplification. The housekeeping gene GAPDH was used as a positive control and to ensure comparable concentrations of cDNA in samples of Nesprin-2 knockout and wild type fibroblasts or tissue. For each quantification three reactions were performed in parallel, quantification results were normalized based on the GAPDH control and mean values were calculated.

### **4.13 Cell culture and transfection**

Primary mouse fibroblasts and human keratinocytes (HaCaT) and cultivated in high glucose DMEM (4.500 mg/ml von GIBCO) supplemented with 10% fetal bovine serum at 37°C in a humidified atmosphere containing 5% CO<sub>2</sub> and 100% humidity. Cells once attain 90% (primary mouse fibroblast) and nearly 60-70% (HaCaT) confluency were trypsinized and split in to 1:2-4 dilution.

The expression of Nesprin-2 Giant was knock down in HaCaT cell line (Lüke et al., 2008). To knock down the HaCaT cells were transfected with 5µg pShag1-Nesprin-2 knockdown and control shRNA plasmid, using the Amaxa nucleofector technology according to the manufacture' instruction (Amaxa Biosystems). To get a higher knock down efficiency HaCaT cells were transfected for two times in each trial.

### **4.14 Chromatin immunoprecipitation assay (ChIP)**

ChIP assays were performed using a ChIP-IT express kit and ChIP-IT control kits (Active motif) as described in the manufacturer's instructions. Briefly, approximately  $4.5 \times 10^7$  HaCaT cells were fixed by 1% formaldehyde for 10 minutes at room temperature. The fixation reactions were stopped by Glycine Stop-Fix solution. Cells were washed once with ice-cold PBS and colleted using ice-cold Cell Scraping Solution. Cells were pelleted by centrifugation and then resuspended in ice-cold Lysis Buffer (supplemented with proteinase inhibitor + PMSF). Samples were incubated on ice for 30 minutes. Nuclei were pelleted and resuspended in the Shearing Buffer. We sheared the DNA to an average length of 200 bp to 1,000 bp. The sheared DNA samples were centrifuged at 10,000 to 15,000 rpm in a 4°C microcentrifuge for 12 minutes. A small aliquot of the sheared chromatin (supernatant) was used for checking the DNA shearing efficiency and

DNA concentration. Protein G Magnetic Beads/Sheared Chromatin/Antibody mixtures were incubated on a rolling shaker overnight at 4<sup>0</sup>C. Nesprin-2 specific mAb K20-478, negative Control IgG and an RNA pol II antibody (positive control) were used for ChIP reactions. The DNA/protein complexes were eluted and treated with 0.4µg/µl proteinase K at 37<sup>0</sup>C for 1 hour. The proteinase K digestion was stopped and the eluted DNA was immediately processed as a template for further PCR analysis. Eluted DNA from the Nesprin-2 antibody, negative control IgG and RNA polII antibody and purified DNA from the sheared chromatin, were assessed for the presence of the GAPDH DNA fragments using PCR and the following primers: 5'GAPDH exon1, 5'-GCGCCCCCGGTTTCTATAAATTGAG-3' and 3'GAPDH exon1, 5'- AGAGAACAGTGAGCGCCTAGTGGCC-3'. 3µl of each eluted DNA was amplified for 34 cycles using the following conditions: 95<sup>0</sup>C for 30 seconds, 70<sup>0</sup>C for 30 seconds and 72<sup>0</sup>C for 40 seconds.

## **4.15 Microarray analysis**

### **Microarray methods**

DNA microarray is a technique that permits the analysis of expression levels of thousands of genes. The principle of DNA microarray is hybridization or base pairing of the unknown DNA sequences in the sample with complementary immobilized DNA probes with known sequences. DNA microarrays are mainly employed to study genetic variations in a sample or to determine the expression levels of genes. Because the expression pattern of a gene is linked to its biological role, microarray studies can provide important information on the biochemical pathways involved, sites of gene expression and most importantly the function of the gene in a particular organ as well as the whole organism (Chikina et al., 2009). Total RNA or mRNA is isolated from the test and reference sample which are then reverse transcribed to cDNA. The cDNA which is synthesised will be later

labelled with fluorescence dyes (Cy3 and Cy5-dUTP dyes). These cDNA labelled with fluorescence dyes (fluorescence targets) are pooled together and hybridized under optimum conditions to the clones on the microarray glass slides. The laser excitation of the fluorescence targets emits a characteristic spectrum which is measured using the Confocal Laser microscope. Monochrome images from the scanner are imported into software in which the images are pseudo-coloured and merged. The signal intensity of each spot from both channels is quantified. The information about the clones, including gene name, intensity value, intensity ratios, normalized constant etc., are attached to each target. The data from a single hybridization experiment is viewed as a normalized ration (ratio of Cy3 and Cy5) in which significant deviations from 1 (no change) are indicative of upregulation (more than 1) or down regulation (less than 1) of genes expression in comparison to the reference sample (control sample) (Duggan et al., 1999) (Figure 4.1). Microarray is widely being used in many clinical investigations and it's a convenient tool to study the expression pattern of thousands of genes.

### **Target preparation**

Target (cDNA sample) was prepared by reverse transcribing 20µg of total RNA per reaction in the presence of aminoallyl dUTP with the FairPlay Microarray Labeling Kit (Stratagene, La Jolla, USA) at high-stringent condition and the cDNA was labeled with activated Cy3 and Cy5 fluorescent dyes (Amersham Biosciences, Uppsala, Sweden). Labelled cDNAs were dye swapped from each independent isolation. Cy3 and Cy5 labelled targets were mixed; ethanol precipitated and then dissolved in 65µl of hybridization buffer (Noegel et al., 1985) with 500 mg/ml Fish sperm DNA (Roche, Mannheim, Germany) and 2µM oligo dA 18-mer.

### **Microarray hybridization and scanning**

The hybridization mixtue was prepared and it was heated to 80°C for 10 min, ap-

plied on the microarray under a cover-slip and incubated in a hybridization chamber (Corning, New York, USA). This hybridization chamber is incubated for the process at 37°C for 16 hours. After hybridization microarray slides were washed with 2 x SSC for two times, 0.1 %SDS and once with 0.1 x SSC, 0.1 %SDS for 5 min each, five times with 0.1 x SSC and once with 0.01 x SSC for 5 sec each and dried by centrifugation at 235g for 5 min. Signal detection was performed with the ScanArray® 4000XL confocal laser Scanner (PerkinElmer Life Sciences, Wellesley, USA). Two image pairs were produced per microarray slide, one with maximum laser intensity so that signals for most probes and also some saturated signals were obtained and a second one with minimum laser intensity so that none of the signals was saturated. This way the dynamic range of the measurement was expanded. Images for Cy3 and Cy5 were obtained, spots were detected and quantified with ScanArray® Express v3.0 (PerkinElmer Life Sciences), then manually inspected and if necessary corrected.

### **Data analysis**

Array tools (<http://www.uni-koeln.de/med-fak/biochemie/transcriptomics/toolsarray.e.shtml>) was used to handle the import and export of microarray data to different analysis programs. Upon import of two data files of the same microarray scanned with different laser powers the saturated spots of the high laser power scan were replaced by non-saturated spots from the low laser power scan. In addition the import also performed data filtering by flagging SpotReport® controls, negative controls, empty spots, spots where only spotting solution was printed and spots whose intensities were below or equal to zero as 'Bad'. Fluorescence ratios were normalized by LOWESS-normalization using R 1.6.2 (BioConductor, <http://www.bioconductor.org/>). Differentially expressed genes were identified with the program Significance Analysis of Microarrays (SAM) (Tusher et al., 2001). Differentially regulated genes that were common between the different experiments

were detected with the program “compare” (<http://www.uni-koeln.de/fak/biochemie/transcriptomics/tools.e.shtml>). Cluster analysis was performed with GeneSpring 7.2 (Agilent Technologies, <http://www.chem.agilent.com>). GO term enrichment was analyzed with GOAT (Xu and Shaulsky, 2005). A complete list of all *Dictyostelium* proteins with GO annotations is available from the GO website (<http://www.geneontology.org/GO.current.annotations.shtml>). To identify enriched GO terms we selected those genes of the array (reference list) and of the identified clusters (gene lists), respectively, whose gene products have GO annotations. Given a gene and a reference list, the GOAT program calculates the enrichment and statistical significance of every GO term by comparing the observed number of genes in a specific category with the number of genes that might appear in the same category if a selection performed from the same reference list were completely random.

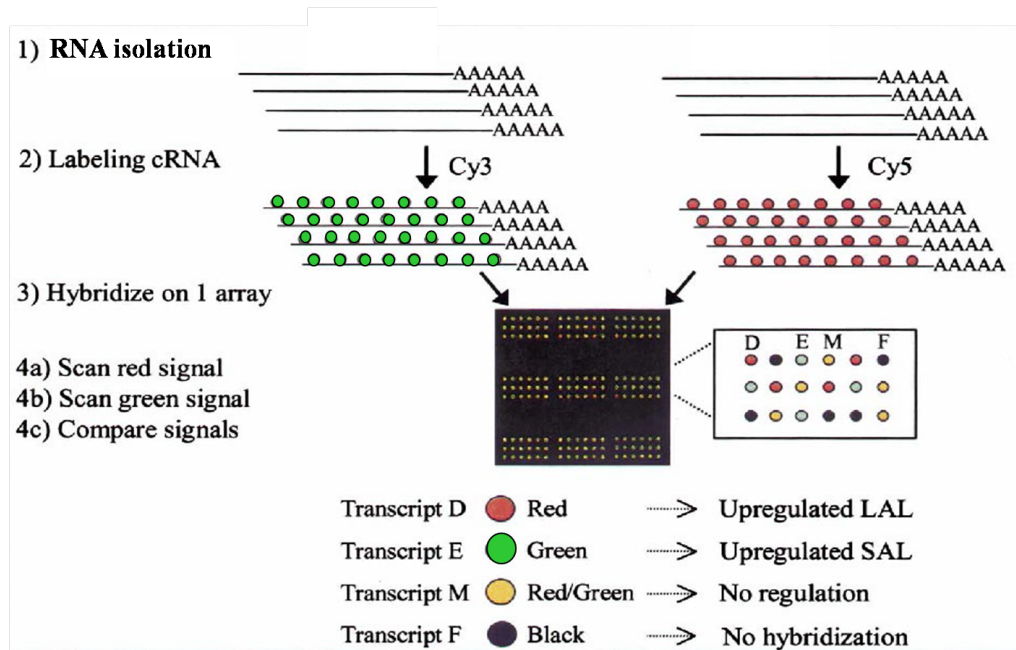


**Figure 4.1: Principle of microarray.** The core principle of microarray is hybridization between two fluorescently labelled DNA strands. The property of complementary nucleic acid sequences to specifically pair with each other by forming hydrogen bonds between complementary nucleotide base pairs. A high number of complementary base pairs in a nucleotide sequence mean tighter non-covalent bonding between the two strands. After washing off of non-specific bonding sequences, only strongly paired strands will remain hybridized. So fluorescently labelled target sequences that bind to a probe sequence generate a signal that depends on the strength of the hybridization determined by the number of paired bases, the hybridization conditions and washing after hybridization. Total strength of the signal, from a spot (feature), depends upon the amount of target sample binding to the probes present on that spot. Microarrays use relative quantification in which the intensity of a feature is compared to the intensity of the same feature under a different condition, and the identity of the feature is known by its position. (Feldker et al., 2003).

# Bibliography

- Akhtar, A. & Gasser, S. M. (2007), 'The nuclear envelope and transcriptional control', *Nature Reviews Genetics* **8**(7), 507–517.
- Angel, P. & Karin, M. (1991), 'The role of jun, fos and the AP-1 complex in cell-proliferation and transformation', *Biochimica et Biophysica Acta (BBA)-Reviews on Cancer* **1072**(2-3), 129–157.
- Ball, A. R. J. & Yokomori, K. (2009), 'Revisiting the role of heterochromatin protein 1 in DNA repair', *Journal of Cell Biology* **185**(4), 573.
- Beck, M. (2004), 'Nuclear pore complex structure and dynamics revealed by cryoelectron tomography', *Science* **306**(5700), 1387–1390.
- Beck, M., Lucic, V., Förster, F., Baumeister, W. & Medalia, O. (2007), 'Snapshots of nuclear pore complexes in action captured by cryo-electron tomography', *Nature* **449**(7162), 611–615.
- Bell, L. A. & Ryan, K. M. (2003), 'Life and death decisions by E2F-1', *Cell Death & Differentiation* **11**(2), 137–142.
- Boban, M., Zargari, A., Andreasson, C., Heessen, S., Thyberg, J. & Ljungdahl, P. O. (2006), 'Asi1 is an inner nuclear membrane protein that restricts promoter access of two latent transcription factors', *Journal of Cell Biology* **173**(5), 695.
- Boyce, M. & Yuan, J. (2006), 'Cellular response to endoplasmic reticulum stress: a matter of life or death', *Cell Death and Differentiation* **13**(3), 363–373.
- Broers, J. L., Peeters, E. A., Kuijpers, H. J., Endert, J., Bouten, C. V., Oomens, C. W., Baaijens, F. & Ramaekers, F. (2004), 'Decreased mechanical stiffness in LMNA-/-cells is caused by defective nucleo-cytoskeletal integrity: implications for the development of laminopathies', *Human molecular genetics* **13**(21), 2567.
- Bryant, M., Drew, G. M., Houston, P., Hissey, P., Campbell, C. J. & Braddock, M. (2000), 'Tissue repair with a therapeutic transcription factor', *Human gene therapy* **11**(15), 2143–2158.
- Burke, B., Mounkes, L. C. & Stewart, C. L. (2001), 'The nuclear envelope in muscular dystrophy and cardiovascular diseases', *Traffic* **2**(10), 675–683.

- Chikina, M. D., Huttenhower, C., Murphy, C. T. & Troyanskaya, O. G. (2009), 'Global prediction of Tissue-Specific gene expression and Context-Dependent gene networks in *caenorhabditis elegans*', *PLoS Computational Biology* **5**(6), e1000417.
- Cikala, M., Alexandrova, O., David, C. N., Proeschel, M., Stiening, B., Cramer, P. & Boettger, A. (2004), 'The phosphatidylserine receptor from hydra is a nuclear protein with potential Fe(II) dependent oxygenase activity', *BMC Cell Biology* **5**(1), 26.
- Cohen, M., Gruenbaum, Y., Lee, K. K. & Wilson, K. L. (2001), 'Transcriptional repression, apoptosis, human disease and the functional evolution of the nuclear lamina', *Trends in biochemical sciences* **26**(1), 41–47.
- Cowin, A. J., Adams, D., Geary, S. M., Wright, M. D., Jones, J. C. R. & Ashman, L. K. (2006), 'Wound healing is defective in mice lacking tetraspanin CD151', *Journal of Investigative Dermatology* **126**(3), 680–689.
- D'Angelo, M. A. & Hetzer, M. W. (2008), 'Structure, dynamics and function of nuclear pore complexes', *Trends in cell biology* **18**(10), 456–466.
- Debril, M. B., Dubuquoy, L., Feige, J. N., Wahli, W., Desvergne, B., Auwerx, J. & Gelman, L. (2005), 'Scaffold attachment factor b1 directly interacts with nuclear receptors in living cells and represses transcriptional activity', *Journal of molecular endocrinology* **35**(3), 503.
- Desmouliere, A., Geinoz, A., Gabbiani, F. & Gabbiani, G. (1993), 'Transforming growth factor-beta 1 induces alpha-smooth muscle actin expression in granulation tissue myofibroblasts and in quiescent and growing cultured fibroblasts', *Journal of Cell Biology* **122**(1), 103.
- Dialynas, G. K., Terjung, S., Brown, J. P., Aucott, R. L., Baron-Luhr, B., Singh, P. B. & Georgatos, S. D. (2007), 'Plasticity of HP1 proteins in mammalian cells', *Journal of Cell Science* **120**(19), 3415–3424.
- Dicker, A. J., Popa, C., Dahler, A. L., Serewko, M. M., Hilditch-Maguire, P. A., Frazer, I. H. & Saunders, N. A. (2000), 'E2F-1 induces proliferation-specific genes and suppresses squamous differentiation-specific genes in human epidermal keratinocytes', *Oncogene* **19**(25), 2887–2894.
- Dorner, D., Gotzmann, J. & Foisner, R. (2007), 'Nucleoplasmic lamins and their interaction partners, LAP2?, rb, and BAF, in transcriptional regulation', *FEBS Journal* **274**(6), 1362–1373.
- Dorner, D., Vlcek, S., Foeger, N., Gajewski, A., Makolm, C., Gotzmann, J., Hutchison, C. J. & Foisner, R. (2006), 'Lamina-associated polypeptide 2alpha regulates cell cycle progression and differentiation via the retinoblastoma-E2F pathway', *The Journal of Cell Biology* **173**(1), 83–93.

- Dreger, M., Bengtsson, L., Schoeneberg, T., Otto, H. & Hucho, F. (2001), 'Nuclear envelope proteomics: novel integral membrane proteins of the inner nuclear membrane', *Proceedings of the National Academy of Sciences* **98**(21), 11943.
- D'Souza, S. J. A. (2001), 'Ca<sup>2+</sup> and BMP-6 signaling regulate E2F during epidermal keratinocyte differentiation', *Journal of Biological Chemistry* **276**(26), 23531–23538.
- Duggan, D. J., Bittner, M., Chen, Y., Meltzer, P. & Trent, J. M. (1999), 'Expression profiling using cDNA microarrays', *Nature genetics* **21**(1 Suppl), 10–14.
- Dyson, N. (1998), 'The regulation of E2F by pRB-family? proteins', *Genes & Development* **12**(15), 2245–2262.
- Eferl, R. & Wagner, E. F. (2003), 'AP-1: a double-edged sword in tumorigenesis', *Nature Reviews Cancer* **3**(11), 859–868.
- Emerson, L. J., Holt, M. R., Wheeler, M. A., Wehnert, M., Parsons, M. & Ellis, J. A. (2009), 'Defects in cell spreading and ERK1/2 activation in fibroblasts with lamin A/C mutations', *Biochimica et Biophysica Acta (BBA)-Molecular Basis of Disease* .
- Eming, S. A., Werner, S., Bugnon, P., Wickenhauser, C., Siewe, L., Utermohlen, O., Davidson, J. M., Krieg, T. & Roers, A. (2007), 'Accelerated wound closure in mice deficient for interleukin-10', *American Journal Of Pathology* **170**(1), 188–202.
- Fang, Z. H. & Han, Z. C. (2006), 'The transcription factor e2f: a crucial switch in the control of homeostasis and tumorigenesis', *Histol Histopathol* **21**, 403–413.
- Feldker, D. E., de Kloet, E. R., Kruk, M. R. & Datson, N. A. (2003), 'Large-scale gene expression profiling of discrete brain regions: potential, limitations, and application in genetics of aggressive behavior', *Behavior genetics* **33**(5), 537–548.
- Fisher, D. Z., Chaudhary, N. & Blobel, G. (1986), 'cDNA sequencing of nuclear lamins a and c reveals primary and secondary structural homology to intermediate filament proteins', *Proceedings of the National Academy of Sciences of the United States of America* **83**(17), 6450.
- Franz, R. C. (2010), 'ROTEM analysis: a significant advance in the field of rotational thrombelastography', *South African Journal of Surgery* **47**(1).
- Fridkin, A., Penkner, A., Jantsch, V. & Gruenbaum, Y. (2008), 'SUN-domain and KASH-domain proteins during development, meiosis and disease', *Cellular and Molecular Life Sciences* **66**(9), 1518–1533.
- Gaines, P., Tien, C. W., Olins, A. L., Olins, D. E., Shultz, L. D., Carney, L. & Berliner, N. (2008), 'Mouse neutrophils lacking lamin b-receptor expression exhibit

- aberrant development and lack critical functional responses', *Experimental Hematology* **36**(8), 965–976.
- Garee, J. P. & Oesterreich, S. (2009), 'SAFB1's multiple functions in biological control-lots still to be done!', *Journal of Cellular Biochemistry* pp. n/a–n/a.
- Geneve, S. (1970), 'actor prevent cteriophage', *J. Mol. Bid* **47**, 69–85.
- Gerace, L., Blum, A. & Blobel, G. (1978), 'Immunocytochemical localization of the major polypeptides of the nuclear pore complex-lamina fraction. interphase and mitotic distribution', *Journal of Cell Biology* **79**(2), 546.
- Gerace, L. & Burke, B. (1988), 'Functional organization of the nuclear envelope', *Annual review of cell biology* **4**(1), 335–374.
- Gerharz, M., Baranowsky, A., Siebolts, U., Eming, S., Nischt, R., Krieg, T. & Wickenhauer, C. (2007), 'Morphometric analysis of murine skin wound healing: Standardization of experimental procedures and impact of an advanced multitissue array technique', *Wound Repair and Regeneration* **15**(1), 105–112.
- Gillitzer, R. & Goebeler, M. (2001), 'Chemokines in cutaneous wound healing', *Journal of Leukocyte Biology* **69**(4), 513.
- Gimona, M., Djinovic-Carugo, K., Kranewitter, W. J. & Winder, S. J. (2002), 'Functional plasticity of CH domains', *FEBS letters* **513**(1), 98–106.
- Gotzmann, J. & Foisner, R. (2005), 'A-type lamin complexes and regenerative potential: a step towards understanding laminopathic diseases?', *Histochemistry and Cell Biology* **125**(1-2), 33–41.
- Greenberg, M. E. & Ziff, E. B. (1984), 'Stimulation of 3T3 cells induces transcription of the c-fos proto-oncogene', *Nature* **311**(5985), 433–438.
- Grose, R., Harris, B. S., Cooper, L., Topilko, P. & Martin, P. (2002), 'Immediate early genes krox-24 and krox-20 are rapidly up-regulated after wounding in the embryonic and adult mouse', *Developmental Dynamics* **223**(3), 371–378.
- Gruenbaum, Y., Margalit, A., Goldman, R. D., Shumaker, D. K. & Wilson, K. L. (2005), 'The nuclear lamina comes of age', *Nature Reviews Molecular Cell Biology* **6**(1), 21–31.
- Hale, C., Shrestha, A., Khatau, S., Stewarthutchinson, P., Hernandez, L., Stewart, C., Hodzic, D. & Wirtz, D. (2008), 'Dysfunctional connections between the nucleus and the actin and microtubule networks in laminopathic models', *Biophysical Journal* **95**(11), 5462–5475.
- Hammerich-Hille, S., Kaipparettu, B. A., Tsimelzon, A., Creighton, C. J., Jiang, S., Polo, J. M., Melnick, A., Meyer, R. & Oesterreich, S. (2009), 'SAFB1 mediates repression of immune regulators and apoptotic genes in breast cancer cells', *Journal of Biological Chemistry* **285**(6), 3608–3616.

- Haque, F., Mazzeo, D., Patel, J. T., Smallwood, D. T., Ellis, J. A., Shanahan, C. M. & Shackleton, S. (2009), 'Mammalian SUN protein interaction networks at the inner nuclear membrane and their role in laminopathy disease processes', *Journal of Biological Chemistry* **285**(5), 3487–3498.
- Harris, D. M., Krogt, Z. A. V. D., Klaassen, P., Raamsdonk, L. M., Hage, S., Berg, M. A. V. D., Bovenberg, R. A., Pronk, J. T. & Daran, J. M. (2009), 'Exploring and dissecting genome-wide gene expression responses of penicillium chrysogenum to phenylacetic acid consumption and penicillinG production', *BMC genomics* **10**(1), 75.
- Heessen, S. & Fornerod, M. (2007), 'The inner nuclear envelope as a transcription factor resting place', *EMBO reports* **8**(10), 914–919.
- Hetzer, M. W., Walther, T. C. & Mattaj, I. W. (2005), 'Pushing the envelope: structure, function, and dynamics of the nuclear periphery'.
- Hinz, B., Celetta, G., Tomasek, J. J., Gabbiani, G. & Chaponnier, C. (2001), 'Alpha-smooth muscle actin expression upregulates fibroblast contractile activity', *Molecular biology of the cell* **12**(9), 2730.
- Hinz, B. & Gabbiani, G. (2003), 'Mechanisms of force generation and transmission by myofibroblasts', *Current Opinion in Biotechnology* **14**(5), 538–546.
- Hinz, B., Gabbiani, G. & Chaponnier, C. (2002), 'The NH<sub>2</sub>-terminal peptide of  $\alpha$ -smooth muscle actin inhibits force generation by the myofibroblast in vitro and in vivo', *The Journal of Cell Biology* **157**(4), 657–663.
- Hotulainen, P. & Lappalainen, P. (2006), 'Stress fibers are generated by two distinct actin assembly mechanisms in motile cells', *Journal of Cell Biology* **173**(3), 383.
- Hutchison, C. J. & Worman, H. J. (2004), 'A-type lamins: Guardians of the soma?', *Nature cell biology* **6**(11), 1062–1067.
- Ishimura, A. (2006), 'Man1, an inner nuclear membrane protein, regulates vascular remodeling by modulating transforming growth factor  $\beta$  signaling', *Development* **133**(19), 3919–3928.
- Ivorra, C. (2006), 'A mechanism of AP-1 suppression through interaction of c-Fos with lamin A/C', *Genes & Development* **20**(3), 307–320.
- Jiang, S. (2005), 'Scaffold attachment factor SAFB1 suppresses estrogen receptor  $\alpha$ -Mediated transcription in part via interaction with nuclear receptor corepressor', *Molecular Endocrinology* **20**(2), 311–320.
- Kandert, S., Luke, Y., Kleinhenz, T., Neumann, S., Lu, W., Jaeger, V. M., Munck, M., Wehnert, M., Muller, C. R., Zhou, Z. et al. (2007), 'Nesprin-2 giant safeguards nuclear envelope architecture in LMNA S143F progeria cells', *Human molecular genetics* **16**(23), 2944.

- Kandert, S., Wehnert, M., Mueller, C. R., Buendia, B. & Dabauvalle, M. C. (2009), 'Impaired nuclear functions lead to increased senescence and inefficient differentiation in human myoblasts with a dominant p. R545C mutation in the LMNA gene', *European journal of cell biology* .
- Kondo, H. & Yonezawa, Y. (2000), 'Human fetal skin fibroblast migration stimulated by the autocrine growth factor bFGF is mediated by phospholipase a2 via arachidonic acid without the involvement of pertussis Toxin-Sensitive G-Protein', *Biochemical and Biophysical Research Communications* **272**(3), 648–652.
- Lai, J., Lai, K., Chuang, K., Chang, P., Yu, I., Lin, W. & Chang, C. (2009), 'Monocyte/macrophage androgen receptor suppresses cutaneous wound healing in mice by enhancing local  $\text{tnf-}\alpha$  expression', *Journal of Clinical Investigation* .
- Lebkowski, J. S. & Laemmli, U. K. (1982), 'Non-histone proteins and long-range organization of HeLa interphase DNA', *Journal of Molecular Biology* **156**(2), 325–344.
- Lee, J. S., Hale, C. M., Panorchan, P., Khatau, S. B., George, J. P., Tseng, Y., Stewart, C. L., Hodzic, D. & Wirtz, D. (2007), 'Nuclear lamin A/C deficiency induces defects in cell mechanics, polarization, and migration', *Biophysical journal* **93**(7), 2542–2552.
- Lee, K. K., Starr, D., Cohen, M., Liu, J., Han, M., Wilson, K. L. & Gruenbaum, Y. (2002), 'Lamin-dependent localization of UNC-84, a protein required for nuclear migration in *caenorhabditis elegans*', *Molecular biology of the cell* **13**(3), 892.
- Libotte, T., Zaim, H., Abraham, S., Padmakumar, V. C., Schneider, M., Lu, W., Munck, M., Hutchison, C., Wehnert, M., Fahrenkrog, B., Sauder, U., Aebi, U., Noegel, A. A., & Karakesisoglou, I. (2005), 'Lamin A/C-dependent localization of nesprin-2, a giant scaffold at the nuclear envelope', *Molecular biology of the cell* **16**(7), 3411.
- Lloyd, D. J., Trembath, R. C. & Shackleton, S. (2002), 'A novel interaction between lamin a and SREBP1: implications for partial lipodystrophy and other laminopathies', *Human Molecular Genetics* **11**(7), 769–777.
- Lovvorn, H. N., Cheung, D. T., Nimni, M. E., Perelman, N., Estes, J. M. & Adzick, N. S. (1999), 'Relative distribution and crosslinking of collagen distinguish fetal from adult sheep wound repair', *Journal of Pediatric Surgery* **34**(1), 218–223.
- Luke, Y., Zaim, H., Karakesisoglou, I., Jaeger, V. M., Sellin, L., Lu, W., Schneider, M., Neumann, S., Beijer, A., Munck, M., Padmakumar, V. C., Gloy, J., Walz, G. & Noegel, A. A. (2008), 'Nesprin-2 giant (NUANCE) maintains nuclear envelope architecture and composition in skin', *Journal of Cell Science* **121**(11), 1887–1898.

- Mansharamani, M. (2005), 'Direct binding of nuclear membrane protein MAN1 to emerin in vitro and two modes of binding to Barrier-to-Autointegration factor', *Journal of Biological Chemistry* **280**(14), 13863–13870.
- Maraldi, N. M., Lattanzi, G., Capanni, C., Columbaro, M., Merlini, L., Mattioli, E., Sabatelli, P., Squarzony, S. & Manzoli, F. A. (2006), 'Nuclear envelope proteins and chromatin arrangement: a pathogenic mechanism for laminopathies', *European Journal of Histochemistry* **50**(1), 1–8.
- Marcotte, R., Lacelle, C. & Wang, E. (2004), 'Senescent fibroblasts resist apoptosis by downregulating caspase-3', *Mechanisms of ageing and development* **125**(10-11), 777–783.
- Martin, P. (1997), 'Wound healing-aiming for perfect skin regeneration', *Science* **276**(5309), 75.
- Mattout, A., Dechat, T., Adam, S., Goldman, R. & Gruenbaum, Y. (2006), 'Nuclear lamins, diseases and aging', *Current Opinion in Cell Biology* **18**(3), 335–341.
- McKeon, F. D., Kirschner, M. W. & Caput, D. (1986), 'Homologies in both primary and secondary structure between nuclear envelope and intermediate filament proteins', *Nature* **319**(6053), 463–468.
- Michalik, L., Desvergne, B., Tan, N. S., Basu-Modak, S., Escher, P., Rieusset, J., Peters, J. M., Kaya, G., Gonzalez, F. J., Zakany, J. et al. (2001), 'Impaired skin wound healing in peroxisome proliferator-activated receptor (ppar) $\alpha$  and ppar  $\beta$  mutant mice', *Journal of Cell Biology* **154**(4), 799.
- Mislow, J. M. K., Holaska, J. M., Kim, M. S., Lee, K. K., Segura-Totten, M., Wilson, K. L. & McNally, E. M. (2002), 'Nesprin-1alpha self-associates and binds directly to emerin and lamin a in vitro', *FEBS Letters* **525**(1-3), 135–140.
- Nayler, O., Stratling, W., Bourquin, J. P., Stagljar, I., Lindemann, L., Jasper, H., Hartmann, A. M., Fackelmayer, F. O., Ullrich, A. & Stamm, S. (1998), 'SAF-B protein couples transcription and pre-mRNA splicing to SAR/MAR elements', *Nucleic acids research* **26**(15), 3542.
- Noegel, A., Welker, D. L., Metz, B. A. & Williams, K. L. (1985), 'Presence of nuclear associated plasmids in the lower eukaryote dictyostelium discoideum', *Journal of Molecular Biology* **185**(2), 447–450.
- Nogami, M., Takatsu, A., Endo, N. & Ishiyama, I. (1999), 'Immunohistochemical localization of c-fos in the nuclei of the medulla oblongata in relation to asphyxia', *International journal of legal medicine* **112**(6), 351–354.
- Okada, Y., Saika, S., Shirai, K., Hashizume, N., Yamanaka, O., Ohnishi, Y. & Senba, E. (1998), 'Immunolocalization of proto-oncogene products in keratocytes after epithelial ablation, alkali burn and penetrating injury of the cornea in rats', *Graefe's Archive for Clinical and Experimental Ophthalmology* **236**(11), 853–858.

- Padmakumar, V. C., Abraham, S., Braune, S., A. A., Tunggal, B., Karakesisoglou, I. & Korenbaum, E. (2004), 'Enaptin, a giant actin-binding protein, is an element of the nuclear membrane and the actin cytoskeleton', *Experimental cell research* **295**(2), 330–339.
- Padmakumar, V., Libotte1, T., Lu, W., Zaim, H., Abraham, S., Noegel, A. A., J.Gotzmann, Foisner, R. & Karakesisoglou1, I. (2005), 'The inner nuclear membrane protein sun1 mediates the anchorage of nesprin-2 to the nuclear envelope', *Journal of Cell Science* **118**(15), 3419–3430.
- Panno, J. P. (1988), 'Symmetry analysis of cell nuclei', *Cytometry* **9**(3), 195–200.
- Paramio, J. M. (2000), 'Opposite functions for E2F1 and E2F4 in human epidermal keratinocyte differentiation', *Journal of Biological Chemistry* **275**(52), 41219–41226.
- Patel, G. K., Wilson, C. H., Harding, K. G., Finlay, A. Y. & Bowden, P. E. (2005), 'Numerous keratinocyte subtypes involved in wound re-epithelialization', *Journal of Investigative Dermatology* **126**(2), 497–502.
- Pekovic, V., Harborth, J., Broers, J. L. V., Ramaekers, F. C. S., van Engelen, B., Lammens, M., von Zglinicki, T., Foisner, R., Hutchison, C. & Markiewicz, E. (2007), 'Nucleoplasmic LAP2alpha-lamin a complexes are required to maintain a proliferative state in human fibroblasts', *The Journal of Cell Biology* **176**(2), 163–172.
- Pierce, A. M., Fisher, S. M., Conti, C. J. & Johnson, D. G. (1998), 'Deregulated expression of E2F1 induces hyperplasia and cooperates with ras in skin tumor development', *Oncogene* **16**(10), 1267–1276.
- Porse, B. T., TA, P., Xu, X., Lindberg, B., Wewer, U. M., Friis-Hansen, L. & Nerlov, C. (2001), 'E2F repression by C/EBPalpha is required for adipogenesis and granulopoiesis in vivo', *Cell* **107**(2), 247–258.
- Porter, A. G. & Jaenicke, R. U. (1999), 'Emerging roles of caspase-3 in apoptosis', *Cell Death and Differentiation* **6**(2), 99–104.
- Puckelwartz, M. J., Kessler, E. J., Kim, G., DeWitt, M. M., Zhang, Y., Earley, J. U., Depreux, F. F., Holaska, J., Mewborn, S. K., Pytel, P. et al. (2009), 'Nesprin-1 mutations in human and murine cardiomyopathy', *Journal of Molecular and Cellular Cardiology* **48**, 600–608.
- Puckelwartz, M. J., Kessler, E., Zhang, Y., Hodzic, D., Randles, K. N., Morris, G., Earley, J. U., Hadhazy, M., Holaska, J. M., Mewborn, S. K. et al. (2009), 'Disruption of nesprin-1 produces an emery dreifuss muscular dystrophy-like phenotype in mice', *Human Molecular Genetics* **18**(4), 607.
- Rando, O. J., Zhao, K. & Crabtree, G. R. (2000), 'Searching for a function for nuclear actin', *Trends in cell biology* **10**(3), 92–97.

- Reddy, K. L., Zullo, J. M., Bertolino, E. & Singh, H. (2008), 'Transcriptional repression mediated by repositioning of genes to the nuclear lamina', *Nature* **452**(7184), 243–247.
- Rosenberg-Hasson, Y., Renert-Pasca, M. & Volk, T. (1996), 'A drosophila dystrophin-related protein, MSP-300, is required for embryonic muscle morphogenesis', *Mechanisms of development* **60**(1), 83–94.
- Schaefer, M. & Werner, S. (2007), 'Transcriptional control of wound repair', *The Annual Review of Cell and Developmental* **23**, 69–92.
- Schaefer, M. & Werner, S. (2008), 'Cancer as an overhealing wound: an old hypothesis revisited', *Nature Reviews Molecular Cell Biology* **9**(8), 628–638.
- Scheijen, B., Bronk, M., Meer, T. V. D. & Bernards, R. (2003), 'Constitutive E2F1 overexpression delays endochondral bone formation by inhibiting chondrocyte differentiation', *Molecular and cellular biology* **23**(10), 3656.
- Schirmer, E. C. (2003), 'Nuclear membrane proteins with potential disease links found by subtractive proteomics', *Science* **301**(5638), 1380–1382.
- Schirmer, E. C. & Foisner, R. (2007), 'Proteins that associate with lamins: many faces, many functions', *Experimental cell research* **313**(10), 2167–2179.
- Schoenthal, A., Herrlich, P., Rahmsdorf, H. J. & Ponta, H. (1988), 'Requirement for fos gene expression in the transcriptional activation of collagenase by other oncogenes and phorbol esters', *Cell* **54**(3), 325–334.
- Senior, A. & Gerace, L. (1988), 'Integral membrane proteins specific to the inner nuclear membrane and associated with the nuclear lamina', *Journal of Cell Biology* **107**(6), 2029.
- Serini, G. & Gabbiani, G. (1999), 'Mechanisms of myofibroblast activity and phenotypic modulation', *Experimental Cell Research* **250**(2), 273–283.
- Setoyama, C., Frunzio, R., Liao, G., Mudryj, M. & Crombrughe, B. D. (1986), 'Transcriptional activation encoded by the v-fos gene', *Proceedings of the National Academy of Sciences of the United States of America* **83**(10), 3213.
- Singer, I. I., Kawka, D. W., Kazazis, D. M. & Clark, R. A. (1984), 'In vivo co-distribution of fibronectin and actin fibers in granulation tissue: immunofluorescence and electron microscope studies of the fibronexus at the myofibroblast surface', *The Journal of Cell Biology* **98**(6), 2091–2106.
- Skalli, O., Ropraz, P., Trzeciak, A., Benzonana, G., Gillessen, D. & Gabbiani, G. (1986), 'A monoclonal antibody against alpha-smooth muscle actin: a new probe for smooth muscle differentiation', *Journal of Cell Biology* **103**(6), 2787.

- Somech, R., Shaklai, S., Geller, O., Amariglio, N., Simon, A. J., Rechavi, G. & Gal-Yam, E. N. (2005), 'The nuclear-envelope protein and transcriptional repressor LAP2  $\beta$  interacts with HDAC3 at the nuclear periphery, and induces histone h4 deacetylation', *Journal of cell science* **118**(17), 4017.
- Squarzoni, S., Sabatelli, P., Capanni, C., Petrini, S., Ognibene, A., Toniolo, D., Cobianchi, F., Zauli, G., Bassini, A., Baracca, A. et al. (2000), 'Emerin presence in platelets', *Acta neuropathologica* **100**(3), 291–298.
- Squier, M. K. & Cohen, J. J. (2000), 'Assays of apoptosis', *METHODS IN MOLECULAR BIOLOGY-CLIFTON THEN TOTOWA-* **144**, 327–337.
- Starr, D. A. (2002), 'Role of ANC-1 in tethering nuclei to the actin cytoskeleton', *Science* **298**(5592), 406–409.
- Stewart, C. L., Roux, K. J. & Burke, B. (2007), 'Blurring the boundary: The nuclear envelope extends its reach', *Science* **318**(5855), 1408–1412.
- Stewart-Hutchinson, P. J., Hale, C. M., Wirtz, D. & Hodzic, D. (2008), 'Structural requirements for the assembly of LINC complexes and their function in cellular mechanical stiffness', *Experimental cell research* **314**(8), 1892–1905.
- Stricker, J., Falzone, T. & Gardel, M. L. (2010), 'Mechanics of the f-actin cytoskeleton', *Journal of Biomechanics* **43**(1), 9–14.
- Stuurman, N., Heins, S. & Aebi, U. (1998), 'Nuclear lamins: their structure, assembly, and interactions', *Journal of Structural Biology* **122**(1-2), 42–66.
- Tan, N. S. (2001), 'Critical roles of PPAR $\beta$  / $\delta$  in keratinocyte response to inflammation', *Genes & Development* **15**(24), 3263–3277.
- Tan, N. S. (2004), 'Genetic- or transforming growth factor-4  $\beta$  1-induced changes in epidermal peroxisome proliferator-activated receptor  $\beta$ / $\delta$  expression dictate wound repair kinetics', *Journal of Biological Chemistry* **280**(18), 18163–18170.
- Terry, L. J., Shows, E. B. & Wente, S. R. (2007), 'Crossing the nuclear envelope: Hierarchical regulation of nucleocytoplasmic transport', *Science* **318**(5855), 1412–1416.
- Tomasek, J. J., Gabbiani, G., Hinz, B., Chaponnier, C. & Brown, R. A. (2002), 'Myofibroblasts and mechano-regulation of connective tissue remodelling', *Nature Reviews Molecular Cell Biology* **3**(5), 349–363.
- Towbin, B. D., Meister, P. & Gasser, S. M. (2009), 'The nuclear envelope a scaffold for silencing?', *Current Opinion in Genetics & Development* **19**(2), 180–186.
- Townson, S. M. (2003), 'SAFB2, a new scaffold attachment factor homolog and estrogen receptor corepressor', *Journal of Biological Chemistry* **278**(22), 20059–20068.

- Townson, S. M. (2004), 'Structure-Function analysis of the estrogen receptor  $\alpha$  corepressor scaffold attachment Factor-B1: IDENTIFICATION OF a POTENT TRANSCRIPTIONAL REPRESSION DOMAIN', *Journal of Biological Chemistry* **279**(25), 26074–26081.
- Tran, E. & Wenthe, S. (2006), 'Dynamic nuclear pore complexes: Life on the edge', *Cell* **125**(6), 1041–1053.
- Usui, M. L., Underwood, R. A., Mansbridge, J. N., Muffley, L. A., Carter, W. G. & Olerud, J. E. (2005), 'Morphological evidence for the role of suprabasal keratinocytes in wound reepithelialization', *Wound Repair and Regeneration: Official Publication of the Wound Healing Society [and] the European Tissue Repair Society* **13**(5), 468–479.
- van den Berg, T. K. & Kraal, G. (2005), 'A function for the macrophage f4/80 molecule in tolerance induction', *Trends in immunology* **26**(10), 506–509.
- Vaughan, M. B., Howard, E. W. & Tomasek, J. J. (2000), 'Transforming growth factor-beta1 promotes the morphological and functional differentiation of the myofibroblast', *Experimental Cell Research* **257**(1), 180–189.
- Volk, T. (1992), 'A new member of the spectrin superfamily may participate in the formation of embryonic muscle attachments in drosophila', *Development* **116**(3), 721.
- Wang, J. Y. & Johnson, L. R. (1990), 'Luminal polyamines stimulate repair of gastric mucosal stress ulcers', *American Journal of Physiology- Gastrointestinal and Liver Physiology* **259**(4), G584.
- Warren, D. T., Tajsic, T., Mellad, J. A., Searles, R., Zhang, Q. & Shanahan, C. M. (2009), 'Novel nuclear nesprin-2 variants tether active extracellular signal-regulated MAPK1 and MAPK2 at promyelocytic leukemia protein nuclear bodies and act to regulate smooth muscle cell proliferation', *Journal of Biological Chemistry* **285**(2), 1311–1320.
- Warren, D. T., Zhang, Q., Weissberg, P. L. & Shanahan, C. M. (2005), 'Nesprins: intracellular scaffolds that maintain cell architecture and coordinate cell function?', *Expert reviews in molecular medicine* **7**(11), 1–15.
- Welch, M. P., Odland, G. F. & Clark, R. A. (1990), 'Temporal relationships of f-actin bundle formation, collagen and fibronectin matrix assembly, and fibronectin receptor expression to wound contraction', *Journal of Cell Biology* **110**(1), 133.
- Wheeler, M. A., Davies, J. D., Zhang, Q., Emerson, L. J., Hunt, J., Shanahan, C. M. & Ellis, J. A. (2007), 'Distinct functional domains in nesprin-1 [alpha] and nesprin-2 [beta] bind directly to emerin and both interactions are disrupted in x-linked Emery-Dreifuss muscular dystrophy', *Experimental cell research* **313**(13), 2845–2857.

- Wilson, K. L., Zastrow, M. S. & Lee, K. K. (2001), 'Lamins and disease:: Insights into nuclear infrastructure', *Cell* **104**(5), 647–650.
- Worman, H. J. & Gundersen, G. G. (2006), 'Here come the SUNs: a nucleocytoskeletal missing link', *Trends in Cell Biology* **16**(2), 67–69.
- Worman, H. J., Yuan, J., Blobel, G. & Georgatos, S. D. (1988), 'A lamin b receptor in the nuclear envelope', *Proceedings of the National Academy of Sciences of the United States of America* **85**(22), 8531.
- Xiong, H., Rivero, F., Euteneuer, U., Mondal, S., Mana-Capelli, S., Larochelle, D., Vogel, A., Gassen, B. & Noegel, A. A. (2008), 'Dictyostelium sun-1 connects the centrosome to chromatin and ensures genome stability', *Traffic* **9**(5), 708–724.
- Zhang, N., Ahsan, M. H., Purchio, A. F. & West, D. B. (2005), 'Serum amyloid a-luciferase transgenic mice: response to sepsis, acute arthritis, and contact hypersensitivity and the effects of proteasome inhibition', *The Journal of Immunology* **174**(12), 8125.
- Zhang, Q., Bethmann, C., Worth, N. F., Davies, J. D., Wasner, C., Feuer, A., Ragnauth, C. D., Yi, Q., Mellad, J. A., Warren, D. T. et al. (2007), 'Nesprin-1 and-2 are involved in the pathogenesis of emery dreifuss muscular dystrophy and are critical for nuclear envelope integrity', *Human molecular genetics* **16**(23), 2816.
- Zhang, Q., Ragnauth, C., Greener, M. J., Shanahan, C. M. & Roberts, R. G. (2002), 'The nesprins are giant actin-binding proteins, orthologous to drosophila melanogaster muscle protein MSP-300', *Genomics* **80**(5), 473–481.
- Zhang, Q., Skepper, J. N., Yang, F., Davies, J. D., Hegyi, L., Roberts, R. G., Weissberg, P. L., Ellis, J. A. & Shanahan, C. M. (2001), 'Nesprins: a novel family of spectrin-repeat-containing proteins that localize to the nuclear membrane in multiple tissues', *Journal of Cell Science* **114**(24), 4485.
- Zhen, Y. Y., Libotte, T., Munck, M., Noegel, A. A. & Korenbaum, E. (2002), 'NUANCE, a giant protein connecting the nucleus and actin cytoskeleton', *Journal of cell science* **115**(15), 3207.

# Abstract

Nesprin-2 is one of the Giant proteins in mammalian cells. It localizes at the ONM through the interaction with SUN domain proteins and performs diverse functions within the cells including maintenance of nuclear morphology, bridging between nucleoplasm and cytoplasm, cell migration and polarity, and regulation of extracellular signalling. There is evidence for roles in clinical disorders as well.

Using a Nesprin-2 Giant knockout mouse model we showed here that the protein participates in vivo in cell migration and tissue repair during wound healing. In the wound healing situation, Nesprin-2 Giant regulates cell proliferation and differentiation as Nesprin-2 KO wounds caused the reduction in keratinocyte proliferation. Nesprin-2 KO mice also showed higher influx of inflammatory cells, mainly macrophages, indicating the protein's importance in the controlled expression of inflammatory cells. In Nesprin-2 KO mice reduced expression of cell proliferation related transcription factors c-Fos, PPAR  $\beta/\delta$ , Egr-1 and E2F1 was also observed which led to reduced keratinocyte proliferation and leading to a delay in re-epithelialization or healing of the wounds. c-Fos was mislocalized and found in the cytoplasm and in the nucleus in Nesprin-2 knock down (KD) HaCat cells whereas in the wild type situation its localization is confined to the nucleus in non-scratched cells. In in vivo wound healing and in vitro cell scratch experiments the localization of c-Fos is shuttling between the cytoplasm and nucleoplasm in WT at different time points. In contrast, in Nesprin-2 KO wounds and KD cells no differential localization was observed. Nesprin-2 KO mice also showed defective myofibroblast differentiation and reduced granulation tissue area (Figure 4.2). We

found that Nesprin-2 absence caused a disorganised distribution of F-actin. In primary dermal fibroblasts and the localization of actin along the NE and at the cell-cell junction is impaired in Nesprin-2 KD human keratinocytes. Microarray analysis showed that Nesprin-2 differentially regulates the transcription of the genes involved in extracellular matrix protein expression and in the inflammation process. It also regulates the transcription of signal transduction and cell cycle associated genes. From the results of loss of cell-cell junction and regulation of extracellular matrix and signal transduction genes in Nesprin-2 KD and KO cells, respectively, we propose it's a role in extracellular signalling. We also showed that Nesprin-2 binds to heterochromatin and centromeric DNA. Through this interaction it may have an effect on transcriptional regulation as well.

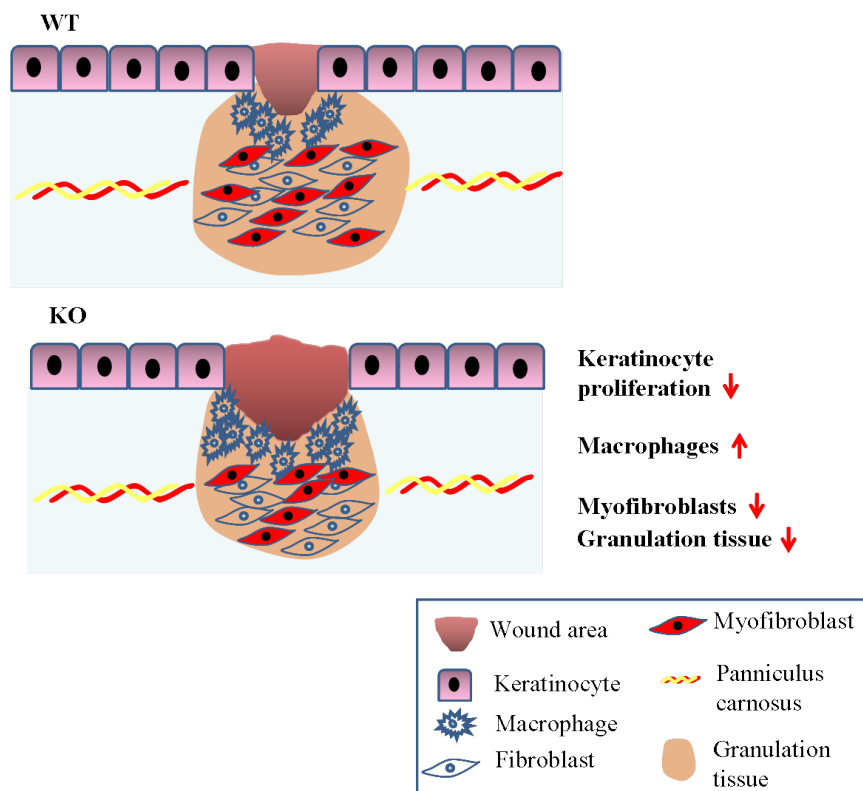


**Figure 4.2: Overview of the research findings.** Keratinocyte proliferation, macrophages population, granulation tissue area and myofibroblasts were studied during in vivo wound healing in nesprin-2 Giant knockout mice.

# Zusammenfassung

Nesprin-2 Giant ist ein riesiges F-Aktin bindendes Protein, das in der äußeren und der inneren Kernmembran lokalisiert ist. In Vorarbeiten ist die Generierung und Charakterisierung einer Nesprin-2 Giant defizienten Maus beschrieben worden, in der eine verdickte Epidermis beobachtet worden war, die mit einer Vergrößerung der Zellkerne und einer Veränderung der Zellmigration und Zellpolarität in isolierten Fibroblasten einherging. Ausgehend von diesen Ergebnissen wurde in dieser Arbeit ein in vivo Wundheilungsexperiment durchgeführt.

Die makroskopische Analyse hat eine Verzögerung im Wundheilungsprozess in den Knockout Mäusen gezeigt. Die anschließenden histochemischen und Immunfluoreszenzanalysen lassen auf Veränderungen in allen drei Phasen der Wundheilung schließen. In der inflammatorischen Phase (Phase I) wurde in den KO Mäusen eine schnellere Heilung beobachtet, die auf eine erhöhte Einwanderung von Makrophagen zurückzuführen war. Parallel dazu waren in Expressionsanalysen inflammatorische Gene hochreguliert in Wunden der KO Mäuse. In den Phasen II und III der Wundheilung findet die Neubildung und die Ummodellierung des Gewebes statt. Keratinozyten vermehren sich und wandern in die Wunde ein und Fibroblasten differenzieren sich in Myofibroblasten um. In den KO Mäusen waren diese Prozesse verlangsamt.

Eine Untersuchung der F-Aktinstrukturen in KO Fibroblasten zeigt Veränderungen. Im Gegensatz zu Wildtyp Fibroblasten sind in den Mutanten Fibroblasten die F-Aktinstressfasern in der Nähe des Zellkern weniger abundant und der typi-

sche "nukleäre Korb", der von Aktinfilamenten gebildet wird, fehlt. Statt dessen ist Aktin in punktaktigen Strukturen angereichert. Daraus schliessen wir, dass Nesprin-2 Giant eine wichtige Rolle für den Aufbau des Aktinnetzwerks spielt, das den Kern umgibt. Diese Ergebnisse konnten in HaCat Zellen bestätigt werden, in denen mit shRNA die Expression von Nesprin-2 stark reduziert war.

Nicht nur das Aktinnetzwerk ist beeinträchtigt in KO Zellen, auch die Expression und Lokalisation des für die Wundheilung wichtigen Transkriptionsfaktors c-Fos war verändert in den Wunden der KO Mäuse. Dieser Befund lässt auf eine Beteiligung von Nesprin-2 Giant in der Transkription schließen. Eine direkte Bindung zwischen Nesprin-2 und c-Fos wurde nicht nachgewiesen. Statt dessen assoziiert Nesprin-2 mit Heterochromatin und ein Verlust von Nesprin-2 führt zu Veränderungen in der Chromatinstruktur, deren Konsequenz eine Veränderung des Transkriptionsmuster einer Zelle sein könnte und für die beobachteten Effekte verantwortlich ist. Wir haben ein Modell entwickelt, das unsere Ergebnisse integriert und sowohl eine zytoplasmatische als auch eine nukleäre Rolle von Nesprin-2 Giant voraussetzt und die Basis für weiterführende Arbeiten zur Funktion dieser Proteine bildet.

# Erklärung

Hiermit versichere ich, dass ich die vorliegende Arbeit selbstständig verfasst und keine anderen als die angegebenen Quellen und Hilfsmittel benutzt habe, dass alle Stellen der Arbeit, die wörtlich oder sinngemäß aus anderen Quellen übernommen wurden, als solche kenntlich gemacht sind und dass die Arbeit in gleicher oder ähnlicher Form noch keiner Prüfungsbehörde vorgelegt wurde.

Köln, den 11. Juli 2011

Rashmi Rudrappa Nanjundappa